MOLECULAR SIMULATION STUDIES IN THE SUPERCRITICAL REGION

PANAGIOTIS PARRIS

A thesis submitted for the degree of Doctor of Philosophy

Department of Chemical Engineering

University College London

London, WC1E 7JE

July 2010

ACKOWLEDGEMENTS

First, I would like to thank my supervisor Dr. George Manos for his continuous support and encouragement throughout my studies.
Many thanks to my colleagues at University College of London: Alfeno, Baowang Errika, Eugenia, Giovanna, Sayed, Nadia, Nick, Nnamso for encouraging me keep going on at difficult times. Many thanks also go to my fiancée

July 2010

P.Parris

CONTENTS

ABSTRACT

In our work, we employed **molecular dynamics** and **Monte Carlo** (MC) simulations to investigate the supercritical phase of carbon dioxide near its critical point. Three systems have been studied. The pure carbon dioxide, mixture methane + carbon dioxide at infinite dilution of supercritical carbon dioxide and water + carbon dioxide at infinite dilution of supercritical carbon dioxide. The usage of molecular simulation methods in supercritical region gave us a distinct advantage of knowing the microstructure of the systems in a qualitative and quantitative way. The Kirkwood-Buff theory, which predicts the influence of the solvent on the solute, enabled us to predict thermodynamic properties of supercritical phase and compare them with experimental values.

We have examined the density effect on structure of the pure carbon dioxide and its solutions along its critical isotherm 4 K above its critical point. We focused our research and we present results for two basic sections,

A. Equilibrium and transport properties, namely

Volumetric properties;

Average configurational energy;

Isothermal compressibility;

Diffusivity; and the

Isochoric heat capacity

B. Solution structures at infinite solutions, namely

Radial distribution function; and

Coordination number

We discuss the outcomes based on the density inhomogeneities of the solvent and critical fluctuations, which are maximised at the critical point. We found that the

addition of methane to supercritical carbon dioxide increases the volume of the solution and a cavitation is formed around it. On the hand, the addition of water gives a cluster around it in local structure and decrease the volume of solution. We report results also of the diffusion coefficients for the pure carbon dioxide and the mixtures in this study, which it shows an anomalous decrease close to the critical point of the pure carbon dioxide. It is a general conclusion for all the properties we have studied that the density dependence along the isotherm is maximised at densities close to the critical one. Further, the usage of both molecular dynamics and Monte Carlo in supercritical regions validates the extension of the techniques in the supercritical region and reveals their limitations.

LIST OF FIGURES

LIST OF TABLES

1 INTRODUCTION

1.1 MOTIVATION

Supercritical fluids have dissolving power comparable to those of liquids, are much more compressible than gases and have transport properties intermediate between gas-like and liquid-like properties. These unique properties can be advantageously exploited in environmentally benign reaction processes, and make SCFs very attractive to industry, where constantly increasing waste disposal costs pose major problems.

Industrial separation processes using SCFs have been well established for decades, with the most famous application being coffee and tea decaffeination. Over the past few years, there was much interest also in industrialisation of reaction processes involving supercritical carbon dioxide. The driving force behind this commercialisation of supercritical reaction technology is the goal of developing economically as well as environmentally acceptable processes achieving set targets. The industrial potential of SCFs as reaction media is enhanced by their capability to fine tune reaction rates and the fact that we can select solvent properties. Due to the large compressibility of supercritical fluids, small changes in pressure can produce substantial changes in density, which, in turn, affect diffusivity, viscosity, dielectric, and solvation properties, thus dramatically influencing the kinetics and mechanisms of chemical reactions. This provides the opportunity to conduct a multistep synthesis in one solvent instead of number of solvents at different conditions.

Furthermore, while there exists a wealth of potential applications of SCF chemistry, realisation of this potential is severely hindered by our inability to predict accurately reactivity in SCFs. The Arrhenius equation can be used to predict the

reaction rate with temperature but there is no similar equation to predict the reaction rate with pressure in SCFs. Solvent properties of SCF are very sensitive to temperature and pressure in the compressible region of the phase diagram in the vicinity of their critical point. This failure reflects the fact that our current theories of solvation and its effect on chemical reaction dynamics do not extrapolate well close to the solvent regime, where novel reactivity has been observed. It is important to keep in mind that the effect of SCF solvents on solubilities, transport properties and the kinetics of the elementary reactions may differ substantially from that expected for non-SCF solvents. An understanding of these effects is needed for the design and optimisation of reaction processes at supercritical conditions (SC). Gaining an understanding of supercritical solvent effects on reaction kinetics from experiment alone is very difficult because of the problems associated with observing the supercritical phase, the reaction rate in such non-ideal environments and characterising their effect on rate constant separately. However, molecular simulation is an appropriate tool for such investigations because these problems do not arise, and system parameters can be precisely controlled and manipulated.

Using molecular simulation techniques for that purpose overcomes major problems associated with experimental studies at SC and gives us the opportunity to study microscopic properties such as solution microstructure and their connection to macroscopic properties. Indeed, we believe the main reason for the lack of quantitative prediction of reactivity at SC is the lack of molecular simulation studies connecting microscopic quantities, which are difficult to measure or hard to predict accurately, to macroscopic properties. Potential ways for affecting reactivity at SC is local density augmentation and preferential solvation resulting from the differential stabilization of reactants, products and activated complexes according to the strength

of their molecular asymmetries with respect to the solvent. As these properties as well as the observed innovative reactivity are maximal in the solvent's compressible regime, they must be accounted for in any computational treatment of such SCF solvent systems. Crucial to the success of any computational study is the implementation of efficient molecular simulation techniques that manage the solvent structure near to the critical point and this was the main task of our work.

1.2 SUMMARY OF CHAPTERS

The overall goal of this work is to explore the solvent properties of CO_2 at the molecular level. The first goal of our work was to gain insight into the solvent properties of a pure SCF close to the critical point and test the validity of molecular simulations methods. **Supercritical carbon dioxide** ($scCO_2$) was well described by an Elementary Physical model. Calculations have been performed with, molecular dynamics/Monte Carlo simulation in canonical ensemble. The validity of molecular simulation methods has been tested in the supercritical region.

The second goal was to gain a solid understanding of the structure of supercritical phase. The tendency of the solvent to form cluster or cavities around different types of solutes was studied extensively. We used the Kirkwood-Buff fluctuation theory to examine the solutions structures.

The following objectives are met in achieving the goals

• Testing the outcome of our developed Monte Carlo code with literature data

• Comparing the outcomes of Monte Carlo vice molecular dynamics in the supercritical region

• Finding the dependence of CO_2 solvent structure on density close to supercritical isotherm

- Understanding the contributing factors to structure of molecules in the supercritical CO_2
- Comparing simulated thermodynamic properties with experimental values
- Comparing the solution process of methane and water solutes in CO_2 solvent
- Examining the role of CO_2 solvent conditions on solute solution environment
- Developing a theory between molecular structure and solution process.

Our work is being presented in three parts, theory, simulation and results. In theory part, we present the background and techniques used in meeting the above objectives. In simulation part, we present the implementation of the molecular methods with technical details and covering programming issues. In results, we present and discuss the outcome of our work by exploring the goals.

In first part, following this introduction, we provide a framework of high pressure reaction kinetics in chapter two. In chapter three, a detailed description of molecular simulation techniques is given for MC and MD. An introduction of supercritical fluids, their properties and their features are presented in chapter four. Subsequently, a review on molecular models (potentials) in supercritical conditions is presented. We discuss the importance of the potential model with a review of different types of potential models produced in literature for carbon dioxide, water and methane.

Computational methods over molecular systems and their implementations for our system are given in second part. We discuss molecular simulation and molecular techniques from the simple to the complex in chapter five. We cover programming issues and their implementation in chapter six. It also includes the technical details of simulation for the initialization, equilibration and production periods.

Finally, third part presents the results. In chapter seven, we verify our Monte Carlo program. In the same chapter we accommodate also a discussion about the efficiency of molecular dynamics and Monte Carlo in the supercritical region. In chapter eight, we examine the dependence of solvent structure on solvent conditions. We show how solvent structures changes with density of CO_2 close to the critical isotherm and we explore the solvent structure on its thermodynamic properties. We examined the solvent structure on isothermal compressibility, isochoric heat capacity and diffusivity. In chapter nine, we explore the structure of infinitely diluted solutes in supercritical carbon dioxide. The water and methane have been chosen to play the role of solutes. Using the Kirkwood-Buff theory, the solution microenvironment of these solutes is predicted from the structure of solute molecule and the solvent conditions. The predictions are verified by against experimental data. Further, we address the effect of the addition of methane or water on the thermodynamic properties of the infinite diluted mixture. We compare the thermodynamics properties with those of pure carbon dioxide at chapter eight.

Finally, in chapter ten, we summarize conclusions of previous chapters. We outline a theory explaining the supercritical nature of solution. We also discuss future research opportunities.

Part I .Theory

2 EFFECT OF PRESSURE ON REACTIONS

This section gives a detailed introduction to transition state theory and pressure effects on chemical reactions. These concepts and tools are used frequently in supercritical fluids reactions studies.

2.1 INTRODUCTION

The main advantage in application of high pressure to gas phase reactions is seen by the increase of concentrations of the reactants due to compression. Thus, the reaction rates increase as well as the equilibrium conversions, since pressure affects directly the equilibrium (Gao *et al.*, 2003; Peck *et al.*, 1989). With knowledge of the P, V, T-behaviour of the system one can calculate this pressure effect, which is defined as '***thermodynamic pressure effect'***. On the other hand, it is less known that the rate constant coefficient of a reaction also depends on pressure. This pressure effect is called '***kinetic pressure effect***' (Brennecke and Chateauneuf, 1999; Viana and Reis, 1996).

However, the kinetic approach to elucidate the mechanism of a chemical reaction involves the measurement of reaction rates and rate constants as a function of many chemical and physical variables. Much emphasis is usually placed on the activation parameters obtained from the temperature dependence of the reaction. The accuracy of the suggested reaction mechanism is likely to increase with increasing number of variables covered during such investigations (Tiltscher and Hofmann, 1987). This is one of the reasons why pressure has been included as a kinetic (or thermodynamic) variable in an increasing number of studies over the past decades (Jenner, 2002; Tiltscher and Hofmann, 1987). Such additional information may assist not only in the elucidation of the intrinsic reaction mechanism, but it may also reveal new fundamental aspects of the studied systems, and thus add to the understanding of underlying principles of reaction kinetics. Pressure is a fundamental physical property that influences the values of different thermodynamic and kinetic parameters. In the same way as temperature dependence studies tell us something about the energetics of

the process, pressure-dependence studies reveal information on the volume profile of the process.

2.2 THEORETICAL BACKGROUND

The theories available to chemists to explain and predict the effects of pressure on reactions, whether the objective of the investigation is a synthetic one or mechanistic one, are thermodynamics and applications of thermodynamics principles within the absolute reaction rate (Atkins, 1994; Moore and Pearson, 1982). We are interested in how the effect of pressure manifests itself on the equilibrium constant K and the free Gibbs energy $\Delta G°$, for the reaction (difference between products-reactants), or upon the kinetic constant k and the free Gibbs energy of activation $\Delta G^{\#}$ (difference between transition state-reactants). If the effect of pressure is to increase the magnitude of K or reduce $\Delta G^{\#}$, the reaction will have a greater yield or a faster reaction rate respectively. Qualitatively it can be said that these effects can arise from the differing pressure effects on the chemical potentials of the reactants and products (equilibrium), or reactants and transition-state (kinetics). The approach favoured by many is one of considering the volume per mol of initial state, the transition-state and when appropriate, the product state. A reaction in which the transition-state has a smaller volume than the initial state is accelerated by application of pressure. Further, if the product has a different volume from the initial state, pressure will induce a change in product yield.

To be more rigorous we must first remember that the volume of a chemical species in a solution is invariably different from that from the pure substance, where the volume per mole can readily be established from the density. The quantity we are interested in is the **partial molar volume**, which may be thought of as the effective volume per mole of a species when its intrinsic volume is modified by the influence

of solvation (McQuarrie and Simon, 1999). It is represented by $\overline{V}$ for a mole substance in the literature but is also written, as $V_{A,\,m}$ for the partial molar volume of A.

$$\overline{V}_A = V_{A,m} = \left(\frac{\partial V}{\partial n_A} \right)_{pT,m_B} \tag{2.1}$$

where the partial derivative signifies the change of volume when the amount of substance A is increased in a binary system (A and B present) and this change is considered at constant temperature, pressure and amount of B.

Chemical reactions under supercritical conditions usually require relatively high pressures due to the nature of the supercritical state and the kind of fluids commonly used (Tucker and Maddox, 1998). Consequently, pressure effects on chemical equilibrium and chemical reaction rates have to be accounted for (Asano and Lenoble, 1978; Drljaca *et al.*, 1998; Vaneldik *et al.*, 1989; Vaneldik and Klärner, 2002).

The effect of pressure on the mole fraction-based equilibrium constant K_x of a chemical reaction depends on the reaction volume ΔV_r of a reaction, i.e. the difference between the partial molar volumes of the product(s) and those of the reactant(s) (Baiker, 1999)

$$\left(\frac{\partial \ln K_X}{\partial P} \right)_{T,x} = -\frac{\Delta V_r}{RT} \tag{2.2}$$

The effect of pressure on kinetics is mostly described in the context of transition state theory and a supposed reaction pathway. According to this theory, the mole fraction based rate equilibrium constant k_x of an elementary reaction depends on the activation volume $\Delta V^{\#}$, i.e. the difference between the partial molar volume of the activated complex and the sum of those of the reactant(s)(Baiker, 1999)

$$\left(\frac{\partial \ln k_X}{\partial P}\right)_{T,x} = -\frac{\Delta V^{\#}}{RT} \tag{2.3}$$

It is worth repeating again that k_X or K_X is the constant expressed in mole fraction units, T and P are the system absolute temperature and pressure, R is the universal gas constant and x is the concentration in mole fractions units. The following formula[•] is used to convert between conventional concentration (mol/L) units k_C or K_C and mole fraction concentration units k_X or K_X

$$k_X = \frac{k_C}{(\rho / M_W)^{(1-\alpha-\beta-\ldots)}} \tag{2.4}$$

where ρ is the mixture fluid density (expressed as g L^{-1}) at the temperature and pressure of the kinetic measurement and M_W is the average molecular weight of all the species in the mixture. In that case

$$\begin{aligned} &\left(\frac{\partial \ln k_X}{\partial P}\right)_{T,x} = -\frac{\Delta V^{\#}}{RT} \Rightarrow \\ &-\frac{\Delta V^{\#}}{RT} = \left(\frac{\partial \ln(k_C(\rho / M_W)^{(1-\alpha-\beta-\ldots)})}{\partial P}\right)_{T,x} \Rightarrow \\ &-\frac{\Delta V^{\#}}{RT} = \left(\frac{\partial \ln k_C}{\partial P}\right)_{T,C} + \kappa_T(1-\alpha-\beta-\ldots) \end{aligned} \tag{2.5}$$

the pressure effect on the rate constant is a function of isothermal compressibility. As we mentioned before the pressure of a gas phase reaction has a direct effect on the rate of the reaction simply as the concentrations of the species are directly proportional to the pressure (‘***thermodynamic pressure effect’)***(Tiltscher and Hofmann, 1987). For a reaction in solution, altering the pressure on the solvent does

---

• For a general reaction **αA + βB ... ⟶ Product**

not affect the concentration yet it is found that at high pressures reaction rates are affected (‘***kinetic pressure effect***’)(Brennecke and Chateauneuf, 1999). The change in the rate is attributed to a change in the rate constant as a result change in pressure. Although pressure is inevitably the experimental controlled variable, sometimes the analysis of rate data can be facilitated by examining how the rate constant varies with the solvent density in that case

$$\left(\frac{\partial \ln k_C}{\partial P}\right)_{T,C} = \left(\frac{\partial \ln k_C}{\partial \rho}\right)_{T,C}\left(\frac{\partial \rho}{\partial P}\right)_{T,C} = \frac{\kappa_T}{V}\left(\frac{\partial \ln k_C}{\partial \rho}\right)_{T,C} \tag{2.6}$$

where V is the molar volume.

2.3 HISTORICAL DEVELOPMENTS AND MODERN KINETICS

The transition state (**TS**) is the critical configuration of a reaction system situated at the highest point of the most favourable reaction path on the potential energy surface. It is regarded as critical in the sense that if it is attained the system will have a high probability of continuing reaction to completion. The concept of the transition state was first broached by M.Polanyi and M.G.Evans (Evans and Polanyi, 1935) and by H.Eyring (Eyring, 1935), both in 1935. Since that time, numerous pieces of work on chemical kinetics and dynamics, both experimental and theoretical, have been published in implicit or explicit reference to the concept. The theory of absolute reaction rates gained popularity under the name ‘transition-state theory’. Admittedly, however the theory has never been considered to be complete. A major reason for this is that little reliance could be place on the methods used to guess the characteristic properties (i.e. geometry, vibrational frequencies and activation energy) of the TS. Transition-state theory (**TST**) is a convenient and powerful formalism for explaining and interpreting the kinetics of elementary reactions. This theory views a chemical

reaction as occurring via a transition-state species (in many presentations the term ‘transition state’ is used synonymously with activated complex). It is better to be avoided, however, because firstly the word ‘complex’ implies an entity, which has a chemically significant lifetime, which the transition state does not, and secondly, the collision complex, which may be formed when two molecules collide, is often called an activated complex. The chemical reaction rate is evaluated by statistical-mechanical methods.

The earliest work on reaction rate theory came from Arrhenius (Arrhenius, 1889). Arrhenius was interested in why activation barriers arose in chemical reactions. He considered a simple reaction:

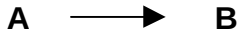

and proposed that if one looked at a chemical system containing A and B, there were two kinds of A molecules in the system: reactive molecules (i.e., A molecules that had the right properties to react), and unreactive A molecules (i.e. A molecules did not have the right properties to react).At the time the work was done, there were many empirical rules to predict how rates vary with temperature. Arrhenius was the first person to derive a theoretical expression. When the expression was found to fit data, Arrhenius’ expression, which was renamed Arrhenius’ law, was universally adopted in kinetics.

$$k = k_o e^{-(E_\alpha / k_B T)} \tag{2.7}$$

Arrhenius was never able to provide a model for k_o in the above expression. Fortunately, Trauntz (Trautz, 1918) and Lewis (Lewis, 1918) independently proposed the collision theory of reactions. The objective of collision theory is to use knowledge of molecular collisions to predict the pre-exponential k_o. Trautz and Lewis proposed a

model to do just that. The model builds on Arrhenius' concept that only "hot" molecules can react (Moore and Pearson, 1982). The model assumes that the rate of reaction is equal to the rate of collisions of molecules. The main weakness of the Trautz-Lewis version of collision theory is that it ignores the fact that one needs a special geometry in order for a reaction to occur. Given this weakness the Trautz-Lewis model, it does not always give a good prediction of the rate. Another weakness of the model is that it does not explain activation barriers. Neither Arrhenius, nor Trautz, nor Lewis was able to explain why reactants needed to be "hot" in order for reaction to occur. Trautz and Lewis just assumed - without explaining this assumption - that reactions had barriers. It was transition state theory that came later to cover this gap.

2.4 BASIC TRANSITION-STATE THEORY

2.4.1 The concept of transition-state theory

The original transition-state theory developed by Eyring as the principal contributor is based on two fundamentals postulates. One *first* assumption the existence of a molecular aggregate called the 'activated complex' $T^{\#}$, which may have a geometry corresponding to that of the transition state. *Second,* the hypothetical complex $T^{\#}$ is assumed to be in quasi-equilibrium with the initial state during the entire course of a reaction. A substitution reaction, for example, can be understood by a scheme as follows:

$$A + BC \rightleftharpoons T^{\#} \longrightarrow AB + C$$

The activated complex was regarded as being 'similar to an ordinary molecule, possessing all the usual thermodynamic properties, with the exception that the motion in one direction, i.e., along the reaction coordinate, would lead to decomposition at a

finite rate (Moore and Pearson, 1982). The transition-state theory is based on the application of statistical mechanics to both reactants and activated complexes.

2.4.2 Transition-state theory and potential energy

In the process of reaction, the reacting molecules come sufficiently close together so the interactions are set up between the atoms involved. The reacting molecules and products are described in terms of all atoms in a single unit made up of all the reacting species and products. For example the reaction

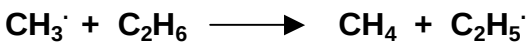

$$CH_3^{\cdot} + C_2H_6 \longrightarrow CH_4 + C_2H_5^{\cdot}$$

is described in terms of the unit

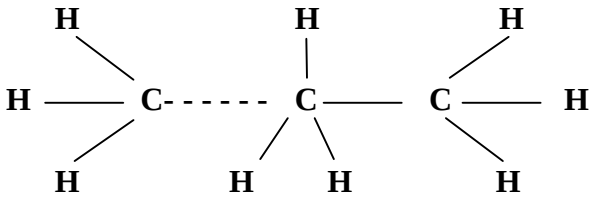

Reaction unit

rather than in terms of as the independent species

$CH_3^{\cdot}$, C_2H_6 , CH_4 , $C_2H_5^{\cdot}$

When the configuration changes the potential energy (**P.E.**) of the reaction also changes. The potential energy surface summarises these changes. A description of what happens during the reaction rests on knowledge of the potential energy surface, as the actual derivation of the theory.

The potential energy surface and its properties can be given for a reaction expressed by a general form

$$\alpha A + \beta B \ldots \rightleftharpoons T^{\#} \longrightarrow \text{Product}$$

Where A, B…are polyatomic molecules. This would give an n-dimensional surface. Fortunately, all the properties of an n-dimensional surface, relevant to kinetics, can be

exemplified by a three dimensional surface which much easier to visualize and to describe. A three dimensional surface describes the reaction

$$A + BC \rightleftharpoons T^{\#} \longrightarrow AB + C$$

where A,B and C are atoms and a linear approach of A to BC and recession of C is assumed, implying a linear configuration for the 'reaction unit'

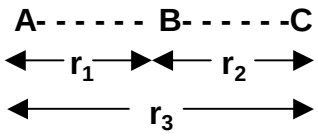

in which all configurations can be described by the distances $r_1$and r_2, with $r_3=r_1+r_2$

There is no interaction between A and B or between A and C when A is at large distances from BC, and so the potential energy is simply that of BC at its equilibrium internuclear distance. When the distance between A and BC decreases an attractive interaction is set up, and this interaction is different at different distances. A quantum mechanical calculation (Martin and Martin J.Field, 2000) gives the potential energy increases as the distance apart, and shows that the potential energy increases at the distance r_1 decreases.

Eventually the interactions between A and B become comparable to those between B and C, and this corresponds to configurations where r_1 and r_2 are comparable. The potential energy for these configurations can be calculated.

Finally, the interactions between A and B become greater than those between B and C. The configurations reached as C recedes from AB and r_2 becomes greater than r_1 result in progressively decreasing potential energies. When C is at very large distances from AB the potential energy of interaction C and AB is zero, and the potential energy becomes virtually that for AB at its equilibrium internuclear distance.

These configurational changes take place at constant total energy so that there is an interconversion of kinetic and potential energy resulting from the changes in configuration.

The calculations involved can be summarised in the form of a table such as:

r_1	r_2	P.E
.	.	.
.	.	.

The potential energy surface considered in this section are based on the Born-Oppenheimer separation of nuclear and electronic motion (Born and Oppenheimer, 1927; Hirst, 1985). For a non-linear molecule, consisting of N atoms, the potential energy surface depends on 3N-6 independent coordinates (Martin and Martin J.Field, 2000), and depicts how the potential energy changes as relative coordinates of the atomic nuclei involved in the chemical reaction are varied. An analytic function, which represents a potential energy surface, is called potential energy function. Understanding the relationship between properties of the potential energy surface and the behaviour of the chemical reaction is a central issue in chemical kinetics.

Let us go back to considering the simplest possible reaction, that of an atom, A, reacting with a diatomic, BC. Then only two distances, r_{AB} and r_{BC} are needed to specify completely the arrangement of the atoms and so the P.E. surface is just a function of two variables, and we have a chance of being able to visualize it. In Figure 2-1, the reactants, A+BC, are found in the upper left part of the surface (r_{AB} large, $r_{BC} \approx$ equilibrium separation). The products, AB+C, are found in the lower right part of the diagram (r_{BC} large, $r_{AC} \approx$ equilibrium separation). The form of the surface is two valleys meeting at right angles, one starting at the products and one at the reactants. As we ‘walk’ up the valley away from the reactants the valley floor rises up; the same thing happens as we ‘walk’ away from the products.

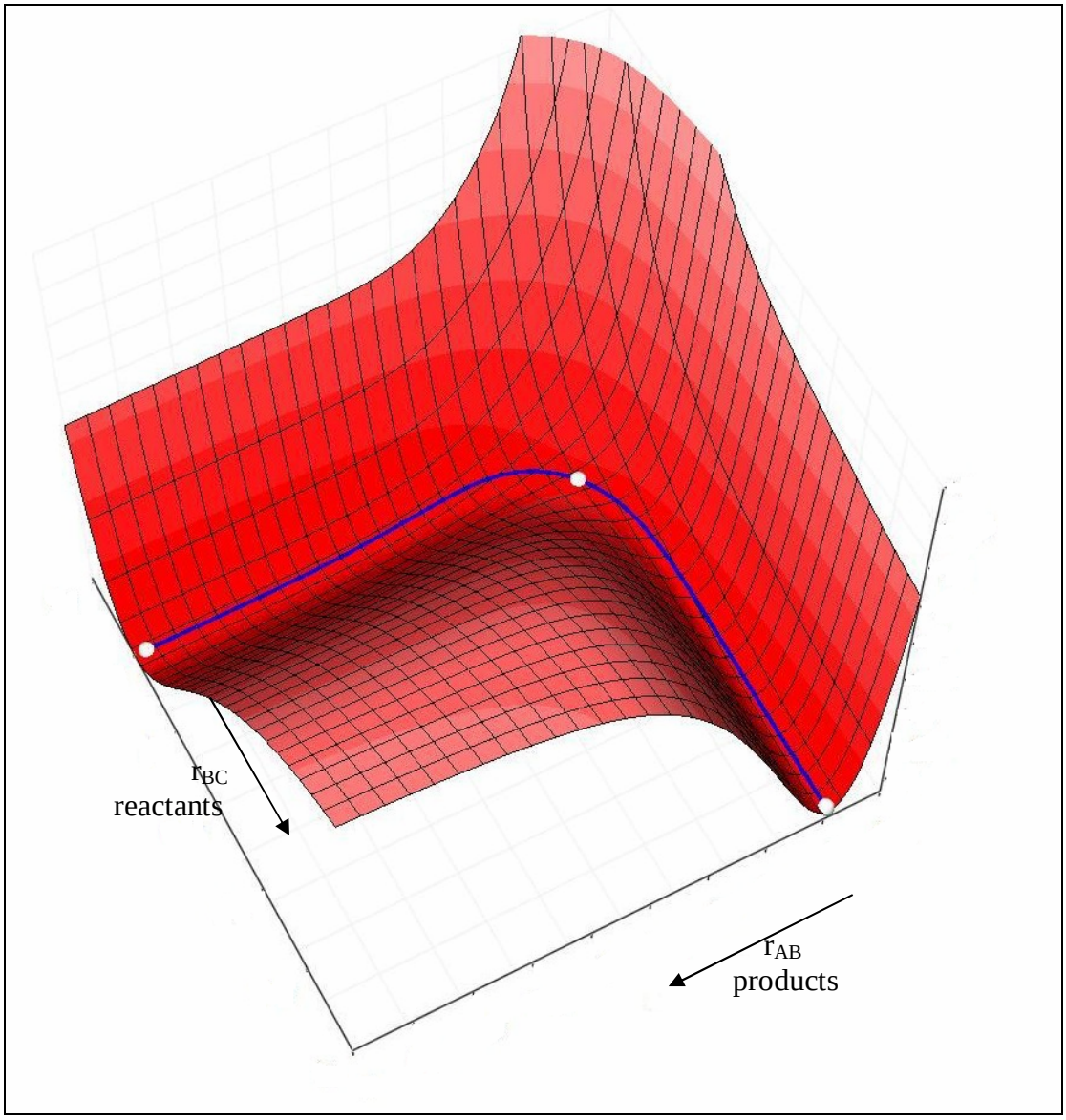

Figure 2-1: Perspective view of the PE surface for the A+BC→AB+C reaction. The arrangement consisting of the separated atoms is the corner coming towards us, while that corresponding to the atoms being compressed together is at rear. Note how the cross-sections at large r_{AB} and r_{BC} are identical to the usual PE curves for diatomics. Modified figure from Hirst work (Hirst, 1985).

There are many path ways of going from reactants to products to produce on the P.E. surface. The transition state path is a special one. It involves going up the floor of the reactant valley, crossing over the pass at its lowest point and then exiting along the floor of the product valley. It is the same path that involves the least expenditure of energy and, we shall see, this is the pathway which the reaction takes. The point of highest energy on this pathway is called the transition state; it

corresponds to a molecule in which the A-B bond is partly made and the B-C bond is partly broken.

2.5 THERMODYNAMIC FORMULATION

Transition-state theory rate constant

Thermodynamics applied to chemical reactions yields useful thermodynamics quantities such as ΔG (change in Gibbs free energy of the chemical system), ΔH (change in enthalpy or heat of the reaction) and ΔS (change in entropy). These quantities refer to the starting and ending states of the system. A general reaction is represented by the form

$$\alpha A + \beta B \ldots \rightleftharpoons T^{\#} \longrightarrow \text{Product}$$

The transition state is in equilibrium with the reactants, and the rate of the reaction is the rate of the product formation from the transition state, given by

$$r = \frac{dC_p}{dt} = -\frac{1}{a}\frac{dC_A}{dt} = \kappa \frac{k_B T}{h} C_T^{\neq} = \kappa \frac{k_B T}{h} K_C C_A{}^{a} C_B{}^{\beta} \ldots$$

So the rate constant (concentration based) can be expressed as

$$k_c{}^{TST} = \kappa \frac{k_B T}{h} K_C^{\neq} \tag{2.8}$$

where κ is the transmission coefficient ($0 \leq \kappa \leq 1$ and always positive (Asano and Lenoble, 1978)), k_B is Boltzmann's constant ($1.381 * 10^{-23}$ J K^{-1}) , T is absolute temperature, h is Planck's constant ($6.626 * 10^{-34}$ J s), and $K_C^{\neq}$ is the concentration-based equilibrium constant for the reaction involving the reactants and the transition state. Equation (2.8) uses the concentration-based equilibrium constant, which combines all chemical and physical effects between the reaction species and the solvent. As already stated above, one of the most important things is to locate the transition state along the reaction coordinate, which corresponds to maximum energy

along the reaction coordinate. The energy required to overcome the barrier (corresponding to the transition state) is the activation energy $\Delta G^{\#}$.

The activation energy is connected to the equilibrium constant though the expression

$$RT \ln K_c^{\neq} = -\Delta G^{\neq} \tag{2.9}$$

The activation Gibbs free energy change can be written in terms of enthalpy (or internal energy) change and entropy change

$$\Delta G^{\#} = \Delta E^{\#} + P\Delta V^{\#} - T\Delta S^{\#} \text{ or } \Delta G^{\#} = \Delta H^{\#} - T\Delta S^{\#}$$

Since $(\partial G^{\#} / \partial P)_T = -V$ we have

$$\Delta V^{\#} = RT\left(\frac{\partial \ln k_X}{\partial P}\right)_{T,x} = \left(\frac{\partial \ln k_C}{\partial P}\right)_{T,C} + \kappa_T(1-\alpha-\beta-...) \tag{2.10}$$

Gas-phase reaction

When a chemical reaction takes place in the gas phase and considered ideal, the free energy barrier is completely determined by the interactions among the reactants. In that case, there is no pressure dependence on kinetic constant and always the activation volume value is zero in equation 2.10

Reaction in Solution

When a reaction takes place in solution, however, the forces exerted by the solvent molecules also influenced the free energy barrier. For reactions in solution, it is usually assumed that the solute follows the same reaction path as it would if the same reaction were to occur in the gas phase, and that the transition state is taken to be located at some point along this path, most frequently at the free energy maximum. Additionally, the solute reaction path is nearly always identified as the reactive degree of freedom (Tucker and Truhlar, 1990) and then κ_{TST} is taken to be one. Note that this set of assumptions, known as the equilibrium solvation approximation, is equivalent to assuming that the solvent rapidly readjusts in response to changes in the solute,

such that at all times during the course of the reaction the solvent remains in equilibrium with the reacting solute (Voth and Hochstrasser, 1996). Within this approximation, the activation energy $\Delta G^{\neq}$ can be written as

$$\Delta G^{\#} = (U^{\#} + \Delta G^{\#}_{solv}) - (U^{R} + \Delta G^{R}_{solv})$$

where the free energy at each location along the solute reaction path is given by the sum of the potential energy, U, of the isolated solute at this location plus the equilibrium solvation free energy of the solute at this location ΔG_{solv}. The equilibrium solvation free energy depends on the pressure and for reaction in solution $\Delta V^{\neq}$ is usually different from zero. Accurate measurements of the kinetic constant k at different pressures (generally in the pressure range 0-150 MPa) lead to a curve $k = f(P)$ whose slope gives $\Delta V^{\neq}$. Viana made a literature review for the common used mathematical approximations for $k = f(P)$ (Viana and Reis, 1996). The conventional interpretation of the activation volume $\Delta V^{\#}$ is that it is an intrinsic solute property (or solute plus local solvent property for solution phase reactions), which represents the difference in the effective volumes of the transition state and reactant complexes, like the Figure 2-2.

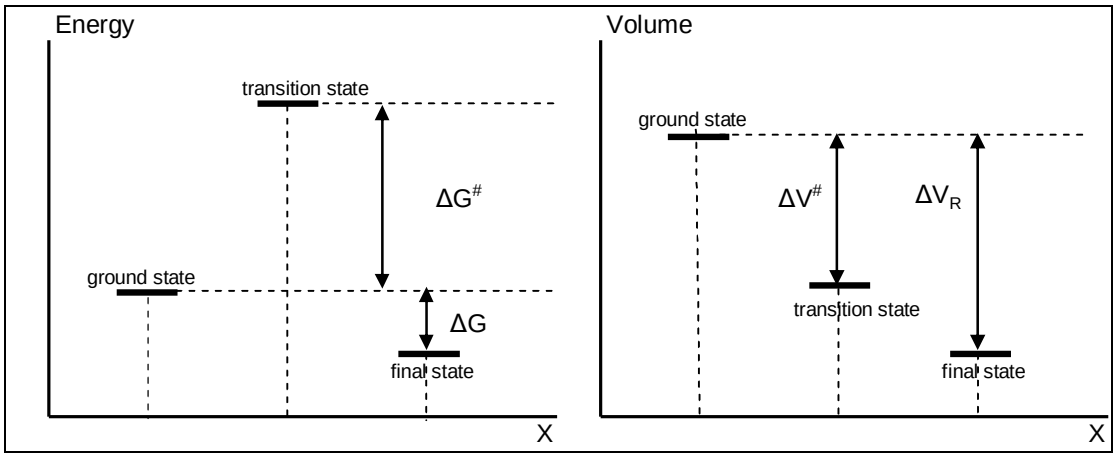

Figure 2-2: Energy and volume profile of a general reaction

To see the relationship between $\Delta V^{\#}$ and pressure, consider the case where the transition state volume is smaller than that of the reactants $V^{\#}$. In this case an increase in pressure would shift the assumed equilibrium between the transition state and reactants toward the transition state, increasing the rate as given by equation (2.10) when $\Delta V^{\#} < 0$. Although there is in principle nothing wrong with the activation volume approach, application of its traditional interpretation to the pressure dependence of reaction rates to SCFs can be misleading and our discussion of these effects is better to be given in terms of the pressure dependence of the activation barriers, $\Delta G^{\#}(P)$.

The problem arises, as we can see from Figure 2-3, the traditional interpretation of the activation neglects the fact that other solvent properties, such as the dielectric constant, can be extremely pressure sensitive in compressible SCFs.

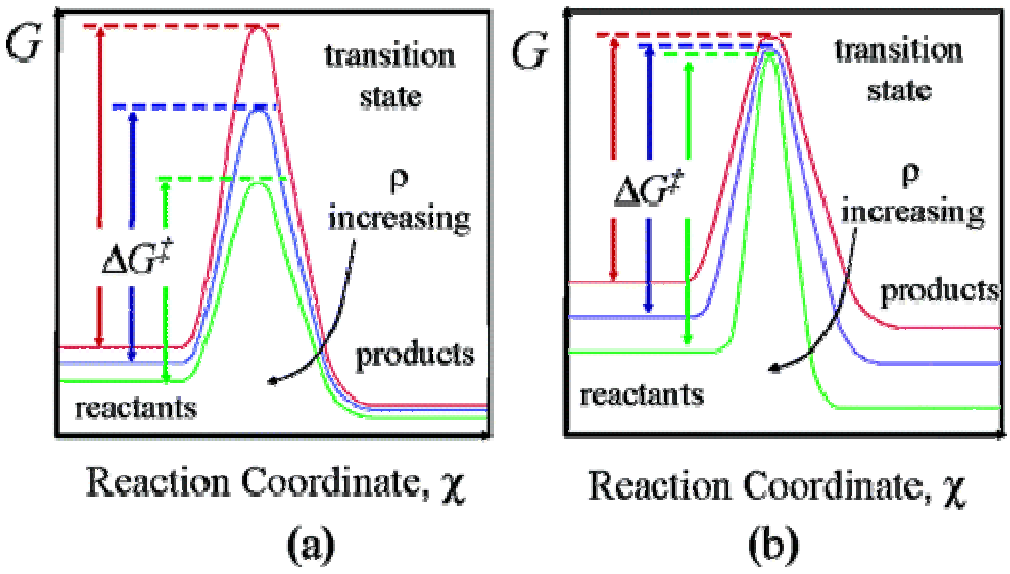

Figure 2-3: Free energy sketches for reaction coordinates representing two different responses to density.(a) preferential solvation of the transition state as density increases, leading to a net decrease in $\Delta G^{\#}$ with increasing density. In (b) the reactants and products are preferentially solvated by increased density. Modified figure from Levert Sengers' book (Levert Sengers, 1998).

When these properties affect the solvation of the transition state and reactants differently, the activation energy will vary rapidly with pressure, causing large changes in the reaction rate, which are not representative of an actual volume effect.

Combining equations (2.8) and (2.9), the reaction rate is related to $\Delta G^{\neq}$ by the equation:

$$k_c^{TST} = \kappa \frac{k_B T}{h} \exp\left(-\frac{\Delta G^{\#}}{RT}\right) \tag{2.11}$$

Equation (2.11) predicts that a decrease in $\Delta G^{\neq}$ leads to an increase in k_c^{TST}
Now, the equilibrium constant accessible from classical thermodynamics•, $K_\alpha^{\#}$ is related to $K_c^{\#}$ as.

$$K_c^{\#} = \frac{K_\alpha^{\#}}{K_\gamma^{\#}} \rho^{(1-\alpha-\beta-\ldots)} \tag{2.12}$$

where $K_a^{\#} = \prod a_i^{\nu_i}$, $K_\gamma^{\#} = \prod \gamma_i^{\nu_i}$,α_i, γ_i and ν_i are activity, the activity coefficient and stoichiometric coefficient (e.g., α, β...), respectively, for component i, and ρ is the molar density of the reacting mixture. We can then write the transition state theory as

$$k_c^{TST} = \kappa \frac{k_B T}{h} \frac{K_\alpha^{\neq}}{K_\gamma^{\neq}} \rho^{(1-\alpha-\beta-\ldots)} \tag{2.13}$$

or as

$$k_x = \frac{k_c^{TST}}{\rho^{(1-\alpha-\beta-\ldots)}} = \kappa \frac{k_B T}{h} \frac{K_\alpha^{\#}}{K_\gamma^{\#}} \tag{2.14}$$

if the concentration - independent units (e.g., mole fraction) are desired for the rate constant. One could also develop an alternative expression for the transition state theory constant that employs fugacity coefficients rather than activity coefficients (Clifford, 1999). This alternative form of the rate constant is convenient to use when an accurate analytical equation of state is available for the fluid phase. The rate constant in equation (2.14) can be written as

---

• from the relationship $\alpha_i = x_i \gamma_i = \frac{C_i \gamma_i}{\rho}$

$$k_x = \frac{k_c^{TST}}{\rho^{(1-\alpha-\beta-\ldots)}} = \kappa \frac{k_B T}{h} \mathrm{K}_x^{\#} \qquad (2.15)$$

3 MOLECULAR SIMULATION

The two sets of methods for computer simulations of molecular fluids are : **Monte Carlo** and **molecular dynamics**. In both cases the simulations are performed on a relatively small number of particles (atoms, ions, and/or molecules) of the order of $100 < N < 10{,}000$ confined in a periodic box, or simulation supercell. The interparticle interactions are represented by pair potentials, and it is generally assumed that the total potential energy of the system can be described as a sum of these pair interactions. Very large numbers of particle configurations are generated on a computer in both methods, and, with the help of statistical mechanics, many useful thermodynamic and structural properties of the fluid (pressure, temperature, internal energy, heat capacity, radial distribution functions, etc.) can then be directly calculated from this microscopic information about instantaneous atomic positions and velocities.

Before embarking on a description of the molecular modelling techniques, we should first briefly explain the role of computer simulations in general. **What is exactly molecular simulation?** Molecular simulation is a computational 'experiment' conducted on a molecular model. The Molecular model is built on the given sufficient knowledge about the intermolecular interactions. Clearly, it would be very nice if we could obtain essentially exact results for a given model system, without having to rely on approximate theories. However, we can compare the calculated properties of a model system with those of an experimental system: if the two disagree, our model is inadequate, i.e. we have to improve on our estimate of the intermolecular interactions. Rephrasing, the validity of any simulation will rest on the suitability and accuracy of the equations/parameters used for the intermolecular potentials. Molecular mechanics

deals with that subject and many forms have been developed for describing the interparticle potentials known as force fields.

3.1 MOLECULAR MECHANICS

The goal of molecular mechanics is to predict the detailed structure and physical properties of molecules. Examples of physical properties that can be calculated include enthalpies of formation, entropies, dipole moments, and strain energies. Molecular mechanics calculates the energy of a molecule and then the bond lengths and angles are adjusted to obtain the minimum energy structure.

3.1.1 Interparticle Interactions

The most fundamental approach is to attempt to calculate the interparticle interactions from first principles by solving the electronic Schrödinger equation

$$H\Psi = E\Psi \tag{3.1}$$

for the electronic energy at each nuclear configuration. Many methods for doing this are available but three of the more commonly used types are passed upon ***density functional theory, molecular orbital theory*** **and** ***valence bond theory***. The last two are first principles or **ab initio methods** in the sense that they attempt to solve the Schrödinger equation with as few assumptions as possible. Although these methods can give very accurate results in many circumstances, they are expensive and hence cheaper alternatives have been developed.

One way of making progress is to drop the restriction of performing first-principles calculations and seek ways of simplifying the *ab initio* methods outlined above. These so called *semi-empirical* methods have the same overall formalism as that of the *ab initio* but they approximate various time-consuming parts of the calculation with simpler approaches. Of course, because approximations have been introduced, the methods must be calibrated to ensure that the results they produce are meaningful. This often means that the values of various empirical parameters in the

methods have to be chosen so that the results of the calculations agree with the results of accurate ab initio quantum mechanical calculations. Semi-emperical versions of all the ab initio methods mentioned above exist.

A second and even cheaper approach is to employ an entirely empirical potential energy function. This consists of choosing an analytic form for the function, which is to represent the potential energy surface for the system and then parametrizing the function so that the energies that it produces agree with experimental data or with the results of accurate ab initio quantum mechanical calculations.

3.1.2 Force Fields

Simulation methods that make use of force fields, parameterised on the basis of quantum mechanical calculations and / or experimental measurements, offer an immediate and practical alternative for the prediction of the properties of molecular fluids. The quality of a given force field model depends on its simplicity and transferability beyond the set of conditions that were used for the parameterisation. Transferability may imply that the force field parameters for a given interaction site can be used in different molecules (e.g. the parameters used to describe a methyl group should be applicable in many organic molecules) or that the force field is transferable to different state points (e.g. pressure, temperature or composition) and to different properties (e.g. thermodynamic, structural or transport). In general, for pure components, the transferability of force fields to different state points is tested against vapour-liquid equilibrium (VLE), heats of vaporization, second virial coefficients (McQuarrie and Simon, 1999) and the prediction of mixture properties. Generally, simulations of molecules and molecular mixtures in a continuum use either united atom (**UA**) models or atomistic (**AA**) models (Jorgensen *et al.*, 1996; Jorgensen *et al.*,

1983; Jorgensen *et al.*, 1984). In the united atom approximation, a molecule or a group of atoms is treated as a single unit, represented by a Van der Waals sphere with a charge point. Atomistic models represent every atom in a molecule. Each atom is usually modelled as a Van der Waals sphere with a point charge. According to Molecular mechanics, ***molecular model is the definition of how a molecule interacts with itself and other molecules***. The total potential energy is composed in two parts intramolecular energy (***how a molecule interacts with itself***) and intermolecular energy (***how a molecule interacts with other molecules.***

A molecule can possess different kinds of energy such as bond and thermal energy. Molecular mechanics calculates the internal energy of a molecule, the energy due to the geometry or conformation of a molecule. Energy is minimized in nature, and the conformation of a molecule that is favoured is the lowest energy conformation. Knowledge of the conformation of a molecule is important because the structure of a molecule often has a great effect on its reactivity. Molecular mechanics assumes the internal energy of a molecule to arise from a few, specific interactions within a molecule. These interactions include the stretching or compressing of bonds beyond their equilibrium lengths and angles, torsional effects of twisting about single bonds, the Van der Waals attractions or repulsions of atoms that come close together, and the electrostatic interactions between partial charges in a molecule due to polar bonds. To quantify the contribution of each, these interactions can be modelled by a potential function that gives the energy of the interaction as a function of distance, angle, or charge. The total internal energy of a molecule can be written as a sum of the energies of the interactions:

$$E_{intramolecular} = E_{str} + E_{bend} + E_{str\text{-}bend} + E_{oop} + E_{tor} + E_{VdW} + E_{qq} \qquad (3.2)$$

The bond stretching, bending, stretch-bend, out of plane, and torsion interactions are called bonded interactions (intramolecular) because the atoms involved must be directly bonded or bonded to a common atom. The van der Waals and electrostatic (qq) interactions are between non-bonded atoms. In addition, Waals and electrostatic (qq) interactions exist between atoms of different molecules. The energy, coming from atoms between different molecules, is called intermolecular energy. It is important to realize that the force field is not absolute, in that not all the interactions listed in Equation (3.2) may be necessary to predict accurately the energy of a system, every time we are considering the most important forces. The total energy of a molecular system is given by the sum of the intermolecular and intramolecular interactions.

$$E_{total} = E_{intramolecular} + E_{intermolecular} \tag{3.3}$$

3.2 STATISTICAL MECHANICS

3.2.1 Introduction

The central question in Statistical Mechanics can be phrased as follows: if particles (atoms, molecules, electrons…) obey certain microscopic laws with specified interparticle interactions, what are the observable properties of a macroscopic system containing a large number of such particles?

According to thermodynamics, a system containing a single pure substance at equilibrium can be completely characterized by three independent variables, say E, V, and N, where E is energy of the system, V the Volume and N represents the number of molecules, generally of the order of 10^{24}. According to classical mechanics, the dynamics of each particle is defined by its three coordinates (e.g. x, y, z) and three momenta (e.g. p_x, p_y, p_z) (Figure 3-1), so the previous system would require immensely greater detail: all the generalized coordinates q_1 (t),q_2(t)…q_n (t) and

conjugate momenta p_1 (t)…p_n (t), each a function of time, would have to be specified and n the number of atoms. The number of degrees of freedom, n, is, for an assembly of atoms, equal to 3N, for systems composed of molecules, internal degrees of freedom (rotations and vibrations) have to be included as well. Thus, even the simplest thermodynamic system corresponds to a mechanical system of immense complexity. Presenting a diatomic molecule in gas phase, we need a trajectory of momenta values (p_1, p_2) and a trajectory with positions (q_1, q_2). For recording the p and q we need to record three coordinates in space x, y and z, like Figure 3-1.

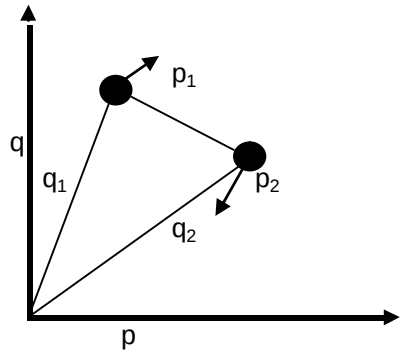

Figure 3-1: A diatomic molecule in phase space. The position and motion of the particle are presented by a point with coordinates (q_{1x}, q_{1y}, q_{1z}, q_{2x}, q_{2y}, q_{2z}, p_{1x}, p_{1y}, p_{1z}, p_{2x}, p_{2y}, p_{2z}) in a 2-dimensional phase space.

A quasi-geometric representation of the dynamical state of a mechanical system, known as phase space specified by the vector x={q, p}, has proved to be invaluable in classical statistical mechanics. The phase space for a system having n degrees of freedom is the composite of the n-dimensional configuration space and the n-dimensional momentum space. A point in its 2n-dimensional phase space represents the instanteous state of the system. The representative point traces out a trajectory in the hypothetical space as the system changes with time in accordance with the laws of mechanics. Given the point in phase space representing the state of the system at time t, the future (as well as the past) trajectory is, in principle, completely and uniquely determined. Only in the case n=1, a system having but one degree of freedom, can the

phase space be explicitly diagrammed as in Figure 3-2. The trajectory in two-dimensional phase space, representing the time development of the system, corresponds to the set of parametric equations.

$$q=q(t),\ p=p(t).$$

For a linear harmonic oscillator with constant energy ε the phase-space trajectory corresponds to an ellipse in the p-q plan (Blinder, 1969)

$$\frac{p^2}{2m}+\frac{kq^2}{2}=\varepsilon$$

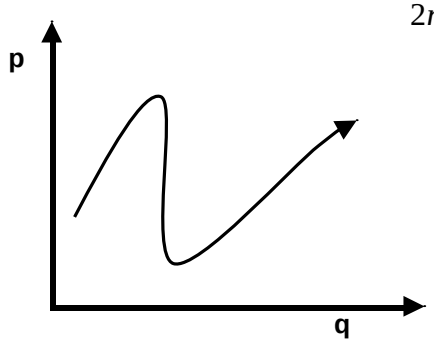

Figure 3-2: Trajectory in two-dimensional phase space

The analogous representation of more complex system mechanical systems, even with $n\sim10^{24}$, introduces no additional conceptual difficulties, notwithstanding the multidimensionality of the corresponding phase space. The trajectory is, in the general case, determined by the 2n equations

$$q_i=q_i(t),\ p_i=p_i(t)\ i=1\ldots n.$$

These are, in turn, determined by classical Hamiltonian's equations of motion

$$\dot{q}_i=\frac{\partial H}{\partial p_i},\ \dot{p}_i=-\frac{\partial H}{\partial q_i}\quad i=1\ldots n$$

in conjugation with 2n initial values $q_i(0)$, $p_i(0)$. The Hamiltonian function $\mathbf{H}(q_1\ldots q_n,p_1\ldots p_n)$ for a multidimensional system will be for convenience, abbreviated $\mathbf{H}(p,q)$ and dot denotes the time derivative. It expresses the total energy of an isolated system as a function of the coordinates and momenta of the constituent

particles. This is essentially equivalent to the system's total energy, kinetic plus potential, and can be written as

$$\mathbf{H}(\mathbf{p}_i, \mathbf{r}_i) = \sum_{i=1}^{N} \frac{1}{2m_i} \mathbf{p}_i^{\,2} + V(\mathbf{r}_i) = K + U = E \tag{3.4}$$

Note that the Hamiltonian is a function of 6N independent variables, the 3N particle momenta and the 3N particle positions. Integration of these equations of motion yields the trajectory

$$x_t = x_t(x_0) \tag{3.5}$$

where x_0 specifies the state of the system at time t=0. Since the laws of classical mechanics are deterministic, the subsequent trajectory from a given point is uniquely determined. Therefore, a trajectory in phase space cannot intersect itself.

3.2.2 The concept of the ensemble

The variables N, V and E are sufficient to specify a thermodynamic system macroscopically, but insufficient to determine the 2n-time dependent variables in order to specify the microscopic state. Moreover, the microscopic mechanical variables can be modified continuously in such way as to leave the macroscopic state unaltered. It must exist an infinite number of microscopic states, which are compatible with the macroscopic specification of a thermodynamic system. Gibbs (McQuarrie and Simon, 1999) denoted as an 'ensemble' a sufficiently representative set of microscopic states corresponding to a specified macroscopic state. For conceptual purposes an ensemble can be defined as a very large number (sometimes taken to the infinity) of systems, each being a replica on a macroscopic scale of a given thermodynamic system.

It is useful to discuss a simple example before discuss further the concept of the ensemble. Consider using a thermocouple (i.e. a digital thermometer) to measure

the average temperature of a small beaker of water. In principle, a thermocouple can be used to measure the water temperature to arbitrary accuracy. However, when one does the measurement, one often finds that the thermocouple reading is noisy because of eddies in the beaker. In order to get very accurate readings, therefore one has to find a way to average over all the noise. One can use a simple beaker and measure the time average. However, an alternative idea is to take a large number of beakers that are identical to the first, place all of them in identical conditions put a thermocouple in each beaker, and average over the readings of all of the thermocouples as illustrated in Figure 3-3

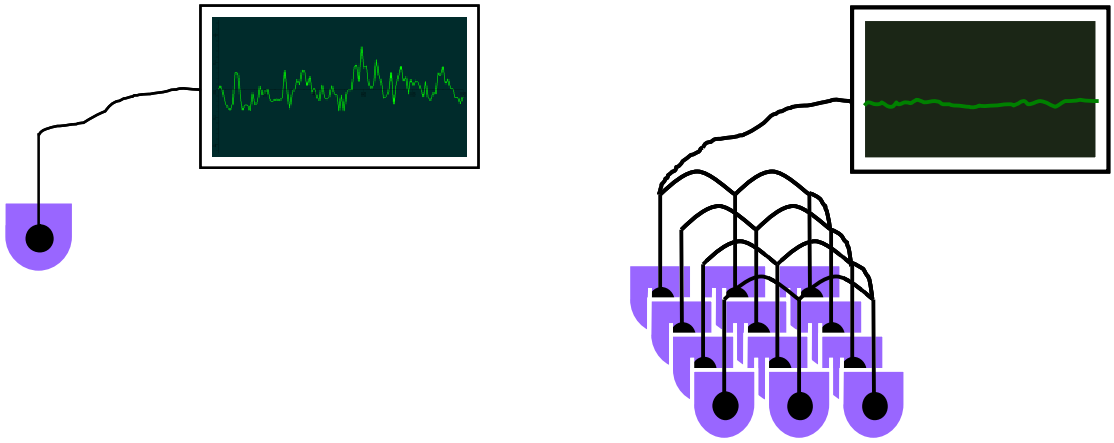

Figure 3-3: A diagram showing how the use of multiple thermocouples can be used to lower the noise in a temperature measurement

In the same way, one can calculate the thermodynamic properties of a system by a time average or by creating a series of systems that are identical to the first and then averaging over all the systems. A basic concept in this calculation is that the system samples all the macroscopic states consistent with the constraints we have imposed to control the system. We perform a multitude N of independent measurements for some property X:

$$X_{obs} = \frac{1}{N}\sum_{i=1}^{N} X_i \qquad (3.6)$$

where X_i is the value during the i-th measurement whose time duration is very short – so short, in fact, that during the i-th measurement the system can be considered to be in only one microscopic state. Then we can partition the sum as

$$X_{obs} = \sum_{\nu} \left[\frac{1}{N} (\text{Number of times state } \nu \text{ is observed in the N observations}) \right] X_{\nu}$$

where X_ν value of property X in microstate ν. The term in the squared brackets is the probability or weight for finding the system during the course of the measurements in state ν. Remember, we believe that after a long time, all states are visited (**ergodic hypothesis**). We give the probability or fraction of time spent in state ν the symbol P_ν and write

$$X_{obs} = \sum_{\nu} P_{\nu} X_{\nu} \equiv \langle X \rangle$$

The averaging operation (i.e., the weight summation over X_ν), indicated by the pointed brackets, $\langle X \rangle$, is called an ensemble average. An ensemble is the assembly of all possible microstates – all states consistent with the constraints with which we characterize the system macroscopically.

The idea that we observe the ensemble average, $\langle X \rangle$, arises from the view in which measurements are performed over a long time, and that due to the flow of the system through phase space, the time average is the same as the ensemble average[*]. The equivalence of a time average and an ensemble average, while sounding reasonable, is not at all trivial. Dynamical systems that obey this equivalence are said to be ergodic or satisfy the ergodic hypothesis. These concepts can be sum up into two postulates.

---

[*] Maxwell (1860) and Boltzmann (1872) showed that one can compute a macroscopic property of a system X as the time average and latter Gibbs (1890) showed that one could replace the time average with an ensemble 'average' of X.

Postulate 1: Ergodic Hypothesis: Given enough time, a system will sample all microstates consistent with the constraints imposed. That is, time averages are equivalent to ensemble averages. Mathematically, we have

$$\langle \mathrm{X} \rangle = \frac{\sum_i x_i \rho_i}{\sum_i \rho_i} = \lim_{x \to \infty} \frac{1}{t} \sum_i x_i \Delta t_i \tag{3.7}$$

where ρ_i is the probability density of state i.

Postulate 2: Equal a Priori Probabilities: All microstates having the same energy are equally probable. Mathematically,

$$\rho_i = \rho_i(E_i) \tag{3.8}$$

3.2.3 Ensembles

Ensembles are classified according to the constraints imposed on the corresponding thermodynamic system. The four most important types are the microcanonical ensemble NVE, the canonical ensemble NVT, isothermal-isobaric NPT and the grand canonical ensemble μVT. The microcanonical ensemble is the assembly of all states with fixed total energy E, and fixed size, usually specified by the number of molecules, N, and volume V. Such a system cannot exchange either matter or energy with its surroundings. Neither can it expand or contract in volume.

The canonical ensemble corresponds to an assembly of all microstates with fixed N and V. The energy can fluctuate; however, the system is kept at equilibrium by being in contact with a heat bath. The canonical ensemble, in which the temperature, number of molecules and volume are imposed, is used for monophasic fluids when density is known. The predicted average properties are then average energy, pressure and chemical potential.

In the isothermal-isobaric or NPT ensemble, pressure is imposed instead of volume of the system. Usually, NPT is used to predict fluid density. This ensemble is

used, for instance, when the properties of a fluid are to be determined at known pressure and temperature. The grand canonical ensemble is defined as the assembly of all states that has a fixed value of μ, V and T, where μ is the chemical potential. The grand canonical ensemble is the ensemble that is most adapted to adsorption in microporous solids, where the temperature, the volume, and the chemical of each species are the imposed variables.

The ensembles summarised in Table 3-1 occur in two broad categories. The microcanonical, canonical and isothermal–isobaric ensembles describe closed systems for which there is no change in the number of particles. In contrast, the grand canonical ensemble is an open system in which the number of particles can change.

Table 3-1: Types of Ensembles

Ensemble	Constraints
Microcanonical	N, V, E
Canonical	N, V, T
Grand Canonical	μ, V, T
Isothermal – Isobaric	N, P, T

Beside common average properties like density, pressure or energy, the analysis of their fluctuations allows to determine thermo physical properties like the heat capacity, the compressibility, the thermal expansion coefficient or the Joule-Thomson coefficient (McQuarrie and Simon, 1999).

3.2.4 Mathematical foundation

The basic idea of statistical mechanics is, therefore, that during a measurement, every microscopic state or fluctuation that is possible does in fact occur, and observed properties are actually the averages from all the microscopic states. To quantify this idea, we need to know something about the probability or distribution of the various microscopic states.

The instantaneous density of representative points can be characterized by a distribution function ρ ($q_1 \ldots q_n$, $p_1 \ldots p_n$, t) abbreviated for convenience ρ(x). To calculate thermodynamic properties• of macroscopic systems, in accordance to ergodic hypothesis, it is necessary to determine explicitly the distribution function ρ (x) for the appropriate ensemble. The distribution function is time –independent, so

$$\frac{\partial \rho}{\partial t} = 0 \tag{3.9}$$

Hence, if the probability density distribution function in a particular ensemble is ρ, the average of a property, X, can be written as an integral

$$\langle X \rangle = \int d\Gamma X(\Gamma)\rho(\Gamma) \tag{3.10}$$

where Γ are the ensemble variables, which will include the coordinates and the momenta of the particles, and $d\Gamma$ indicates the volume element for a multidimensional integration over these variables.

Practically, there are two main methods to simulate statistical ensembles. The first is though molecular dynamics, which solves the equations of motion, and the second is Monte Carlo simulation, in which a statistical method is used. Although the total energy appearing above is the sum of the kinetic energy and potential energy, only the latter needs to be provided as an explicit function of coordinates through a suitable intermolecular potential energy model for Monte Carlo simulation.

3.3 MONTE CARLO SIMULATION

3.3.1 Principles

Consider the integral I, of a function f(x) over a region [a,b]:

• The thermodynamic $\langle X \rangle = \int \ldots \int dq_1 \ldots dp_n \rho(q, p, t) X(q, p)$ properties estimating by the ensemble average as and the time average as $\overline{X}(q, p) = \frac{1}{\tau} \int_0^{\tau} dt X\left[q(t), p(t)\right]$

$$I = \int_a^b f(x)dx \tag{3.11}$$

A normal way to estimate the integral, for well-behaved functions, would be to divide the region [a, b] into n equally spaced slices, each of width Δ=(b-a)/n and then use a standard integration formula of the type

$$I \cong \Delta \sum_{i=0}^{n} w_i f(a + i\Delta) \tag{3.12}$$

where the w_i are weights whose values depend upon the formula being used. For the well-known Euler formula, these would be 1 except at the end points, where they would be ½.

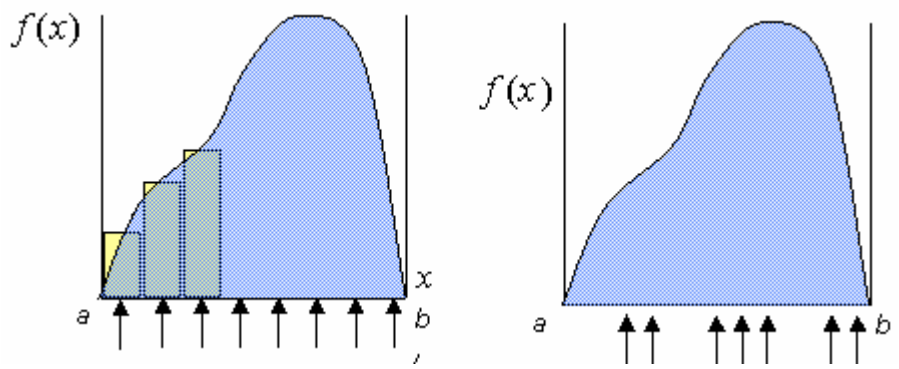

Figure 3-4: Integration sampling between a and b

The basis of the **Monte Carlo** approach is to realize that, instead of using a regular discretization of the integration variable, as in equation (3.12) , **it is possible to use a stochastic method in which the values of the integration variable are chosen at random**. Let n denote the number of trials and x_i (with i=1,…, n) the values between a and b. The integral can be evaluated as

$$I = \Delta \sum_{i=1}^{n} f(x_i) \tag{3.13}$$

where, as before Δ=(b-a)/n, but this time it represents the average distance between integration points rather than the exact distance.This formula works reasonably well

for functions whose values do not change too much from one place to another in the integration range. For a function whose values vary greatly or are peaked in certain areas, the formula will be inefficient because the values of the function at many of the randomly chosen integration points will contribute negligibly to the integral. In these cases, it is more useful to be able to choose values of x that are concentrated in areas in which the function will be significant. In any case, the problem we have to solve is **to find a manner for producing random number between [a, b]**. We have to invent a random generator.

One way to produce random number is by using roulette. In our problem for a '***well-behaved***' function we can use roulette with discrete numbers between [a, b] in order to produce L random numbers. We denote $\langle f(x) \rangle$ the unweighted average of f(x) over the integral [a, b], and it is clear, as L→∞ (many trials with the roulette!) the value (b-a) $\langle f(x) \rangle$ should yield the proper value. For 'non-well-behaved' functions, we can use a biased roulette for generating the random number.

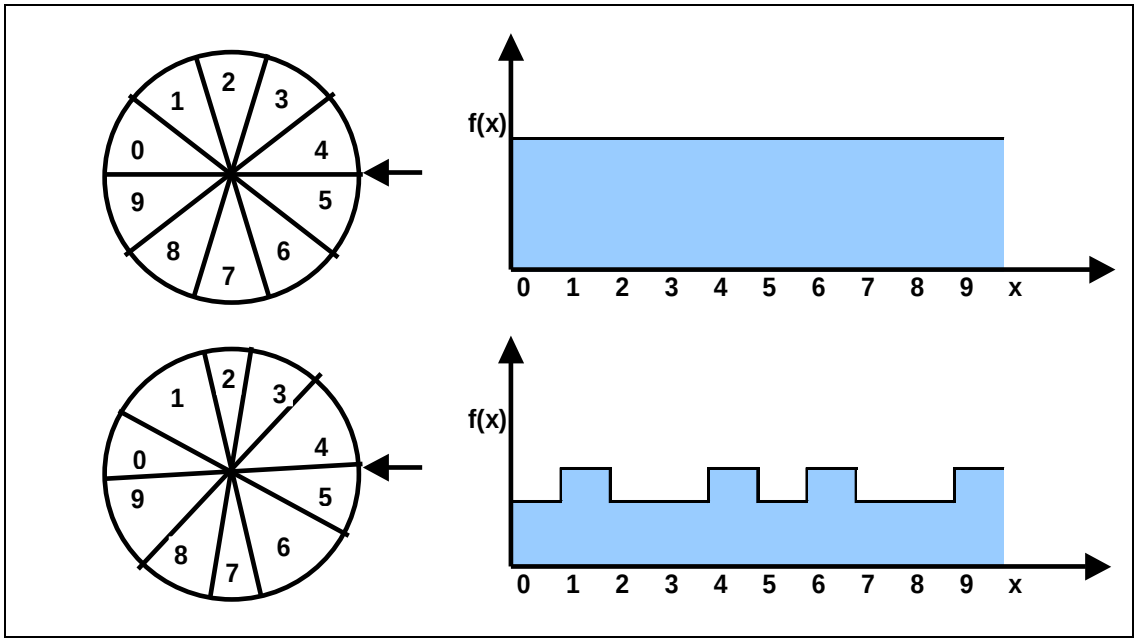

Figure 3-5: Unbiased and biased sampling for Monte Carlo integration. The biased roulette is not proportional in size, different sized portions.

However, when one wants to estimate an integral for a ‘non-well-behaved’ it does not need each time a biased roulette. To do this the integral of equation above can be written as

$$I = \int_a^b \left(\frac{f(x)}{\rho(x)} \right) \rho(x) dx \tag{3.14}$$

where ρ(x) is a probability density function that is large where it is thought that the function will be large. The integral can now be approximated by choosing values of the integration variable randomly from ρ(x) in the range [a, b], instead of from the uniform distribution, and averaging over the values of $f(x_i)/\rho(x_i)$ that are obtained

$$I \cong \frac{1}{n} \sum_{i=1}^{n} \frac{f(x_i)}{\rho(x_i)} \tag{3.15}$$

this formula is the same as equation (3.13) in the case of a uniform distribution follows because the probability distribution function for the uniform distribution is 1/(b-a). The use of a function ρ in this way to enhance sampling in certain regions is known as importance sampling. Choosing perfect weight function is same as solving integral

The stochastic method outlined above cannot usually compete with numerical methods of the type given in equation (3.12) if there is a small number of integration variables. However, the number of function evaluations required by simple discretization schemes for the estimation of an integral becomes prohibitively large as the number of dimensions, N_{dim}, increases. To see this, suppose that n points are chosen for the discretization in each direction, and then the number of function evaluations required is N_{dim}. It is in these cases that stochastic methods are often the only realistic approaches for tackling the problem.

The integrals that are of interest in thermodynamics are usually multidimensional. Usually, a property, X, of the system is a function of the 3N coordinates of the atoms (Sadus, 2007).

3.3.2 Metropolis Monte Carlo Algorithm

As we mentioned in the previous section, the integrals that are of interest in thermodynamics are usually multidimensional. As an example, consider a property, X, of the system that is a function of the 3N coordinates of the atoms **R**, only. The ensemble average of the property in the canonical ensemble is then the ratio of two multidimensional integrals:

$$\langle X \rangle = \frac{\int dRX(R)\exp\left[-U(R)/(k_B T)\right]}{\int dR\exp\left[-U(R)/k_B T\right]} \tag{3.16}$$

where U is the potential energy of the system. This equation can be written in a form reminiscent of equation (3.14) by employing the probability density distribution function for the canonical ensemble, ρ_{NVT}. Thus

$$\langle X \rangle = \int dRX(R)\rho_{NVT}(R) \tag{3.17}$$

If, somehow (and this is the difficult part!), it is possible to choose configurations for the system drawn from the function, ρ_{NVT} then the average, $\langle X \rangle$ can be calculated using a formula analogous to equation(3.15), i.e.

$$\langle X \rangle \cong \frac{1}{n}\sum_{I=1}^{n} X_i = \frac{1}{n}\sum_{I=1}^{n} X(R_I) \tag{3.18}$$

Where n is the number of configurations generated in the simulation and R_I is a vector of the coordinates of the atoms at each configuration. The solution was given by the Metropolis Monte Carlo method. The Monte Carlo for integration was formalized in the late 1940s by N. Metropolis, J. von Neumann and S. Ulam, but a Monte Carlo method for generating configurations drawn from a canonical distribution was

introduced by Metropolis (Allen and Tildsley, 1989) and co-workers in the early 1950s to study atomic systems. In outline, it is as follows:

1. Choose an initial configuration for the system, $\mathbf{R_o}$, and calculate its potential energy U_o. Set I=0.
2. Generate, at random, a new configuration for the system, $\mathbf{R_J}$, from the current configuration. Metropolis et al. used a recipe in which the probability, $P_{IJ,}$ of generating the state J from state I was equal to the probability, P_{JI}, of generating the state I from the state J. They also insisted that the method should allow, in practice, every state to be accessible from all other possible states, if not as a result of a single, then as a result of a sequence of changes.
3. Calculate the potential energy of the new state ,$U_{J.}$
4. If the difference in the potential energy of the two states, $U_J - U_I$, is less than zero, choose state J as the new configuration, i.e. set $\mathbf{R_J}$ to $\mathbf{R_{I+1}}$.
5. If $(U_J-U_I)>0$ fetch a random number in the range (0,1). If the number is less than $\exp[-(U_J-U_I)/k_BT]$ accept the new configuration, otherwise reject it and keep the old one.
6. Accumulate any averages that are required using equation (3.18) and the new configuration, $\mathbf{R_{I+1}}$. Note that even if the 'new' configuration is the same as the old one, it still must be re-used if proper averages are to be obtained.
7. Increment I to I+1 and return to step 2 for as many steps are desired in the simulation.

3.4 MOLECULAR DYNAMICS

In contrast to the Monte Carlo procedure, molecular dynamics simulation follows the time evolution of a molecular system by numerically integrating Newton's equations of motion for a set of N particles (Allen and Tildsley, 1989). The result is a

trajectory file that specifies how the positions and velocities of particles vary with time. In many respects, MC and MD are equivalent technique (periodic boundary conditions, potentials). Identical results should be obtained for structural analysis and thermodynamic properties. However, thermodynamics properties can be studied only with MD, either at equilibrium or far from equilibrium.

3.5 KIRKWOOD-BUFF THEORY

The Kirkwood-Buff (KB) theory of solution (Kang and Smith, 2007) (often called fluctuation theory) employs the grand canonical ensemble to relate macroscopic properties, such as the derivatives of the chemical potentials with respect to concentrations, the isothermal compressibility, and the partial molar volumes, to microscopic properties in the form of spatial integrals involving the radial distribution function. This theory allows one to obtain information regarding some microscopic characteristics of multicomponent mixtures from measurable macroscopic thermodynamic quantities. However, despite its attractiveness, the KB theory was rarely used, until the evolution of computer simulation for two main reasons:

(1) The lack of precise data (in particular regarding the composition dependence of the chemical potentials) and

(2) The difficulty to obtain simulated radial distribution functions

We will use the KB theory to examine the solution behaviour with regard to local composition. The KB theory correlates the local structure with thermodynamic properties .The mathematical formulation of KB theory is given at sections 4.5.3 and 8.4.

4 SUPERCRITICAL FLUIDS

In the last decade, supercritical fluids more and more have been proved as environmentally benign media for chemical and related processes. Many new processes and products have been developed, using the inherent physical and chemical properties of supercritical fluids. We interested in

1. Determining the behaviour of pure SCF solvents, as such information provides a backdrop against which to understand solvation in these fluids.
2. Predicting solvation structure in SCFs, as these properties critically effect solute reaction, and
3. Examining how such SCF effects alter chemical reaction kinetics.

4.1 INTRODUCTION

In 1869, Thomas Andrews (Andrews, 1869) first recognized the presence of the critical point, which gave birth to a new world of critical phenomena and supercritical fluid science. A SCF is defined as a substance above its critical temperature T_C and critical pressure P_C. This definition should arguably include the clause "but below the pressure required for condensation into a solid", however this is commonly omitted as the pressure required to condense a SCF into a solid is generally impracticably high. However, we will refer to any fluid above its critical temperature as 'supercritical' regardless of its pressure or density. ***The critical point represents the highest temperature and pressure at which the substance can exist as a vapour and liquid in equilibrium***. The phenomenon can be easily explained with reference to the phase diagram for pure carbon dioxide (Figure 4-1). This shows the areas where carbon dioxide exists as a gas, liquid, solid or as a SCF. The curves represent the temperatures and pressures where two phases coexist in equilibrium (at the triple point, the three phases coexist). The gas–liquid coexistence curve is known as the boiling curve. If we move upwards along the boiling curve, increasing both temperature and pressure, then the liquid becomes less dense due to thermal expansion and the gas becomes denser as the pressure rises (Licence *et al.*, 2004). Eventually, the densities of the two phases converge and become identical, the distinction between gas and liquid disappears, and the boiling curve comes to an end at the critical point. The critical point for carbon dioxide occurs at a pressure of 7.38 MPa and a temperature of 304.128 K. The Table 4-1 and the Figure 4-2 lists the critical data of SCFs most frequently used in chemical reactions. A single supercritical fluid can be tuned to mimic the properties (dielectric constant, solubility)

of a wide range of conventional solvents by merely varying the pressure, which is one of the more prominent advantages of supercritical fluids.

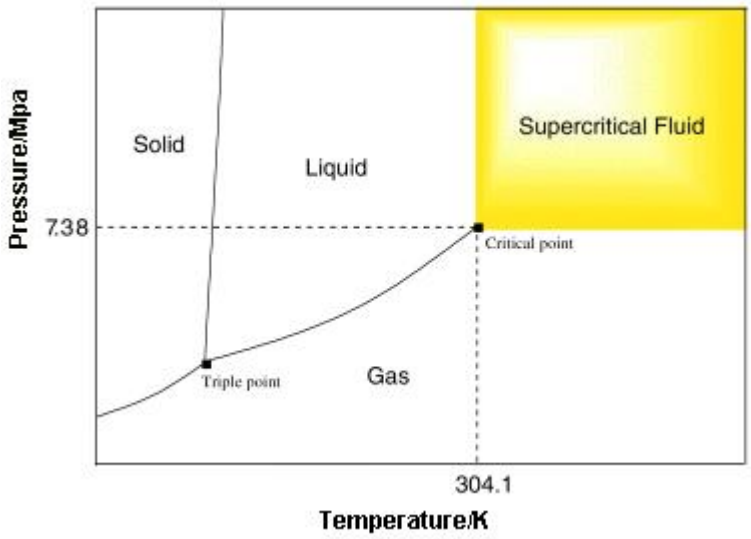

Figure 4-1: Phase diagram for pure carbon dioxide.

Table 4-1: Critical Data (temperature, pressure, and density) of supercritical fluids most frequently used in chemical reactions(source:(Reid *et al.*, 1977))

solvent	T_c,K[a]	P_c, MPa[a]	ρ_c, kg m^{-3} [b]
CO_2	304.04	7.375	735
CH_4	190.44	4.600	452
CH_3OH	512.54	8.092	322
C_2H_6	305.34	4.884	235
C_2H_4	282.24	5.041	468
CH_3CH_2OH	513.84	6.137	162.6
C_3H_8	369.74	4.250	272
$CH_2CH_2CH_3$	364.74	4.601	276
$CH_3CH_2CH_2OH$	536.74	5.170	217
BUTANE	698.3	3.796	275
C_5H_{12}	496.44	3.374	203
C_6H_{14}	507.24	2.969	214
H2	306.12	1.284	233
H2S	373.14	8.937	273

[a] The number of digits given indicates the estimated accuracy of this quantity.[b] Although values for the critical density are given to three decimal places, they cannot be assumed accurate to better than a few percent.

Reactions under supercritical conditions have been used for large-scale industrial production (Vaneldik and Klärner, 2002) for most of the twentieth century, but the application of supercritical fluids in the synthesis of complex material is only

just emerging. Research in this field has been particularly active in the last decade of the 20th century, because the special properties of SCFs make them attractive solvents for modern synthetic chemistry. Moreover, these processes also promise economic and environmental effects. The prerequisites for this success however, are a sound knowledge of physico-chemical properties, phenomena in supercritical mixtures and the availability of chemical engineering data. This requires an effective exchange of knowledge between a large number of branches of science. Werner summarises in a review the recent advances with supercritical fluids which cover the advances in a large number of branches of science (Hauthal, 2001).

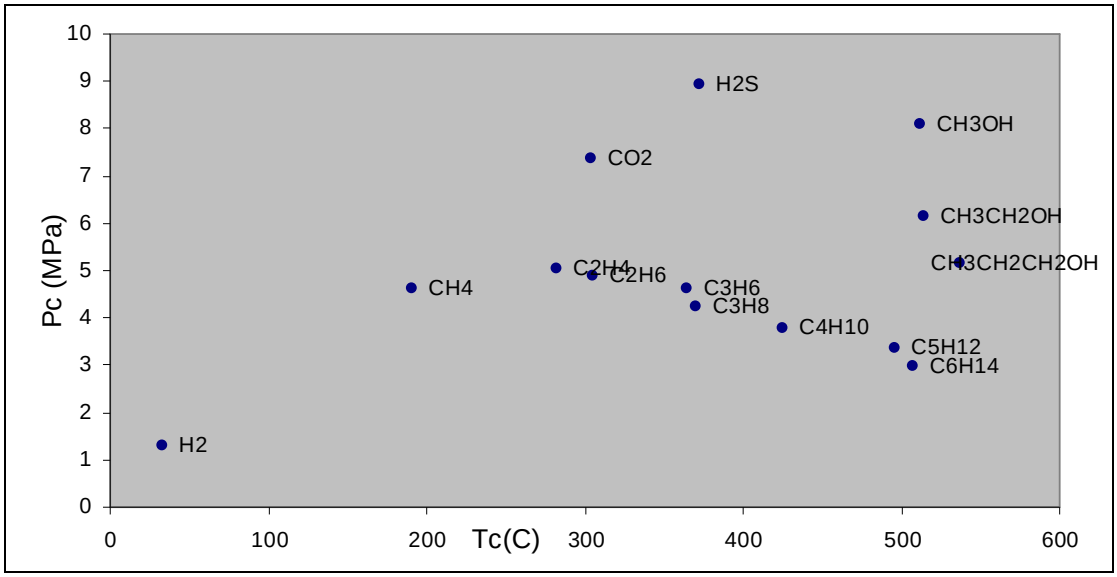

Figure 4-2: The critical points of selected solvents in table 4-1.

4.2 SUPERCRITICAL FLUID PROPERTIES

Using supercritical fluids, such as supercritical carbon dioxide, as a reaction medium has gained considerable attention in recent years, due to the environmental benefits and to the favourable processing conditions. These benefits are due to in part to the increased diffusivity, lowered viscosity, and enhanced mass transfer, as compared to traditional organic liquids solvents. However, chemical reactions are expected to behave differently in supercritical fluids than in the gas or in traditional

liquid phase solvents (Clifford, 1999; Levert Sengers, 1998; Tucker and Maddox, 1998). If we are able to understand and accurately model this behaviour, then we may be able to increase reaction rates, enhance selectivity, and develop more efficient separation process.

To gain insights into the reactions taking place in supercritical fluids, one should first know the characteristics of supercritical fluids. The key characteristics of supercritical fluids are the inhomogeneity in space and the fluctuation in time. It is believed; when a solute molecule with attractive solute–solvent interactions is placed in a supercritical fluid near the critical point, fluid solvent molecules quickly gather around the solute molecule due to solvent attractive interaction.

The inhomogeneity thus caused in supercritical fluids is quite pronounced as compared with ordinary liquids. This process is often called ‘solvation’ or ‘clustering’. It is also called ‘density augmentation’ or ‘enhanced local composition’. The definitions of these terms are rather ambiguous. In our work, the attention is focused on the effect of these phenomena on the chemical reactions of the solute molecule. Therefore, the term “solvation” is better than clustering because clustering sometimes implies the gathering of an enormous number of solvent molecules around the solute molecule. When the term clustering is used in our study, it means the enhancement of solvent density within the first two or three solvation shells. Such a group of molecules consisting of a solute molecule and solvent molecules in the nearby solvation shells is called a cluster. Although the fluctuation in the solvation structure with time has attracted less attention (Kajimoto, 1999) so far, the coupling of such fluctuation with dynamic processes in supercritical fluids will be an attractive target of future research.

The local density enhancement of a fluid, in particular, is expected to influence chemical reactions in supercritical environments. In supercritical fluids, the solvent in the region around a solute molecule will typically be higher than the mean fluid density, and this deviation is often on the order of 50% to 300% (Song *et al.*, 2000). This density enhancement, as well as selective partitioning between solute clusters or the surrounding solvent, can potentially influence the reaction dynamics. The inhomogenities and cluster effect on chemical reactions is not well understood at present. Studies have to be done to examine the lifetime of clusters and compare it with transition state lifetime.

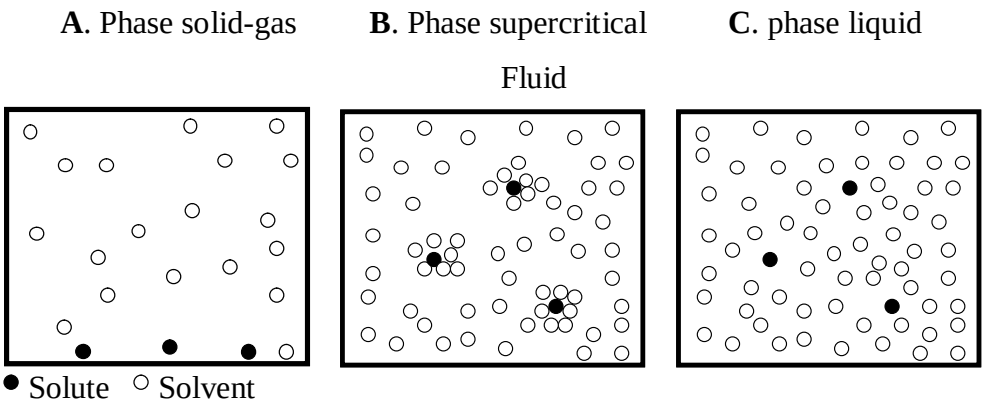

Figure 4-3: Reagent clustering in a supercritical fluid.

Figure 4-3.(A) demonstrates a two phase system in which a solid solute is under pressure of a gas. Interactions between the molecules are very weak and no significant solvation occurs. In (C) the system is in liquid phase, the bulk density is high, offering high solvation and we therefore see a single phase. (B) represents SCF conditions. The bulk density is moderate, higher than the gas phase but much lower than of a liquid. Solvent clustering around the solute molecules does however mean that the local density is relatively high and therefore a moderate solvation is offered and we observe a one phase system for low concentration solutions. The characteristics of clusters vary with temperature a schematically shown in Figure 4-4.

Near the critical point at $T \approx T_C$, the solvent fluid molecules themselves are apt to form clusters of extremely large size.

The effect of pressure on the rate of chemical reactions was originally revealed in solutions under pressure (Asano and Lenoble, 1978; Tiltscher and Hofmann, 1987; Vaneldik and Klärner, 2002). These researches were initiated much earlier than researches in supercritical solvents. Elementary chemical reactions are generally classified according to whether or not the reacting complex must surmount a potential energy barrier in the course of reaction. Reactions for which this is true are called activated processes, while those for which it is not are called diffusion controlled processes. The features of supercritical fluids originate mainly from the intermolecular interactions can affect both of the processes. It is obvious that the study on intermolecular interactions in SCF is very important to their applications.

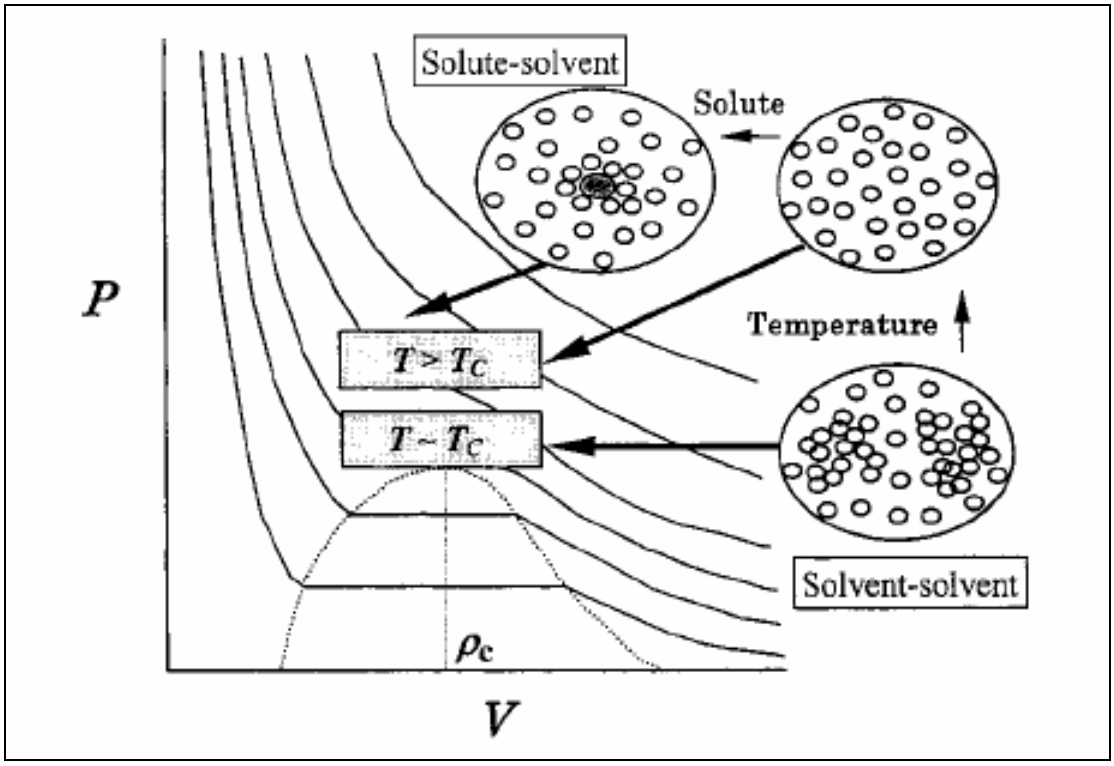

Figure 4-4: Different character of clusters formed in different temperature ranges. Near the critical temperature, the solvent molecules tend to form a large cluster even without a solute molecule. At higher temperatures, the solute molecule with strong attractive interaction is necessary to trigger the clustering of solvent molecules (Reprinted from Baker's work (Baiker, 1999).

4.3 CARBON DIOXIDE

4.3.1 Background

Although $scCO_2$ has received much attention within academic and chemical industrial laboratories both as a green alternative to conventional organic solvent and as a simple, linear triatomic molecular system, the solvent behaviour of $scCO_2$ is not well understood on a microscopic level. The non-toxicity, low cost, abundance, and ease of recycling are some of the key attributes of this environmentally benign solvent. The low critical temperature of CO_2 (T_c =31.1°C) ensures that $scCO_2$ is a safe solvent for biomolecular separations, pharmaceutical applications, and in other thermally labile systems. CO_2 is a major by-product in several industrial processes, and in terms of availability, it is almost as readily abundant as H_2O. Additionally, because CO_2 is recognized as a “green house” gas, recycling of by-product gas and its industrial utilization are an important mode of reducing emissions into the atmosphere. Over the past two decades, there are several areas where CO_2 research has progressed with developments in applications such as CO_2-based dry cleaning, polymer synthesis, extraction and separation of natural products, chemical transformations, synthesis and dispersion of nanoparticles, and materials processing. However, the large-scale utilization of this solvent suffers from the lack of a molecular level understanding of the solvation phenomenon in CO_2. How is CO_2 classified as a solvent? What are the basic characteristics concerning solvation in CO_2, and how is it different from common solvents such as hexane and H_2O? What sort of molecular systems can CO_2 dissolve, and what types of interactions predominate? These are some of the important issues that need to be addressed before it is possible to expand the use of CO_2 as an industrial solvent.

Computational approaches provide excellent insight into understanding the microscopic solute-solvent interactions, microscopic properties and microscopic properties. The development of accurate computational studies for solute solubility and reactions rates in liquid and supercritical carbon dioxide requires a model for intermolecular interactions between this solvent and any solutes. Once a model for carbon dioxide has been selected, it is important to characterize it with its predictions of the equation of state, the liquid-vapour coexistence curve, and the critical properties.

4.3.2 Equation of State for Carbon Dioxide

The current standard National Institute of Standards and Technology (NIST) equation of state for CO_2 was developed by Span and Wagner (Span and Wagner, 1996). For reference, Table 4-2 gives the critical point and triple point conditions for CO_2. The critical temperature for CO_2 is slightly above room temperature.

Table 4-2: Critical point and triple point for CO_2.

	T/K	P/MPa	ρ_g/(Kg/m^3)	ρ_g/(Kg/m^3)
Critical Point	304.128	7.3773	467.6	467.6
Triple Point	216.59	0.5180	13.73	1178.5

4.3.3 Models for Carbon Dioxide

Most frequently, simulations of model fluids at near- and supercritical conditions have been performed without the knowledge of the model's vapour-liquid equilibrium envelope, i.e., by simply taking the state conditions from the phase diagrams of the real substances. The recent development of powerful new simulation techniques for the direct determination of phase equilibria, such as the Gibbs Ensemble Monte Carlo (Panagiotopoulos, 1987), the Gibbs-Duhem intergration (Kofke, 1993), and the Grand Canonical Monte Carlo with histogram re-weighting method (Kiyohara *et al.*, 1998) make it possible to determine the phase diagram of

fluid models with unprecedented accuracy and computational efficiency (Errington *et al.*, 1998).

A large number of efforts has been devoted to the development of an accurate potential model for carbon dioxide. The simplest model is the spherical model with only short-range interactions. This kind of models has great advantage of computational efficiency. On the other hand, several atomic models have been introduced. In those, many single-site Lennard-Jones parameters have been used to describe the carbon dioxide. Most common choices correspond to fits to viscosity data **(model: S_1)** (Reid *et al.*, 1977) or **(model:S_2)** (Nicolas *et al.*, 1979) from a direct fit to the critical temperature and density. The Lennard-Jones parameters adopted usually for molecular fluids determined from the method proposed by Nicolas et al (Nicolas *et al.*, 1979) or the Reid et al for **.** More recently, Virnau et al. (Virnau *et al.*, 2004) present a coarse-grained model for CO_2 which behaves well with the combination with n-alkanes in supercritical solution. The solvent molecule CO_2 is represented by a single particle and the solvent particles interact via a truncated and shifted Lennard-Jones potential,

$$U_{LJ} = \begin{cases} 4\varepsilon_{SS}\left[\left(\frac{\sigma_{SS}}{r}\right)^{12} - \left(\frac{\sigma_{SS}}{r}\right)^{6} + \frac{127}{16384}\right] if \ r<r_C \\ 0 \end{cases} \quad (4.1)$$

where r denotes the distance between particles and the cut-off radius of the potential.

Table 4-3: Parameters for united models of CO_2

model	United Atom	Sigma Å	Epsilon Kcal/mol	Charge e
S1	CO_2	3.720	0.4692	0
S2	CO_2	3.910	0.4477	0

Beyond the simple united atom approaches, there are three potential models designed to fit the properties of CO_2: a 2-point, a 3-point model and 5-point model. The "two-center Lennard-Jones quadrapole" model developed by Möller and Fischer (Moller and Fischer, 1994) fits empirical saturation data to two Lennard-Jones sites and a quadraupole. The model of Möller and Fischer was used by Colina et al (Colina *et al.*, 2003) to describe the thermal properties of supercritical carbon dioxide, except in the extend critical region. The Murthy (Murthy *et al.*, 1983) potential was used by Iwai group (Higashi *et al.*, 2000) to describe the density dependence of structure of supercritical carbon dioxide along an isotherm. The 5-point model of Murthy, O'Shea and McDonald (Maillet *et al.*, 1998; Murthy *et al.*, 1983) uses three Lennard-Jones sites and five Coulombic sites along the molecular axis. The "elementary physical model" (EPM) of Harris and Yung (Harris and Yung, 1995) simplifies the 5-point model by using three Lennard-Jones sites each with a Coulombic charge. The EPM was optimized to get the correct pressure at 239 K, and it has a gas phase quadrapole of 4.3×10^{-26} statcoulomb cm^2 near the experimental value of 4.1×10^{-26} statcoulomb cm^2. The model is designed to be either completely rigid or have a flexible bond. The rigid EPM fits the critical point within 3%. Harris and Yung rescaled the EPM using corresponding states theory to obtain a model (EPM2) that matched the critical properties of CO_2. EPM and EPM2 use a combination Lennard Jones site and point charge at each atom centre.

Table 4-4: Parameters for EPM2 and EPM model

model	Atom	Sigma Å	Epsilon Kcal/mol	Charge e
EPM2	C	2.757	0.0559	+0.6512 e
	O	3.033	0.1600	-0.3256 e
EPM	C	2.785	0.0576	+0.6645 e
	O	3.064	0.1649	-0.3322 e

Accordingly site-site interaction models are the most popular choice for carbon dioxide. A number of the potential models for carbon dioxide can be regarded as EPM based models. The first variation of the EPM model was proposed by Potoff and Siepmann (Potoff and Siepmann, 2001) and is well known with the abbreviation TraPPE. Zhang and Duan (Zhang and Duan, 2005) proposed another version of EPM model by optimizing its parameters by obtaining a better predictability of phase behaviour. Potoff (Potoff and Siepmann, 2001) proposed a model for carbon dioxide with using only the term of power of six in Lennard Jones function, which shows improved accuracies for the PVT properties at high densities. All of the EMP based models have the angle of OCO fixed as 180^{o} .Based on their structural experimental studies, Zhang and Duan (Zhang and Duan, 2005) proposed a new molecular potential abbreviated as EPM-M and EPM2-M with the only difference from EPM model the intermolecular bond angle which is 174.2^{o}. Up to date the EPM2 is the widely used potential, although developed over ten years ago (Nieto-Draghi *et al.*, 2007).

4.4 OTHER COMMON SUPERCRITICAL FLUIDS

4.4.1 Fluoroform

Fluoroform (CHF_3) has a conveniently located critical point (T_C = 26.1°C, P_C = 4.8 MPa), is non-toxic and relatively benign to the environment, and is available in high purity at modest cost. For these reasons, fluoroform has served as the prototype for polar supercritical solvents in numerous experimental studies over the past decade. Several simulation models of fluoroform have already been developed (Hloucha and Deiters, 1998; Lisal and Vacek, 1996; Potter *et al.*, 1997; Song *et al.*, 2002) and successfully applied to study a number of properties of the fluid (Okazaki *et al.*, 1995; Song *et al.*, 2002). The model proposed by Song et al is a 2-site model developed for use in simulations in the near critical regime. The model was optimized

to reproduce the critical point and the liquid-vapour coexistence curve of the real fluid using the Gibbs Ensemble Monte Carlo method.

The model is a Lennard-Jones potential plus a Coulombic interaction (Song *et al.*, 2002). The 2-site model of fluoroform has been used by Song and Maroncelli (Song and Maroncelli, 2003) to examine the role of electrostatic forces on density augmentation on supercritical fluoroform.

Table 4-5: Model parameters of the 2-site model for CHF_3 molecule. The distance between the 2 sites is 1.670 Å

site	Sigma Å	Epsilon Kcal/mol	Charge e
1	3.500	0.1699	+0.275e
2	3.500	0.1699	+0.275e

4.4.2 Ethane

After methane, ethane is the second-largest component of natural gas. Ethane is isolated on an industrial scale from natural gas, and as a by-product of petroleum refining. Ethane is of great interest in separation industry. Many molecular potential have been developed for ethane for different conditions, the most commonly used is the UA-OPLS model developed by Jorgensen et al (Jorgensen *et al.*, 1984) and TraPPe model developed by Siepmann group (Martin and Siepmann, 1998). Ethane (CH_3CH_3) has a critical point (T_C = 32.18°C, P_C = 4.8718 MPa) close to fluoroform. To date all of the developed potentials have been tested across their ability to predict the critical point (Nath *et al.*, 1998). The TraPPe model gives good agreement with experimental critical properties. The 2-site model parameters of the TraPPe model are given in the Table 4-6

Table 4-6: Model parameters of the 2-site model for CH_3CH_3 molecule. The distance between the 2 sites is 1.54 Å

site	Sigma Å	Epsilon Kcal/mol	Charge e
1	3.750	0.1947	0
2	3.750	0.1947	0

4.4.3 Water

Water at elevated and supercritical temperatures is found at the bottom of the oceans as well as in electric power plants (Ulrich Franck, 1987). Supercritical water (SCW) can be a suitable reaction medium for reactions usually carried out in organic solvents. The SCW except the well-known advantages (Levert Sengers, 1998) using a supercritical fluid as a reaction medium also influences the rates of chemical reactions. During a reaction, the transition state may be higher or lower polarity than the initial state. A high relative dielectric constant lowers the activation energy of the reaction of a transition state of higher polarity than the initial state. By variation of the relative dielectric constant, achieved by adjusting the temperature and pressure, the reaction rates maybe controlled. As a consequence, these reactions show a high activation volume. Fundamental chemical properties, which are well-known in aqueous chemistry at 298 K, are much less available for SCW (T_c=647.13, $\rho_c = 0.322 g/cm^3$, $P_c = 220.55\ bar$) solutions (Reid *et al.*, 1977).

Modelling the behaviour of water has been the subject of extensive research. To describe the molecular structure of water, the most widely used effective pair potential models use rigid multiple interaction sites with partial charges, such as the three-site TIP3P (Jorgensen, 1981), SPC (de Pablo *et al.*, 1990), and SPC/E (Berendsen *et al.*, 1987), the four-site TIP4P (Jorgensen *et al.*, 1983), and the five-site ST2 (Stillinger and Rahman, 1974) models, whose merits have been well documented (Paschek, 2004). In particular, the three-site TIP3P, SPC, and SPC/E models are commonly used in biochemical simulations, in part because of their reasonable descriptions of solvation and dielectric properties. The model parameters for TIP3 are given in Table 4-7 . The TIP3 have chosen to be used in this study, due to its compatibility with EPM2.

Table 4-7: Model parameters of TIP3 model.

model	Atom	Sigma Å	Epsilon Kcal/mol	Charge e
TIP3	H	0	0.0000	0.417 e
	O	3.151	0.1521	-0.834 e

4.4.4 Methane

During the last two decades, the properties of fluid methane have been studied by several groups using various experimental and theoretical techniques. The reason for this long-lasting interest is that methane is the major constituent of natural gas. Note that natural gas is one of the most promising fuels in reducing carbon dioxide emissions. Further, it is much cheaper and environmental friendly than petroleum-based fuels. Methane is one of the simplest polyatomic molecules. Its spherical symmetry allows it to be modelled as a single site molecule with more accuracy than almost any other polyatomic molecule. Modelled as a single site molecule the majority of potentials for methane are based Lennard Jones potentials. The OPLS-UA potential proposed by Jorgensen (Jorgensen *et al.*, 1984) is the one widely is in use. An alternative generic effective pair potential is given by the Bunckingham (Martin and Siepmann, 1998) potential, but it is not easily compatible with Lennard-Jones in case of mixture simulations.

Table 4-8: Model parameters of OPLS-AA model.

model	Atom	Sigma Å	Epsilon Kcal/mol	Charge e
OPLS-AA	H	2.500	0.0300	-0.24 e
	C	3.500	0.0660	0.06 e

The most common used potential is the all-atom (AA) five-centre semi empirical Lennard–Jones (LJ) potentials, with or without electrostatic interactions, proposed by Jorgensen et al. (Jorgensen *et al.*, 1996) and Murad–Gubbins (MG) (Quirke and Gubbins, 1996), provide the most accurate description of the liquid compared with other site–site potentials (Skarmoutsos *et al.*, 2005). The OPLS-AA

model is choosen for this study as it is compatible with EPM2. Its parameters are given in Table 4-8.

4.5 SUPERCRITICAL FLUID KINETICS

Chemical processes in SCFs can be controlled by a variety of factors, such as enhanced transport coefficients, increased reactant solubilities, facilitated separation, and strong "***kinetic pressure***" effect on the rate constants. For any given reaction, several aforementioned factors can be affecting the reaction rate simultaneously, which makes the analysis of chemical processes in SCFs rather involved. Therefore, it is important to study simple, well-defined reactions, where it is possible to isolate a few dominant factors influencing the reactivity. In this regard, the investigation of chemical equilibria in SCFs provides a particularly appealing area of research, since the values of the equilibrium constants are largely determined by the structural aspects of supercritical solvation.

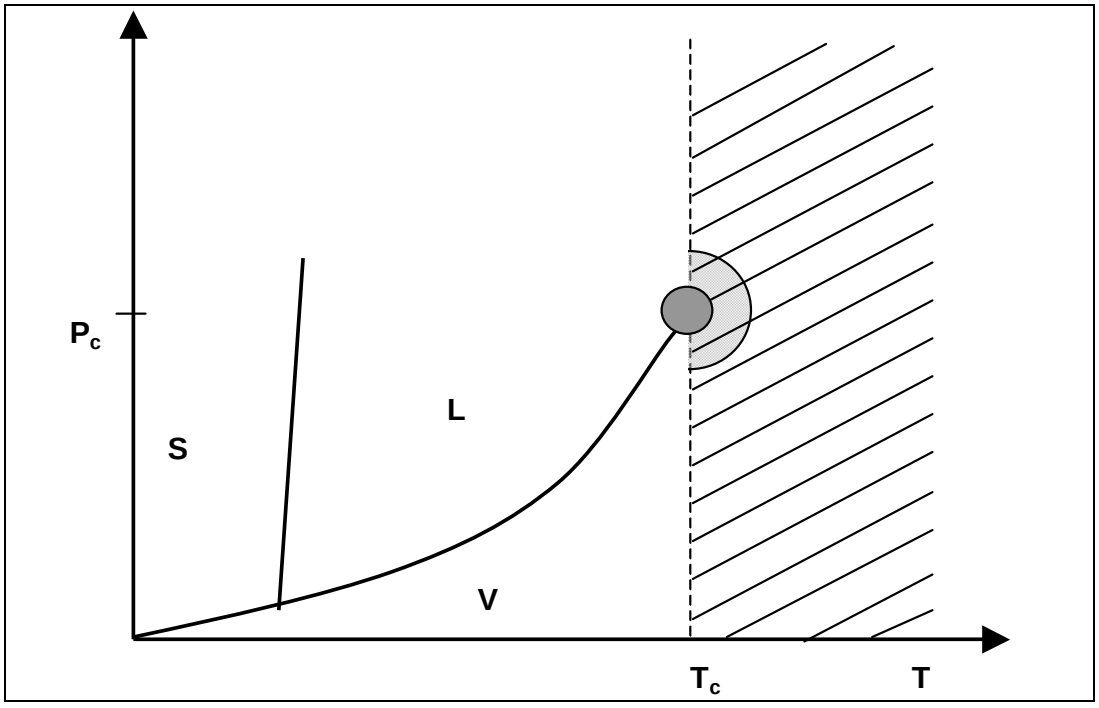

Figure 4-5: Schematic illustration of regions of the phase diagram; near-critical regime (dark area); compressible-regime (light dark area); supercritical regime (slanted hatch)

At present, however, the properties of SCFs and their effects on solute reaction are not well understood, and the way is open for computation to provide the underlying insight necessary for efficient development of SCF technologies.

When T exceeds T_c, there can be no phase transition between the vapour and liquid phases. Instead, as the pressure is increased the fluid density is changed continuously from gas-like to liquid-like densities. Consequently, density-dependent solvent properties, such as the dielectric constant and the viscosity, will also vary continuously. Pressure thus provides direct control of the fluid's solvating properties. This tunability is more effective when large changes in density accompany small changes in pressure, i.e., when the isothermal compressibility is large. Coincidentally, the compressibility of a fluid diverges as its critical point is approached, and there exists a region of the phase diagram surrounding the critical point (with the restriction that $T>T_c$) within which the fluid's compressibility is anomalously large (Figure 4-5). Evidentially, it is in this compressible regime that pressure-controlled tunability of the solvent properties is maximised, and it is thus of primary interest to understand solute reactivity in this solvent regime.

4.5.1 Effect of density on Equilibrium Constant

The effect of pressure (P) on reaction equilibrium constant $(K_c)^{\bullet}$, which is the ratio of forward and reverse rate constants k_f / k_r, is expressed in terms of the reaction volume ΔV_{rxn} :

$$\left(\frac{\partial K_c}{\partial P}\right)_T = -\frac{\Delta V_{rxn}}{RT} + \kappa_T \sum \nu_i \qquad (4.2)$$

$$\alpha A + \beta B \ldots \underset{k_r}{\overset{k_f}{\rightleftharpoons}} \gamma \Gamma + \delta \Delta \ldots$$

$^{\bullet}$ For a general reaction

where $\sum \nu_i$ is the sum of the stoichiometric coefficients for the reaction, and κ_T is the isothermal compressibility. The reaction volume is defined as the sum of the products of the stoichiometric coefficient and the partial molar volume V_i for each species in the reaction. The reaction volume is

$$\Delta V_{rxn} = (\gamma V_\Gamma + \delta V_\Delta + ...) - (aV_A + \beta V_B + ...) \tag{4.3}$$

The difficulty in using (4.2) and (4.3) with experimental data is that experimental measurements of partial molar volumes are challenging (Guo and Akgerman, 1998). Measuring partial molar volumes is very difficult because of the problems associated with observing the supercritical phase the low concentrations and short lifetimes of highly reactive species. An alternative approach to experimental measurements of partial molar volumes or equilibrium constants is theoretical determination of these quantities.

4.5.2 Effect of density on Kinetic Constant

In conventional transition state theory, the pressure dependence of a rate constant is related to the activation volume as it described by Equation (2.5)

$$\left(\frac{\partial \ln k_C}{\partial P}\right)_{T,C} = -\frac{\Delta V^{\#}}{RT} - \kappa_T(1-\alpha-\beta-...) \tag{4.4}$$

where κ_T is the isothermal compressibility of the solvent. The activation volume is calculated as the difference in the partial molar volumes of the transition state ("TS") and the reactants.

$$\Delta V^{\#} = V_{TS} - aV_A - \beta V_B \tag{4.5}$$

The partial molar volumes can be calculated like the equilibrium constant case from the pair correlation functions for infinitely dilute mixtures.

4.5.3 Partial Molar Volumes

When solutes are introduced into such a fluid, substantial solvent density enhancements (clustering) or depletion (cavitation) are often observed around solute molecules. Debenedetti and co-workers identified 3 solute behaviours: repulsive, weakly attractive, and attractive, as follows (Debenedetti and Mohamed, 1989; Petsche and Debenedetti, 1991).

1. Repulsive solutes are those for which the repulsive part of the solute-solvent potential dominates the solute-solvent interactions. In this case, the solute and solvent molecules repel each other and, consequently, the average solvent density around a solute is less than the bulk density. Thus, addition of solute increases the volume of the solution and gives **positive** partial molar volumes (PMV).
2. Weakly attractive solutes are those for which the solute-solvent potential interaction is dominantly attractive but are less so than the solvent-solvent potential interaction. So, the addition of solute still increases the volume of the solution and gives **positive** partial molar volumes.
3. Attractive behaviour results when the dominant solvent-solute interaction is more attractive than the solvent-solvent interaction, so that the solute-solvent correlations exceed the solvent-solvent correlations. In this case, addition of solute decreases the volume of the solution and gives **negative** partial molar volumes.

The observed partial molar volumes provided the main impetus for a whole new realm of investigations seeking to better understand the intermolecular interactions between the solute and the other species in SCF solutions. For example the partial molar volume of naphthalene at infinite dilution in a mixture of naphthalene and supercritical carbon dioxide is -2300cm^3/mol at P=76 bar and

T=308.38 K (Eckert *et al.*, 1986), while the partial molar volume of ethane at infinite dilution in a mixture of ethane and supercritical carbon dioxide is +350 cm^3 /mol at P=73.97 bar and T=305.65 K. According to the classification of Debenedetti and Mohamed the above mixtures (CO_2/naphthalene and CO_2/ethane) belong to different types of supercritical mixtures; CO_2/naphthalene is an 'attractive' mixture and CO_2/ethane is a 'weakly attractive' mixture.

The research group of X.Zhang (Zhang *et al.*, 2002a; Zhang *et al.*, 2002b) reported new data of PMVs of solutes in dilute supercritical solution. In their study, the PMVs of two polar solutes (H_2O and H_2S) in supercritical CO_2 are negative, and a minimum can be observed in each PMV versus pressure curve at the pressure where isothermal compressibility of the fluid is largest. On the opposite site the PMVs of two non-polar solutes (H_2 and CH_4) are positive.

For a solute (u) in solvent (V), the partial molar volume is defined as

$$\overline{V}_u = \left(\frac{\partial V}{\partial n_u} \right)_{pT,n_V} \tag{4.6}$$

with n_u and n_V being the numbers of moles of the solute and solvent, respectively. At infinite dilution, $\overline{V_u^{\infty}} = \lim_{n_u \to 0} \left(\partial / \partial n_u \right)_{p,T,n_V} \approx V(n_u=1,n_s,T,P)-V(n_u=0,n_s,T,P)$, so $\overline{V_u}$ can be computed in the isothermal-isobaric ensemble (NPT) from Monte Carlo simulations (Iwai *et al.*, 1997). The computational method is not limited to Monte Carlo simulations; molecular dynamics simulations are equally applicable. Partial molar volume studies have been reported with this method (Stubbs *et al.*, 2005) for naphthalene carbon dioxide mixture near the critical point with reasonable accuracy.

An alternative approach is to use the Kirkwood-Buff (KB) fluctuation theory (Kang and Smith, 2007). This theory and its extension have been applied to study dilute supercritical fluid mixtures (Akiya and Savage, 2000a; Akiya and Savage,

2000b; Chitra and Smith, 2001a; Chitra and Smith, 2001b; Lin and Wood, 1996). In this formalism, the partial molar volume at infinite dilution can be calculated as

$$\rho\overline{V}^{\infty} = 1 - \rho_v (G^{\infty}_{uv} - G^{0}_{vv}) \tag{4.7}$$

where G_{uv} and G_{vv} are solute-solvent and solvent-solvent fluctuation integrals, respectively. The subscript u refers to the solute and v to the solvent. The superscript 0 and ∞ refer to the pure solvent or infinitely dilute co-solvent, respectively. These fluctuation integrals are a function of pair correlation functions ($g_{ij}(r)$):

$$G_{ij} = 4\pi \int_0^{\infty} \left[g_{ij}(r) - 1 \right] r^2 dr \tag{4.8}$$

Thus partial molar volumes depend on the relative strengths of the solute-solvent and solvent interactions. Pair correlation functions can be calculated directly from molecular simulations.

The KB theory relates fluctuations in particle densities in the grand canonical ensemble to thermodynamic properties of mixtures. The pair correlation function or radial distribution function (RDF) can be calculated through simulations in canonical ensemble. The values of the integrals though RDFs can be obtained for

a. solvent-solvent

b. solvent-solute

c. solute-solute

The same integrals can be calculated for solvent and co-solvent, for mixture where we don't have diluted solutions with introducing some modifications.

4.5.4 Isothermal Compressibility

The way in which the volume of a material decreases with pressure at constant temperature is described by the isothermal compressibility, κ_T. Isothermal compressibility is one on the important properties of the fluid, which gives very

strong indication of the unusual behaviours at supercritical conditions. The isothermal compressibility (κ_T) can be obtained from densities of the fluids according to equation (4.9)

$$\kappa_T = -\frac{1}{V}\left(\frac{\partial V}{\partial P}\right)_T = \frac{1}{\rho}\left(\frac{\partial \rho}{\partial P}\right)_T \tag{4.9}$$

The theory of critical phenomena (Tucker and Maddox, 1998) tells us that, as the critical point of a fluid is approached ($T \rightarrow T_c$), the isothermal compressibility diverges (i.e., it becomes infinite). Since this divergence occurs smoothly, there must exist a region of the phase diagram with $T > T_c$ for which the compressibility κ is large, by which we mean that $\kappa_T > \kappa_T^0$, where κ is the compressibility of an ideal gas (The compressibility of a perfect gas is given as κ_T^0). As it turns out, this region of large κ, which is called the'compressible regime' extends well beyond the near-critical region of the phase diagram in which all fluids behave universally and the theories of critical phenomena apply (Tucker, 1999).

Macroscopically, a large compressibility means that there is very little cost associated with an increase in solvent density, so we can easily compress the fluid. From a molecular point of view, a large compressibility means that there is enough free space, (a big voidage) between molecules, allowing the system to be compressed. In this case, there are two pictures of molecular microstructure that can satisfy this situation. Firstly, if the voidage is uniformly distributed between the molecules, or secondly, if there are high and low density regions. In the first case, a little effort is required to compress and condense the molecules together. In second case, a little cost is required to transfer a molecule from a low-density region to a high-density one. According to Morita (Nishikawa and Morita, 2000) there is a ridge that separates the supercritical region into more liquid-like and more gas-like regions in the supercritical

region. The ridge is shown in Figure 4-6. According to their research group, the ridge is the locus of the points where the values of the density fluctuation becomes maximum in isothermal changes.

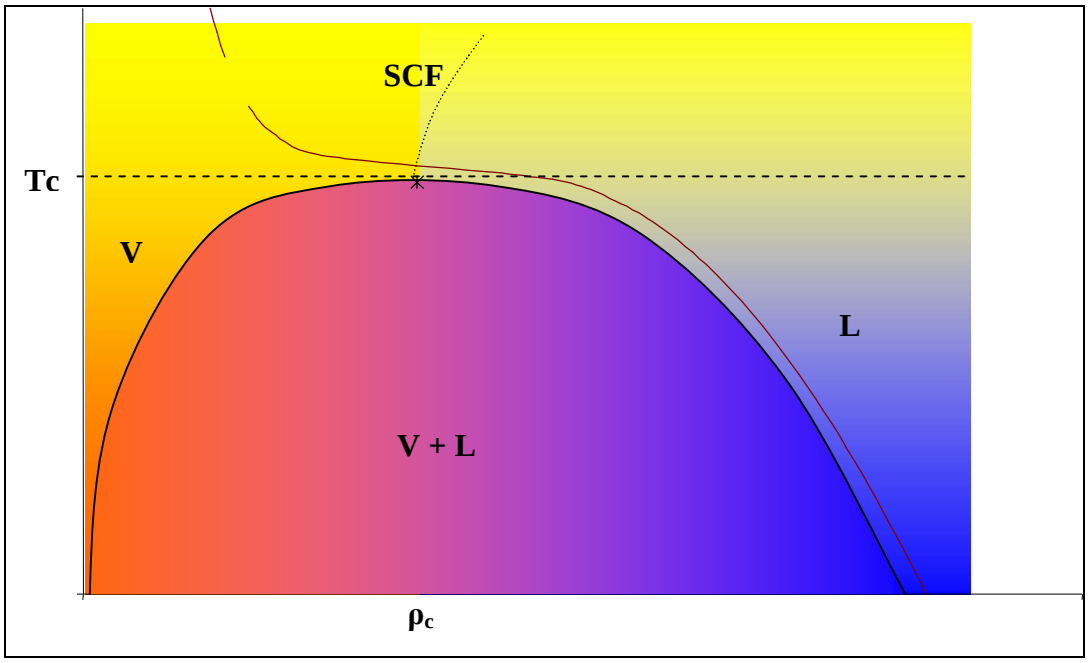

Figure 4-6: The gas–liquid coexistence curve. The blue colour indicates a high density region (liquid like) and the red colour a low density region (gas like). The dashed line represents the locus of the points with the maximum local densities fluctuation (drawn on data representing vapour-liquid curve for carbon dioxide).

Density fluctuation and correlation length are quantitative expressions of the static structural fluctuation from the standpoints of number of molecules and size of molecular aggregates, respectively. The isothermal compressibility obtains its maximum value on the locus of the points of ridge. The isothermal compressibility is related to the Gibbs free energy through the equation

$$\kappa_T = -\frac{1}{V}\left(\frac{\partial^2 G}{\partial P^2}\right)_T = \frac{1}{V}\left(\frac{\partial V}{\partial P}\right)_T \qquad (4.10)$$

Many physicochemical properties of supercritical fluids are related to the second derivative of the Gibbs or Helmholtz free energy, so we expect a unique behaviour on the ridge. From this point of view, little work has been done connected rate constants, equilibrium properties or solubilities with the ridge. However, rate

constants or equilibrium constants of various chemical reactions in supercritical fluids show a singular behaviour on the ridge (Ikushima *et al.*, 1992). Also infinite solution studies reported an anomalous behaviour of solute partial molar volumes at pressures where the ridge located (Guo and Akgerman, 1998).

4.5.5 Diffusion

The most commonly used description of diffusivity on a quantitative basis is via the measurement of the well-known self diffusion coefficient. The diffusion is the rate of transfer of diffusing molecules through unit area of a section and is proportional to the concentration gradient

$$J = -D(\frac{\partial C}{\partial x}) \tag{4.11}$$

where D is the self diffusion coefficient. The self-diffusion is a single particle property and can be obtained from molecular simulation dynamic simulations with great accuracy. The common form to derive the diffusion coefficient through molecular dynamics is the through the Einstein equation. Detailed explanation for the intuiting aspect of the diffusion coefficient at supercritical conditions is given in the results section of diffusivity.

Part II. Simulation

5 COMPUTATIONAL METHODOLOGY

Molecular simulation has reached a stage where it can be reliably used for a large array of equilibrium and non-equilibrium properties of molecular liquids. The purpose of this chapter is to present the technical details of the Monte Carlo simulation and molecular dynamics.

The two most widely used methods for atomic-level modelling of fluids Monte Carlo statistical mechanics and molecular dynamics have been used in our studies in the supercritical region. Both procedures typically have the same system setup including representation of molecules as collections of atom-centred interaction sites, utilization of classical force fields for the potential energy terms, and implementation of periodic boundary conditions. The principal differences are in the modes of sampling the configuration space available to the system. For MC, a new configuration is generated by selecting a random molecule, translating it, rotating it. Acceptance of the new configuration is determined by the Metropolis sampling algorithm; application over enough configurations yields properly Boltzmann-weighted averages for structure and thermodynamic properties. For MD, new configurations are generated by application of Newton's equations of motion to all atoms simultaneously over a small time step to determine the new atomic positions and velocities. In both cases, the force field controls the total energy (MC) and forces (MD), which determine the evolution of the systems. In our simulations, we used both of the methods.

5.1 INTRODUCTION

Typically, a molecular system simulation is carried out with anywhere from 10 to 100,000 molecules. Larger systems are generally prohibited due to memory requirements, and (more importantly) speed considerations. Force calculations increase with number of particles. However, because we are using a very small number of particles and trying to determine macroscopic properties one must be ***very careful*** that the results are not ***system size-independent***. Unless the actual system being studied is very small (a droplet, microstructure etc) a simulation box with 1000 molecules will have a disproportionate number (nearly half) of molecules at the "surface". This would completely skew the behaviour of the system. In order to get around this problem, we employ a trick called periodic boundary conditions. In this model, one chooses a small part of the full system to simulate and then makes the assumption that the rest of the system can be modelled as an infinite series of copies of the central box. This consideration of periodicity makes the simulation of condensed phase systems applicable.

5.2 PERIODIC BOUNDARY CONDITIONS

In the periodic boundary condition approximation, an infinite system is constructed as a periodically repeated array of the finite system that is being studied. A schematic diagram of a two-dimensional system is shown in Figure 5-1, each replica containing the same number of molecules in the same configuration (positions and orientations). Thus when a molecule moves through a boundary and so out of the sample it is automatically replaced by a molecule moving into the sample through the opposite face of the box.

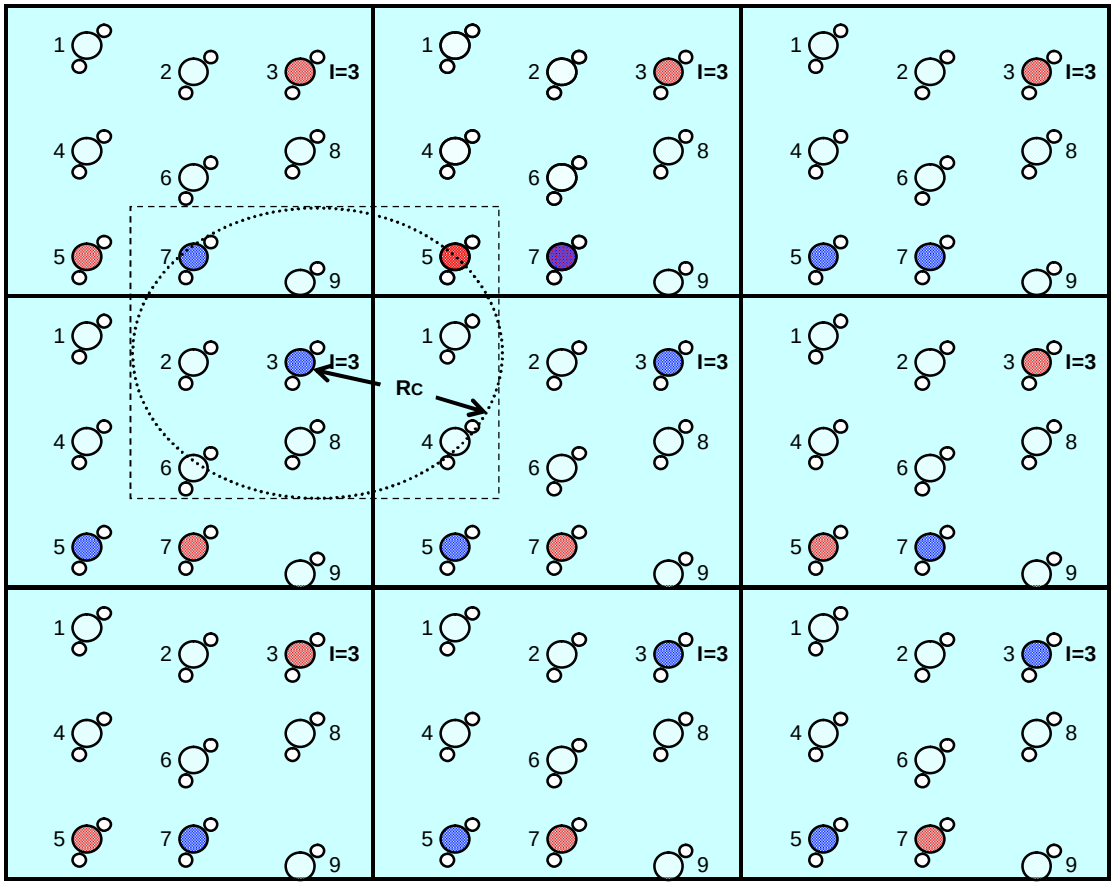

Figure 5-1: Schematic representation of periodic boundary conditions for two–dimensional system

Anyone who has played video games such as Pacman, Asteroids, Galaxians etc. will be familiar with this periodic boundaries trick. The primary simulation box can be envisioned as being surrounded by images of itself; for a "cube", there would be 26 images around the central box. The central box is the "unit cell". With such periodic boundaries it is only necessary to store the coordinates of the molecules in the central box, the periodic images being copies of these.

Here we have to repeat ***that the heart of a Monte Carlo simulation program is the calculation of the energy***. However, the assumption of periodicity immediately makes the simulation of such system ***tractable*** even through all the molecules in it are modelled explicitly.

In order to calculate the intermolecular interaction of any molecule, we position it at the centre of a box with dimensions identical to the simulation box. The

central molecule interacts with all molecules whose centres fall with this region, i.e., the closest periodic images of the other N - 1 molecules. The simplest procedure is to use a spherical cutoff such the interactions are evaluated with the nearest images of the other molecules out to a cutoff distance R_C, as illustrated in Figure 5-1. In order to avoid evaluation of interactions with more than the one image of another molecule R_C is always chosen to be less than or equal to half the length of the shortest edge of the periodic cell. Typically, values for R_C are 10-15 Å. Historically, an alternative approach with a cubic cutoff was used occasionally used whereby the interactions were evaluated with the nearest image of each of the remaining N-1 molecules. This procedure was abandoned since the boundary conditions do not reflect the normal spherically symmetric nature of the intermolecular forces and it requires the calculation of roughly twice as many pair interactions as spherical cutoff. The spherical cutoff is an approximation that could (and does) have important consequences for the behaviour of a system during a molecular simulation. It would be obviously better to have methods that allow the interaction after the cutoff to be considered. A class of such approximations exists and they are called long range corrections techniques.

5.3 CONFIGURATIONAL ENERGY

The potential energy controls the outcome of the Monte Carlo simulations. It is computed from the pairwise sum of the intermolecular interaction energies between molecules. Because our studying systems comprised of small molecules, we shall restrict ourselves to treat the molecules as rigid molecules and we will ignore the intramolecular interactions. So the intermolecular interaction is restricted to pairs of N molecules and total potential energy (U) is obtained by summing over the contribution all of the individual pairs.

$$U = \sum_{I=1}^{N_{mol}} \sum_{J=1}^{I-1} U_{IJ} \tag{5.1}$$

This calculation is known as **Naïve Energy Calculation** (Sadus, 2007), it is obvious that the "self" interactions do not contribute to the potential energy of the system and we avoid the "double" calculation of the pair interactions. Obviously, the type and nature of the terms in the energy function and the values of the parameters will depend upon the force field that we choose to use.

To model intermolecular interactions, we adopt pairwise additive effective potentials of the sort commonly employed in computer simulation. Specifically, the interaction between two molecules I and J is assumed to be given by the sum of site-site terms of the Lennard-Jones plus Coulomb form

$$U = \sum_{i \in I} \sum_{j \in J} \frac{q_i q_j}{4\pi\varepsilon_o r_{ij}} + 4\varepsilon_{ij} \left[\left(\frac{\sigma_{ij}}{r_{ij}} \right)^{12} - \left(\frac{\sigma_{ij}}{r_{ij}} \right)^{6} \right] \tag{5.2}$$

where ε_o=8.85419·10^{-12}C^{2}N^{-1}m^{-2} is the dielectric constant of the vacuum, q_i is the charge on site i of the molecule I, r_{ij} is the distance between sites i and j, and σ_{ij} and ε_{ij} are Lennard-Jones interaction parameters between sites i and j located at molecules I and J. Sometimes simulation models involve with united-atom (**UA**) (Jorgensen *et al.*, 1984) representations wherein multiple atoms are combined into a single interaction site or all-atoms (**AA**) versions (Jorgensen *et al.*, 1996).

For the Lennard-Jones interactions between unlike atoms, the Lorenzt-Berhelot combining rules were used. The Lennard-Jones interactions were calculated using the arithmetic mean of the core diameters and the geometric mean of the well depths.

$$\sigma_{ij} = \frac{\sigma_i + \sigma_j}{2} \tag{5.3}$$

$$\varepsilon_{ij} = \sqrt{\varepsilon_i \varepsilon_j} \tag{5.4}$$

The exact form of the energy within the cutoff distance is given by the form below

$$U = \sum_{I=1}^{Nmol} \sum_{J=1}^{I-1} \left\{ \sum_{i \in I} \sum_{j \in J} \frac{q_i q_j}{4\pi\varepsilon_o r_{ij}} + 4\varepsilon_{ij} \left[\left(\frac{\sigma_{ij}}{r_{ij}} \right)^{12} - \left(\frac{\sigma_{ij}}{r_{ij}} \right)^{6} \right] \right\} \tag{5.5}$$

5.4 LONG RANGE CORRECTIONS

So far, we have discussed the concept of periodic boundary conditions and the output for the configurational energy. In all these theories we assume "perfect" structure. Although, we know that real materials do have order and structure, particularly on short length scales. The basic idea behind this concept is that, elucidation of the structure of fluids is important to understanding fluid behaviour. Considering Figure 5-2, which represents a snapshot of a collection of spherical molecules, with an arbitrary particle picked as a reference. At a distance r from the reference particle, the density of other particles $\rho(r)$ will depend on time. However, on average the density will be a quantity dependent ***only upon distance, r***

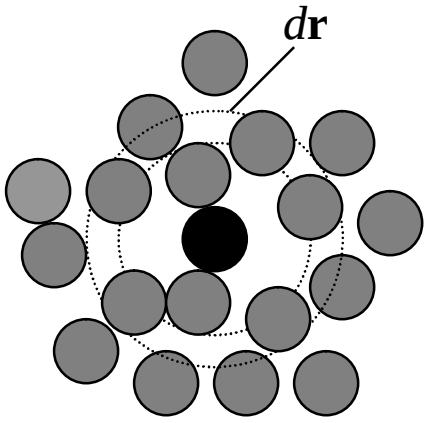

Figure 5-2: Typical arrangement of a fluid of spherical particles. The density at a given radius r with respect to a reference particle is shown.

We can immediately recognize several qualitative features from Figure 5-2. First, $\rho(r)$ must tend toward zero, as r goes to zero, since additional particles cannot occupy the same location as the reference particle. Second, at large r, the influence of

the reference particle is zero, and $\rho(r)$ must approach ρ, the macroscopic density. Third, at intermediate separations, $\rho(r)$ may be less than or exceed ρ, depending on whether the distance r corresponds to distances of repulsion or attraction between particles.

Now, we define a function $g(r) = \rho(r)/\rho$ the behaviour of g(r) is such that

$$g(r) \to 0 \text{ as } r \to 0$$

$$g(r) \to 1 \text{as } r \to \infty$$

g(r) is called the radial distribution function.

We mentioned that the Monte Carlo algorithm it depends on the ***outcome of the total energy***. The ***potential energy*** is defined as

$$U = \langle U_{IJ} \rangle \tag{5.6}$$

The differential number of molecules dN_r in an element of spherical volume at a distance $dr = 4\pi r^2 dr$ between r and r + dr from the central molecule is

$$dN_r = g(r)4\pi^2 dr \tag{5.7}$$

The potential energy of this differential system is

$$U_{IJ}(r)g(r)4\pi^2 dr \tag{5.8}$$

For all distances from the reference molecule, the total potential energy is

$$\int_0^\infty U_{IJ}(r)\rho(r)g(r)4\pi^2 dr \tag{5.9}$$

What about the portion of the potential energy that was "***cut off***"? The contribution to U from the truncated "***tails***" of the pair potential function (the so–called "***long range correction***") is calculated by direct integration, using the energy equation. To obtain the total potential energy of the system, we would sum over all molecules, letting each one be the reference. Each integral would be the same as the

above expression. Thus, we would expect that the total internal energy would be obtained by multiplying the above expression by N, the total number of molecules. However, this would over count, since each pair interaction would be counted twice. Consequently, U_{full} is obtained from

$$U_{full} = U_c + U_{lrc} = \sum_{I=1}^{N_{mol}} \sum_{J=1}^{I-1} U_{IJ} + 2\pi N \rho \int_{R_C}^{\infty} V(r) g(r) r^2 dr$$

But how strong are these long range interactions and what part of the total part of energy they account of?. Let's have a look on the EPM2 model for carbon dioxide. The EPM2 model is presented in Figure 5-3

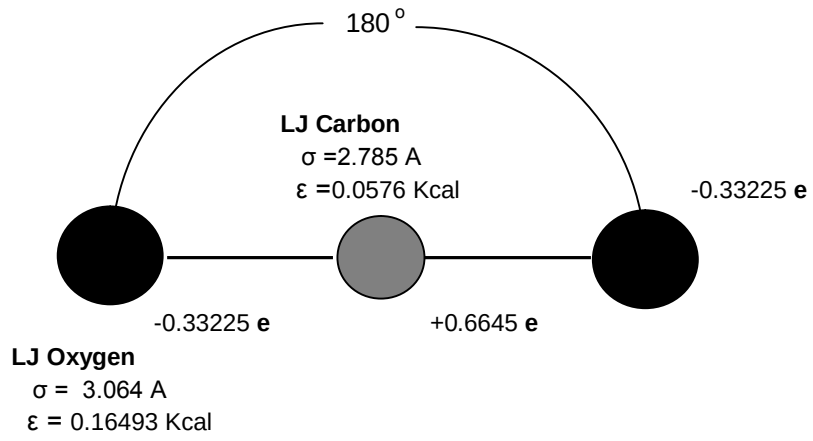

Figure 5-3: Parameters for EPM2 model for carbon dioxide. The distance between carbon and oxygen at 1.149Å

The influence of the potential never vanishes for electrostatic interactions. Therefore, it is clear that the treatment of long-range electrostatic interactions must be performed. Long-range Van der Waals interactions are less strong and decay more quickly with distance.

The Coulomb potential vanishes as 1/r, which is a much slower decay than the $1/r^6$ dispersion interaction characterized by the LJ model potential. Representative curves are shown in Figure 5-4 and Figure 5-5. Whereas the LJ model can quite reasonably be truncated at about 2.5 LJ diameters, the Coulomb potential is at five LJ

diameters nowhere near approaching zero. There are many methods have been developed to treat the long range interactions. The most widely used are analytical forms for Van der Waals (Allen and Tildsley, 1989) interactions and reaction field method (Lisal *et al.*, 2002)`for electrostatic interactions.

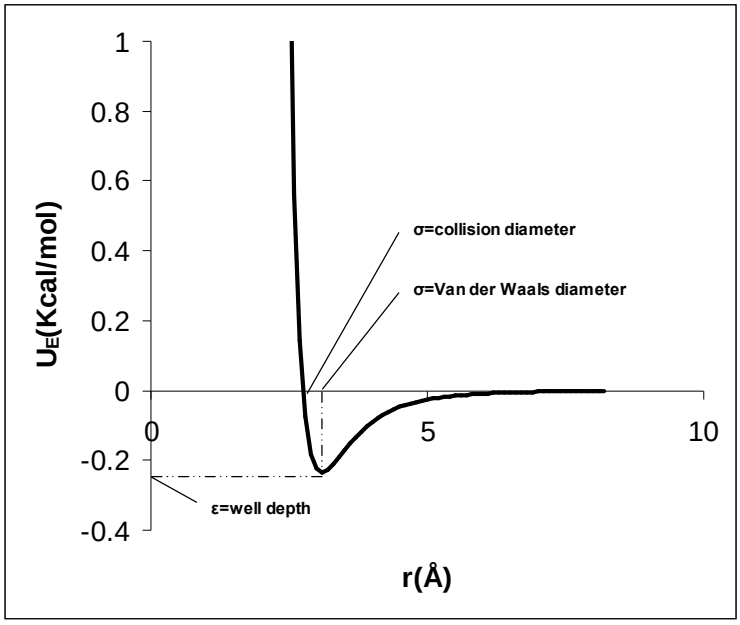

Figure 5-4: Van der Waals interactions between two carbon atoms in carbon dioxide molecule

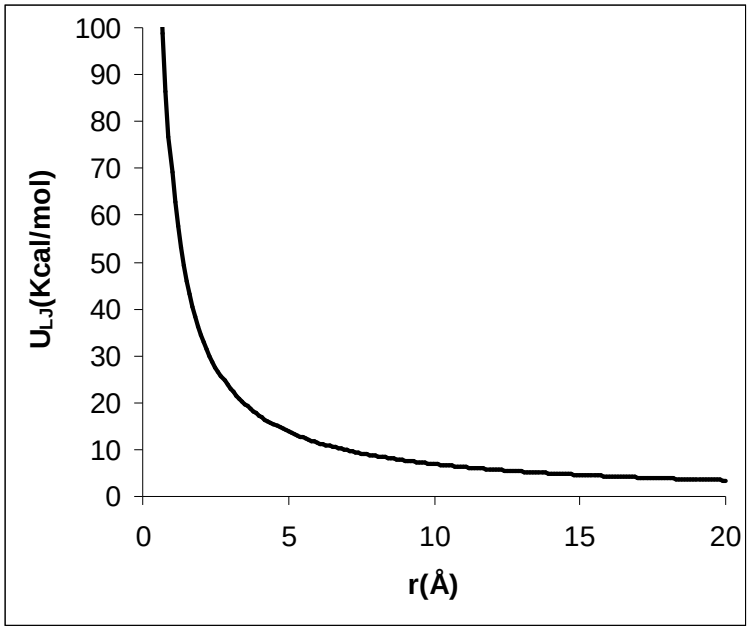

Figure 5-5: Coulomb repulsion of the two Carbons in CO_2

5.4.1 Van der Waals interactions

It is known that long range contributions have a significant influence on the simulation of inhomogeneous systems, even with large number of molecules used in the simulation.

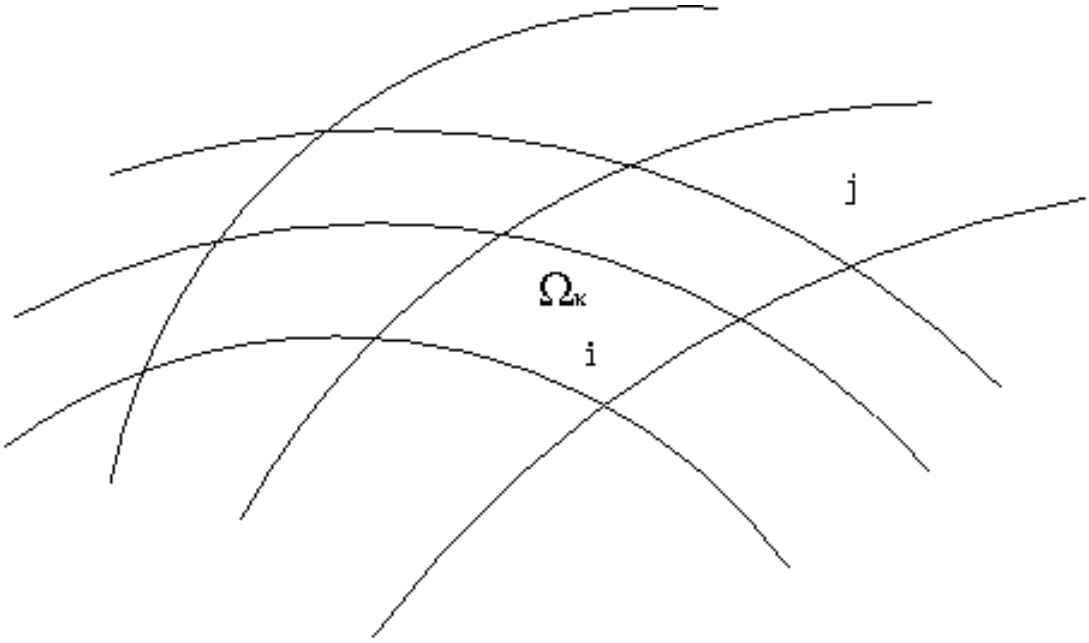

Figure 5-6: A two dimensional diagram of an inhomogeneous system. In the Ω_κ physical space there, M elements interact with elements with the other elements of different physical spaces

For an inhomogeneous fluid system, the total long range corrections (LRC) X_{LRC} to an extensive thermodynamic property X is estimated in terms of all the local values X_{LRC}

$$X_{LRC} = \sum_{k=1}^{M} x_{LRC}(\Omega_\kappa) \tag{5.10}$$

where Ω_κ is the physical space occupied by the κth local element having a uniform density and M is the total number of local elements, like the Figure 5-6. In the presentation of Figure 5-7, the term LRC refers to the LRC from Van der Waals interactions. For a molecular system, the LRC to the Van der Waals configurational energy of a molecule i interacting with molecules (molecule j) in the κth element, is expressed by

$$U_i^{LRC} = \sum_{k=1}^{M} \Delta u_{ij}^{\kappa,LRC}(i, dV_{\kappa_{th}}) \tag{5.11}$$

where $\Delta u_{ij}^{\kappa,LRC} = \int_{dV_{\kappa th}} u_{ij}(r)\rho_j(dV_{\kappa th})dV$.

The $\rho_j(dV_{\kappa th})$ is the density of the fluid in a volume element dV away from the central molecule **i** in the $_{\kappa}$th local region, $u_{ij}(r)$ is the pair potential function, r is the distance between the central molecule i and another molecule j in dV .

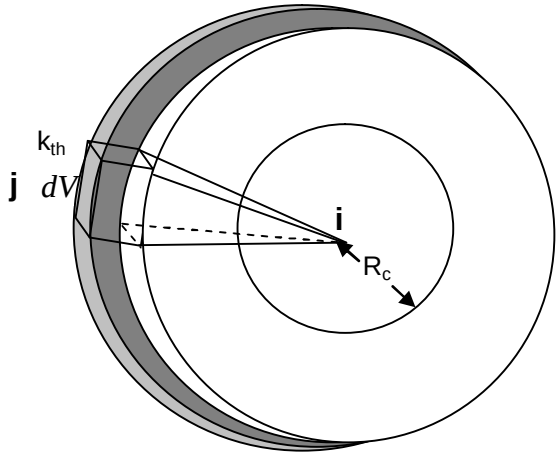

Figure 5-7: The molecule i interacts with the molecules in the molecules within the $_{k}$th element, volume dV. The element is outside the cutoff and Rc is the cutoff.

Assuming a homogeneous system, ρ_j is equal to bulk density ρ, so we can recover the standard expression for long range corrections to the energy of molecule *i* used in bulk simulations by evaluating following integral:

$$U_i = \rho \int_{rc}^{\infty} 4\pi r^2 u(r)dr = (\frac{8}{9}\pi\rho r_c^{-9} - \frac{8}{9}\pi\rho r_c^{-3}) \tag{5.12}$$

The assumption is valid for our system as the potential function $u(r)$ decays very quickly.

5.4.2 Electrostatic interactions

Although the Ewald summation method can be used to estimate the long-range electrostatic interactions with results similar to that the reaction field method (Hirst, 1985; Kettler *et al.*, 2002; Lisal *et al.*, 2002), it is computationally expensive. Therefore, the reaction field method is selected to handle the long-range electrostatic forces in this work. In this method, the long range corrections is given by

$$U_{Coul} = \sum_{i \in I} \sum_{j \in J} q_i q_j \left[\frac{1}{r_{ij}} + \frac{\varepsilon_{rf} - 1}{2\varepsilon_{rf} + 1} \frac{r_{ij}^{\,2}}{r_{cut}^{\,3}} - \left(\frac{1}{r_{cut}} + \frac{\varepsilon_{rf} - 1}{2\varepsilon_{rf} + 1} \frac{r_{cut}^{\,2}}{r_{cut}^{\,3}} \right) \right] \tag{5.13}$$

where i and j are the interaction sites on two different molecules I and J respectively, ε_{rf} and r_{cut} denote the reaction field dielectric constant and the cutoff distance, respectively. ε_{rf} is assumed to be infinity and this conducting boundary ($\varepsilon_{rf} = \infty$) leads to both reasonably consistent results and good computational efficiency.

6 COMPUTATIONAL IMPLEMENTATION

In this chapter, technical details of the Monte Carlo and molecular dynamics simulations are presented. We describe the approach used to perform Monte Carlo simulation in terms of code developing. Programs to accomplish simulations were all written in the programming language FORTRAN 90 and they were then executed on some full-size servers like C^3, Xenon, Plato and Socrates at University College London. Modified modules from the Dynamo library (Martin and Martin J.Field, 2000) and modified programs from Allan and Tildsley's book (Allen and Tildsley, 1989) were used to support the code development. The NAG compiler was utilized to run the programs on these servers.

6.1 ALGORITHM DEVELOPMENT

The algorithm below describes the Monte Carlo pseudo code in canonical ensemble. The code developing was a rigorous task, since the MC simulation needs enough space and time even for a single run. In order to describe the code developing we give below an overview of the primary parts of the code scheme.

Initialisation:

Part 1 Assign initial coordinates r_{xi}, r_{yi}, r_{zi} for the N atoms, N, V, T.
Evaluate and store U_{Total}

Part 2 **Production: Generate Markov Chains**
Assign values for *Ncycles, Nsteps.*
loop $n \leftarrow 1 \ldots NCycles$
loop $n \leftarrow 1 \ldots Nsteps$

Part 2.1 **Generate a trial position:**
$r_{xTrial} \leftarrow (r_{xi} + r_{Max} \text{ x } (2 \text{ x rand() } -1))$
$r_{yTrial} \leftarrow (r_{yi} + r_{Max} \text{ x } (2 \text{ x rand() } -1))$
$r_{zTrial} \leftarrow (r_{zi} + r_{Max} \text{ x } (2 \text{ x rand() } -1))$

Part 2.2 **Calculate energy of molecule i at the trial position:**
$(U_{trial}i)$

Part 2.3 **Calculate change in the energy:**
$\Delta U \leftarrow U_{trial}i - U_i$

Part 2.4 **Apply acceptance criterion:**
if $(\Delta U < 0)$! accept new position
$r_{xi} \leftarrow r_{xTrial}$
$ry_i \leftarrow r_{yTrial}$
$rz_i \leftarrow r_{zTrial}$
$U_i \leftarrow U_{triali}$
$U_{total} \leftarrow U_{total} + \Delta E$! update energy.
else
$BF \leftarrow \exp(-k_B \Delta U)$! Boltzmann factor
if $(BF >$ rand()) ! accept new positions
$r_{xi} \leftarrow r_{xTrial}$
$r_{yi} \leftarrow r_{yTrial}$
$r_{zi} \leftarrow r_{zTrial}$
$U_i \leftarrow U_{triali}$
$U_{total} \leftarrow U_{total} + \Delta U$!update energy.
end if
end if
if $(n > NEquilibrium)$!end of equilibrium period

Part 3 **Accumulation :Accumulate averages**
end if
end *i* **loop**
End *n* **loop**

An explanation of each part displayed in the algorithm is given in the next three parts initialization, production and accumulation.

6.2 INITIALIZATION

The initialization procedure is consisting of two steps. The first one is building the simulation box and the second one, calculating the total potential energy of the system.

6.2.1 Solvent Box

It is very important, how we are creating the first simulation box. The approach adopted for the determination of the coordinates of the molecules in the box is to start off by placing molecules at random within a box much larger than a box of the target size. The coordinates of atoms are stored in a large Fortran 90 array: ATMCRD (1:3, 1:NATOMS).

The size of the large box is then gradually reduced until the target size is reached. The reason for starting off with a large box size is that the probability of having molecules overlap will be small. The initial box length was ten times the target length and the reduction procedure was carried out in ten steps. The number of ten steps has been chosen arbitrary, the more steps the better is but they increase the computational time. After the reduction procedure, the solvent box will have attained the desired volume but the molecules will be by no means fully equilibrated. Thus, the procedure finishes by performing a long Monte Carlo simulation, before writing out the final coordinates to an external file. The coordinates of the last file can be considered as an equilibrated box. Molecular dynamics can be used for the equilibration of the initial box. A different approach is to start all the molecules from a lattice. As moves progress, the lattice “melts” and a simulation box is obtained. The initial period of the simulation is an equilibration period, and must be discarded. We

know that the final result should be independent of the starting configuration, so we checked this by checking the results with using different initial boxes.

As pointed out before, the choice of number of molecules is crucial for the calculation of any thermodynamic property. We choose to use 1000 solvent molecules as a solvent box. The number 1000 is chosen as it is sufficient to describe the system and efficient for keeping down the computational time. Furthermore, other research groups use relevant amount of particles at similar conditions (Song and Maroncelli, 2003).

6.2.2 Potential Energy

The calculation of the potential energy is crucial for the Monte Carlo procedure. As we mentioned in the previous chapter, the energy is calculating by adding the energy of pairs of particles. If intermolecular interaction is restricted to pairs of N molecules, the total potential energy is obtained by summing over the contribution all of the individual pairs. A pseudo-code scheme for the calculating the total energy is given below:

loop i ←1 ... N

loop j ←1 ... i-1

Evaluate r_{ij}.

Evaluate $u(r_{ij})$.

Accumulate energy.

end j **loop**

end i **loop**

The above pseudo code illustrates the nesting of loops required for the Naïve evaluation of energy by equation (5.1). If there are N molecules in the simulation, then to calculate the pairwise energy experienced by each other molecule involves a

summation of N - 1 terms. Care is taken to avoid identical molecules and a total of N(N-1)/2 iterations will be performed. At Fortran 90 code, the above was implemented with the following statements:

```
! . Outer loop over the molecules.
DO IMOL = 1,NMOLECULES

! . Get the some data IMOL(position)
CALL POSITION (IMOL)

! . Pick the center of the molecule.
 X=
 Y=
 Z=

      ! . Inner loop over the molecules.
      DO JMOL = 1,(IMOL-1)

      ! . Get the some data JMOL(position)
      CALL POSITION (JMOL)

      ! . Pick the center of the molecule.
      X=
      Y=
      Z=


      ! . Calculate the distance between the molecule centers
          rxij=
          ryij=
          rzij=
      ! . Applying the minimum image convention
          rxij=
          ryij=
          rzij=
     . . .

     . . .

      END DO

END DO
```

To calculate the intermolecular interaction of any molecule, we position it at the centre of a box with dimensions identical to the simulation box. The central molecule interacts with all molecules whose centres fall with this region, i.e., the closest periodic images of the other N - 1 molecules. This can be coded in FORTRAN using the intrinsic anint(x) to determine the nearest integer of x. For example, to add

the correct number of box lengths to the molecular coordinates r_{ij} or the pair separation vector, we write:

```
rxij(i) = rxij(i) - boxl * anint( rxij(i) / boxl )
```

The above statement is evaluated in the loop, during the evaluation of energies. The procedure for calculating the energy using periodic boundary conditions is given below.

loop i ←1 ... N

loop j ←1 ... i-1

Evaluate r_{ij}.

Convert r_{ij} to its periodic image (r_{ij}).

if (r_{ij}< cut_off_distance)

Evaluate u (r_{ij}').

Add corrections to energy.

end if

end j **loop**

end i **loop**

The above algorithm is different from the naïve approach in two important respects.

a) The accumulated energy is calculated for the periodic separation distances. Secondly,
b) Only molecules separated by a distance less than the cut-off distance contribute to the calculated energy or forces.

The cut-off distance is a consequence of the periodic boundary conditions. It can be any distance up to half the length of the simulation box. A higher cut-off is not permitted because it would violate the minimum image convention. Consequently, the above algorithm evaluates the properties of a truncated intermolecular potential rather

than the full potential. When PBC are used, the full contributions of the intermolecular potential have to be obtained by using long-range correction terms. The full energy was obtained by adding the long-range correction. The contribution of the long-range correction was implemented into the loops though equations (5.12) and (5.13).

6.3 PRODUCTION

The Monte Carlo simulation was performed in blocks (Part 2).Every block consists of number of steps. During each step, a displacement and rotation is attempted for every molecule (Part 2.1). The molecule to be displaced is chosen randomly. It also possible to displace every particle and apply the acceptance criterion to the combined move. This procedure has not been chosen, as it increases dramatically the computational time. The displacement of the molecule is coding though:

1. Choosing a molecule at random.

```
Choosen= INT ( NMOLECULES * rand(iseed))
```

Essentially, the above statement multiply the number of molecules (`NMOLECULES`) with a random number (`rand(iseed))and the INT function` converts the result to an integer.

2. Displacing the molecule.

```
rxtrial = rx(i) + (2.0 * rand(iseed) - 1.0) * drmax
rytrial = ry(i) + (2.0 * rand(iseed) - 1.0) * drmax
rztrial = rz(i) + (2.0 * rand(iseed) - 1.0) * drmax
```

where `drmax` a parameter, controls the “length” of the attempted, `rand(iseed)`is a function for generating random number between 0 and 1.The rand is equal to the fuction `RANDOM_NUMBER()`in Fortran 90. The `iseed` is the starting number for random generator. After a displacement is made, the energy of the new

state is compared to the energy of the old state. The Metropolis selection rule is used to decide whether or not this new state is accepted

6.4 ACCUMULATION

After the equilibration time, it is important that the successive values of any observable be statistically independent when calculating mean fluctuations around average values. So the calculations are often carried out in series of blocks (*Nblocks*) containing a number of m steps (*Nsteps*). As the number of configurations (steps) in each block increases, it would be expected that the block averages become uncorrelated and successive values become independent. We monitored the potential energy U by plotting in MS excel (see Figure 7-5). A schematic diagram of evaluation of potential energy is given at Figure 6-1.

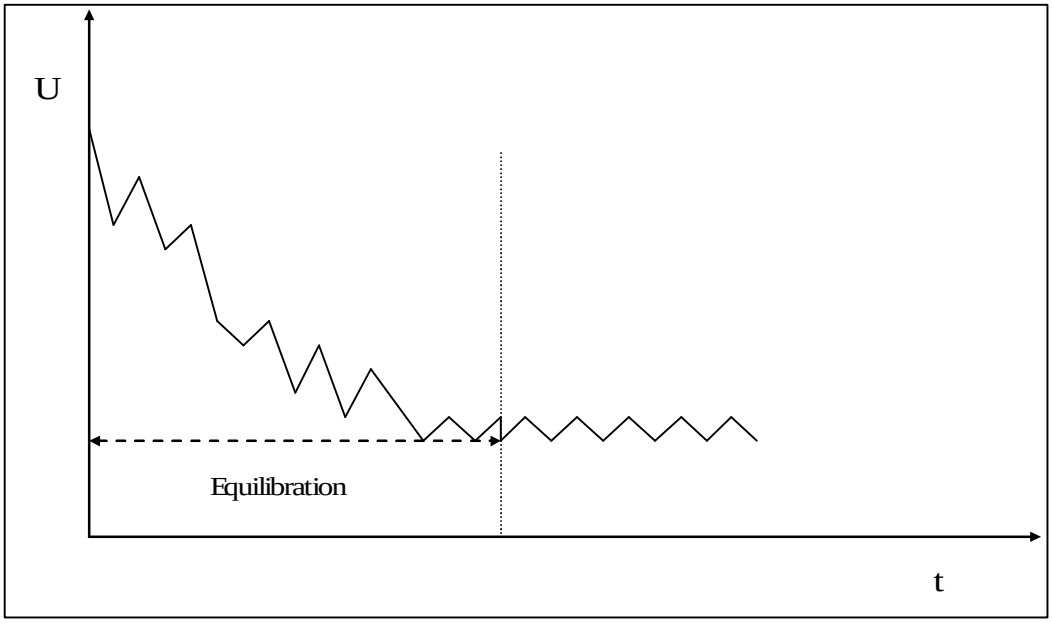

Figure 6-1: Schematic representation of potential energy during the Monte Carlo progress

6.5 TECHNICAL DETAILS

MC simulations were carried in the canonical ensemble (NVT) using periodic boundary conditions. A system with the 1000 molecules was studied at all times.

Simulations were organised in cycles, each cycle consisting of 100000 attempts to displace or rotate a randomly chosen molecule. A variable spherical cut-off radius, equal to half the box length was used and long-range corrections were recalculated after each move. Acceptance ratio of all trial moves was adjusted to 40%. In each run, more than 10^7 Monte Carlo configurations were generated to reach equilibrium and the structural and thermodynamic properties were obtained from the following 200 x 10^6 MC moves. We have studied three systems, ethane, fluoroform and carbon dioxide. Details about the potential are given in results section. The main program is given in appendix.

In all MD simulations, a spherical cut-off equal to the half of the simulation boxed is used. A time step of 2 femtosecond is used in leapfrog verlet algorithm with Berendsen thermostat (Allen and Tildsley, 1989). A time period equals to 0.5 nanoseconds is used for equilibration and 1.5 ns for production.We have studied three systems, pure carbon dioxide, mixture of methane + carbon dioxide at infinite dilution and water + carbon dioxide at infinite dilution. All simulations were performed at temperature 308.15 K (T_r=1.02) in NVT ensemble. When in the text we refer to solvent, we mean carbon dioxide except when we state differently and when we refer to solute either to methane or to water. The methane molecule was represented by OPLS-AA potential model and water by TIP3 model (see section 4.4.3 and 4.4.4). The main program is given in appendix.

Rigid molecules are being used in the simulations. The geometries of water molecule is the same with H-O bond distance of 0.9572Å and H-O-H bond angles of 104.52^o. The methane molecule has tetrahedral symmetry, with C-H bond lengths of 1.090 Å and H-C-H bond angles of 104.47^o.

Part III. Results and Discussion

7 RELIABILITY OF THE METHOD

There are two elements required to successfully predict physical properties in molecular simulation. The first part requires the development of appropriate molecular simulation techniques, in order to describe a physical system as efficiently as possible. The second part is the development or use of a suitable interaction potential model. Given the two perquisites, physical systems can be described successfully.

In this chapter, we evaluate the outcome of our Monte Carlo program by presenting the analogous results. Then, we are examining the validity of the molecular potential in the supercritical region for supercritical carbon dioxide. In this study, we have used a semi-empirical classical potential for carbon dioxide. It is an atomistic model, which is mimicking carbon dioxide geometry and quadrupole momentum. It is well known with the abbreviation EPM2 (Harris and Yung, 1995) and its parameters are adjusted to reproduce the vapour-liquid curve.

7.1 INTRODUCTION

Examining the supercritical phase, in the vicinity of the critical temperature (T_c≈1.01-1.103) though molecular modelling techniques, is a rigorous task for three reasons. Firstly, there are few experimental data because of the problems associated with observing the supercritical phase experimentally, in order to be compared with computational studies. Clearly, without a comparison to experiment, the accuracy of simulation results cannot be gauged.

Secondly, molecular simulation requires very large simulated systems (number of molecules-simulated box) because the correlation length of the system becomes macroscopic as the critical point is approached (Quirke and Gubbins, 1996), which makes simulation run's time consuming and approximations necessary on the estimation of long range interactions. Surely, the rapid growth of computers has provided scientists and engineers great advances in computational power, and has made solving of numerous variable problems possible in many cases. By applying appropriate approximations, it is now possible to run molecular simulations, which were impossible in past. Although, approximations carefully applied in simulation will not always give a complete physical picture of the real systems. In other words, molecular modelling proves itself as a valuable tool only when it is not computationally prohibitive and accuracy moves between acceptable levels.

Thirdly, there are only a few molecular potentials; they can predict the critical point accurately, being used in the phase equilibrium simulation techniques (Panagiotopoulos, 1987). Most of existing potentials were tailored to yield correct thermodynamic properties even closely to supercritical region, and never tried for liquid–vapor coexistence curve (Colina *et al.*, 2003). The use of potentials with an unknown critical point poses a high risk and can lead to flawed results, especially

when the results are compared with real data. This is not applying for the models we use in this study, the fluoroform, the ethane and the carbon dioxide as their potentials are describing properly the vapour-liquid curve.

7.2 EVALUATION OF THE METHOD

In order to check the reliability of our code and our approximations in the implementation, we run simulations for fluoroform and ethane near their critical points. We checked our results against the simulation results of Song and Maroncelli (Song and Maroncelli, 2003). A standard output during an NVT Monte Carlo simulation is the potential energy. Song and Maroncelli performed simulations for fluoroform and ethane in the supercritical region by employing molecular dynamics. The potential energies are given by them as an ensemble average.

Their simulations were carried out at 310K on a sample of one thousand molecules by using the DL_POLY package (Todorov and Smith, 2004). We performed identical simulations at the same conditions. We have chosen the study of Song and Maroncelli because they had examined in their work two completely different systems, one with very strong electrostatic interactions and an apolar one. We checked the validity of Monte Carlo program against two extreme cases.

It is believed that the long range interactions play an important role at molecular simulation at supercritical conditions (Tucker, 1999). Electrostatic interactions belong to this category and decay very slowly with long correlation lengths. Two methods (Sadus, 2007) can be used to treat long range electrostatic interactions, the Ewald method and reaction field method. In our code, we implemented the reaction field method. The Ewald method is more suitable for systems with strong electrostatics interactions (Allen and Tildsley, 1989). We implemented the reaction field method firstly, because it is computationally less

costly and secondly because our final aim is to simulate the carbon dioxide. Historically CO_2 was treated as a nonpolar solvent, primarily because of its low dielectric constant and zero molecular dipole moment. Further, the reaction field method has been used by Harris and Young group for EPM2 studies (Harris and Yung, 1995).

The reliability of our Monte Carlo code for those systems was tested successfully. The calculated configurational energy from the present Monte Carlo simulation is compared with the literature values from Song and Maroncelli in Figure 7-1 and Figure 7-2 for fluoroform and ethane, respectively.

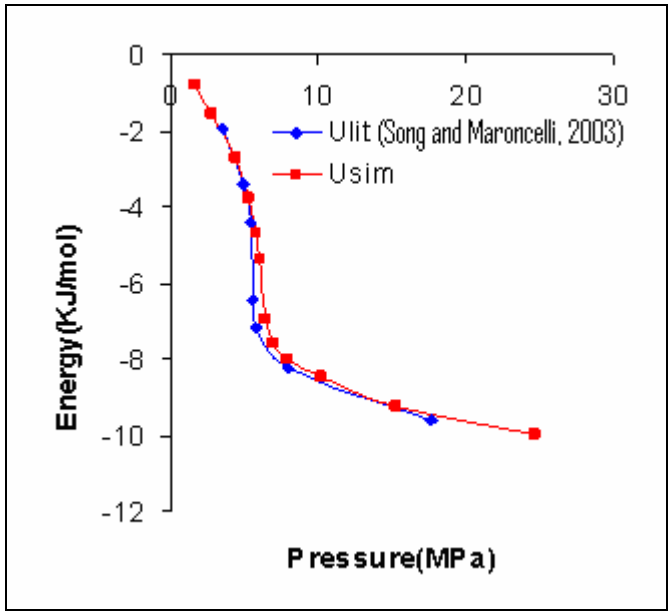

Figure 7-1: Dependence of residual potential energy with pressure along an isotherm (T=310K) for fluoroform (T_c=299.1K). Comparison between simulated literature values (Ulit) and simulated values (Usim).

The simulation was performed very close to the critical point for both of the components. However, the agreement is better for the ethane. We have expected that as ethane molecule is an apolar molecule without any electrostatic interactions near critical pressures. The small discrepancy observed for fluoroform near critical pressures can be attributed to the dominant role of the electrostatic interactions, which the reaction field method underestimates. The discrepancy is not posing any risk on

using the developed code for simulating the CO_2, as CO_2 lacks of strong electrostatic interactions. However, we can conclude that a system with strong electrostatic interactions close to critical point is better to be treated with the Ewald method.

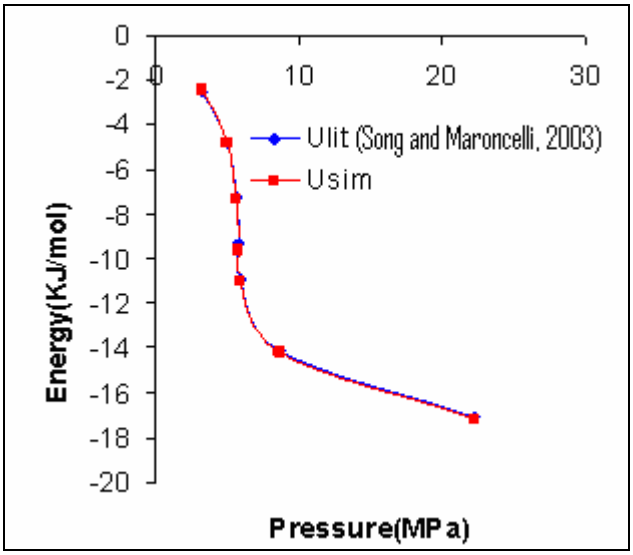

Figure 7-2: Dependence of residual potential energy with pressure along an isotherm (T=310K) for ethane (Tc=305.33K). Comparison between simulated literature (Ulit) values and our simulated values (Usim).

There was no need to check the validity of molecular dynamics since it has been used successfully by Maroncelli and Song (Song and Maroncelli, 2003) in supercritical region. Furthermore, Maroncelli and Song have used the DL_POLY code for their studies, so there is no need to test their results with DL_POLY.

7.3 EVALUATION OF THE MOLECULAR POTENTIAL

Successfully tested the Monte Carlo program, the next step is the evaluation of the interaction potential. We comprehensively evaluated different potential models proposed for carbon dioxide in our literature survey in section 4.3.3. The EPM2 which was optimised to reproduce the critical (Harris and Yung, 1995) point and liquid-vapour coexistence curve of the real fluid using the Gibbs ensemble Monte Carlo method (Skarmoutsos *et al.*, 2005) matches the purposes of our study. The aim of our evaluation is to examine the validity of EMP2 in supercritical region by simulating its

configurational energy, before its adoption and systematic use for evaluating thermodynamic and solutions properties.

7.3.1 Experimental Configurational Energy

The internal energy data for the single component CO_2 were obtained from the NIST database (2006). The NIST database uses the Span-Wagner equation of state, which is the current standard for CO_2 and it is accepted as essentially equivalent to experimental data.

In order to calculate the ideal part of the internal energy, we assume the classical approximation of statistical mechanics where one hypothesises that the energy for a system can be written as sum of energies, each comes from a different property of the system. Within this approximation, the ideal partition function can be written as a product of the partition functions pertaining to the different types of energy. In the case, of a polyatomic gas like CO_2 the ideal partition function is a product of electronic, nuclear, rotational, translational and vibrational partition functions (McQuarrie and Simon, 1999). In that case the ideal part of the internal energy is given by the equation (Van P.Carey, 1999)

$$\frac{U}{Nk_BT} = \frac{5}{2} + \sum_{j=1}^{3n-5}\left[\frac{\theta_{vib,j}/T}{2T} + \frac{\theta_{vib,j}/T}{e^{\theta_{vib,j}/T}-1}\right] - \frac{D_e}{k_BT} \qquad (7.1)$$

The experimental potential energy is obtained from the total experimental potential energy (NIST database) by subtracting the ideal part, which calculated through equation (7.1).

The potential energy for the single component CO_2 was calculated through three methods:

1) Monte Carlo simulations in NVT ensemble conditions, where temperature and volume remain constant.

2) Molecular dynamics simulations in NVT ensemble conditions, where temperature and volume remain constant.

3) Using the Redlich-Kwong equation of state.

7.3.2 Simulated Configurational Energy

The internal energy using Redlich-Kwong equation of state has been represented only in the terms of potential energy and can be given as (Van P.Carey, 1999)

$$U_{EOS} = -\frac{3a_R N}{2b_R T^{1/2}} \ln\left(\frac{V + Nb_R}{V}\right) \tag{7.2}$$

where, N is the number of molecules, T is the temperature, V is the volume and a_R and b_R are constant, which depends on the critical temperature and pressure of the fluid. The value of a_R and b_R for carbon dioxide that have been used in order to calculate the potential energy are, 18 x 10^{-48} (Pa m^6 $K^{1/2}$ / $molecule^2$) and 4.93 x 10^{-29} (m^3 / molecule) (Van P.Carey, 1999), respectively.

For both MD and MC we used the same set-up and the results were obtained at constant temperatures of 308.15 K. Under the respective isothermal conditions, the pressure was varied in the ranges 2 to 12 MPa. The temperature is 4K above ($T=1.02T_c$) the critical temperature of carbon dioxide (T_c=304.1 K), while the pressure varies from a point below the critical to one above the critical pressure of carbon dioxide P_c=7.38 MPa. The results for configurational energy have been compared with the experimental data we calculated from NIST. The objective behind computing the potential energy and comparing them with experimental data is to check the viability of the potential model EPM2. The comparison has been represented through graph in Figure 7-3 and Figure 7-4 in two different graphs which allows making a better assessment and easy understanding.

Comparison of the results obtained by MC, MD and Equation of States (EOS) with experimental database, establishes a good agreement between MD and experimental results from low to high densities. Hence, molecular dynamics technique is reliable in predicting different properties, if a correct potential model is used. Usage of the EPM2 model for predicting potential energy of CO_2 also seems to be very valid.

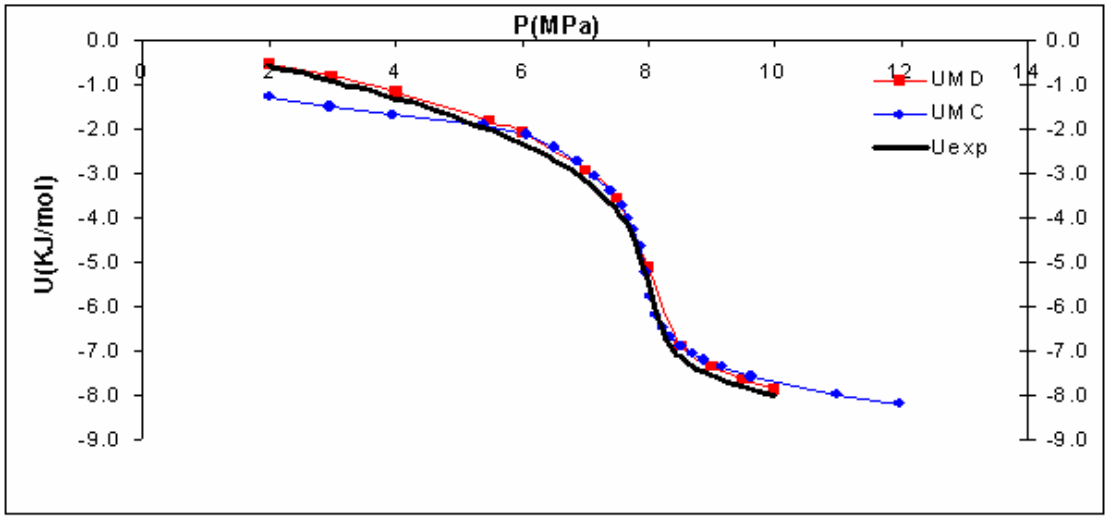

Figure 7-3: Comparison of Configurational calculated through MC and MD with Experimental values at T = 308.15 K for CO_2

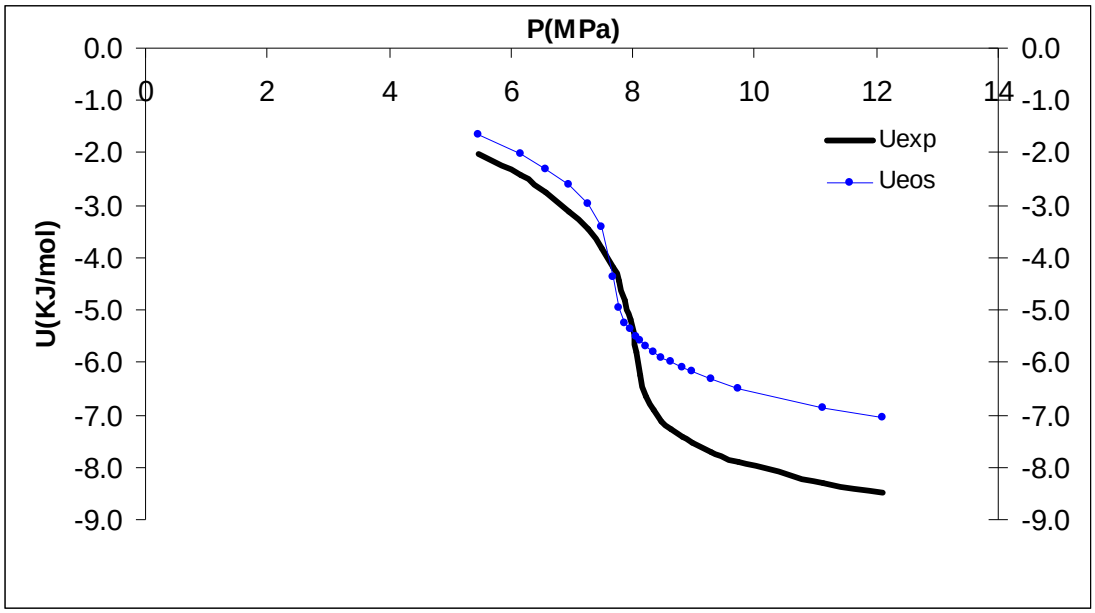

Figure 7-4: Comparison of Configurational calculated through EOS with Experimental values at T = 308.15 K for CO_2

The MC results are close to the experimental ones even at pressures near the critical. More specifically, the MC results match well with experimental values and MD predictions expect the low pressure region. The fact that the MC and MD, two different methods which give almost same results for predicting the potential energy, proves that the molecular potential is valid and can be used for describing the CO_2 in the supercritical region. In the case that the molecular potential has a weakness both methods should give flawed results.

On the other hand, the EOS results are deviating considerably from experimental ones. Traditionally, the performance of EOS has been improved by introducing many interaction parameters (Lue and Prausnitz, 1998) for studying pure solvents and mixtures in the supercritical regime. However, the use of a simple EOS is inadequate to predict even simple thermodynamic properties like internal energy and density, like the one we observe for the case of internal energy Figure 7-4. The results predicted with EOS deviate significantly at pressure above the critical, since the packing of molecules increases quickly with pressure and the Van der Waals theory of EOS meets its weakness.

Conventional Monte Carlo technique except the low pressure region, can be used as a tool for studying difficult systems, like supercritical fluids in comparison with EOS. Furthermore, it gives us an insight to the systems on atomic scales, which can be used to establish a relationship between intermolecular potential and thermodynamic properties. Molecular dynamics technique can be improved with using methods that are more sophisticated on integration algorithms; however, it is adequate for studies in supercritical region for carbon dioxide even for low pressures. In the next section, we discuss the Monte Carlo limitation at the low pressure region.

7.3.3 Molecular Dynamics vs Monte Carlo

Despite the great validity of MC and MD, during Monte Carlo simulation near the critical point, we did come across an unexpected situation, at low densities. The Monte Carlo method does not properly predict the configurational energy of the system, despite the fact that the molecular dynamics results agrees well with the experimental ones. As we have justified that, the molecular potential we used is adequate to describe the CO_2 in the supercritical region, so the inadequacy belongs to the Monte Carlo method.

Despite the identical procedure (system set up, representation of molecules, periodic boundaries conditions, long range corrections) the potential energy of the system, which calculated through molecular dynamics, agrees well with experimental, but Monte Carlo does not. In view of the importance of these methods, there has been surprisingly little research carried out comparing their efficiencies (Jorgensen and Tirado-Rives, 1996). Another fact is that the discrepancy of Monte Carlo and molecular dynamics can not be attributed to long range interactions of the model. As the research group (Kettler *et al.*, 2002) of Kettler studied the effect the of long range corrections on the EPM2 molecular potential and they concluded that their effect is not important, their findings are in accordance with our opinion as CO_2 lacks of strong electrostatic interactions.

The procedure which has been used to build up the initial configuration described in the section 6.2 .We present the evaluation of the configurational energy with the progress of the Monte Carlo (successive steps) at the lowest density ρ=37.94 Kg/m^3 in Figure 7-5. In order to investigate this peculiar effect we used the last configuration produced through the Monte Carlo simulation to start a molecular dynamics simulation and we left the system to equilibrate. After the equilibration, the system ends up with a different configurational energy.

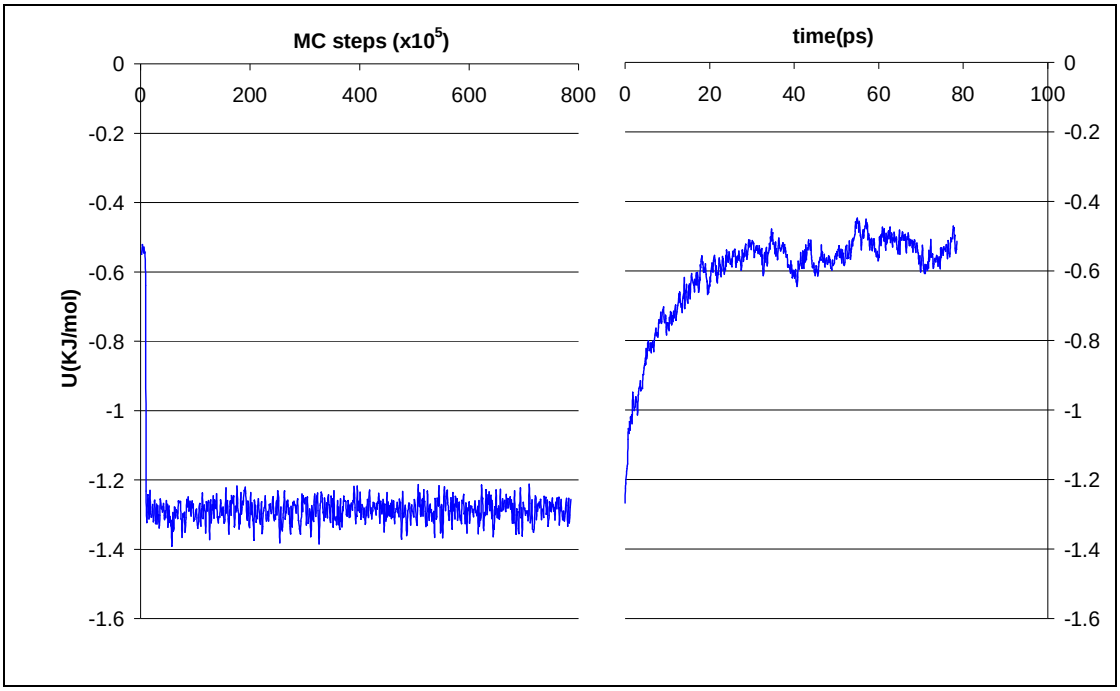

Figure 7-5: Evaluation of the configurational energy at Pressure P=2MPa during progressive configurations left) Monte Carlo simulation right) molecular dynamics simulation. The same system equilibrates at different value of configurational energy. (A small part of MD simulation is shown in figure for a better representation)

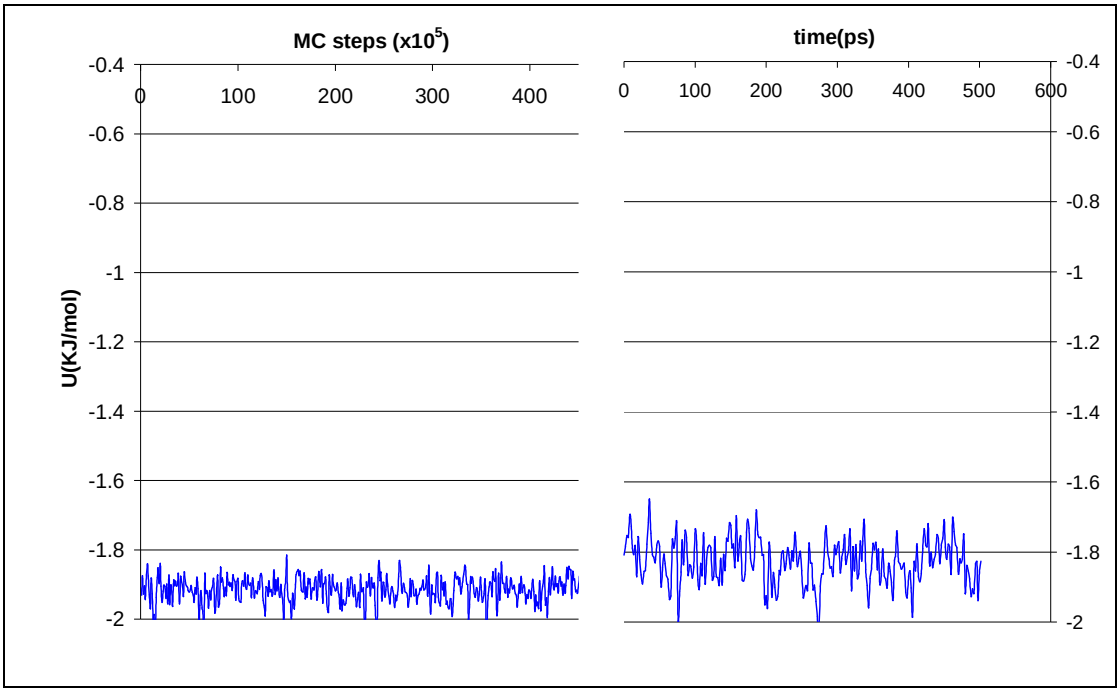

Figure 7-6: Evaluation of the configurational energy at Pressure P=5.5MPa during progressive configurations left) Monte Carlo simulation right) molecular dynamics simulation. The same system equilibrates at same value of configurational energy, but molecular dynamics simulation is sampling systems in a greater range.

We did exactly the same for higher pressures and we present the results for pressure P=5.5 MPa in Figure 7-6. At this pressure, the Monte Carlo configurational

energy starts to diverge from the molecular dynamics one as we move to lower pressures. Traditionally, the Monte Carlo has a weak performance (Kofke, 1993) with simulation of systems at low density (gas phase) and strongly associating fluids, in which molecules can find each other to bond. In other words, there are regions of phase space having a large contribution to the properties of the system, but the simulation cannot find them. In our case we believe that this discrepancy between Monte Carlo simulation and molecular dynamics is problem is attributed to the nature of the Monte Carlo simulation.

In the Metropolis algorithm, the criterion of the acceptance of a random generated configuration depends on its energy, since the fixed variables in the canonical ensemble are the number of particles, volume and temperature. We believe that the problem is that the Markov chain process does not properly represent the statistical distribution of states for energy particularly for low densities.

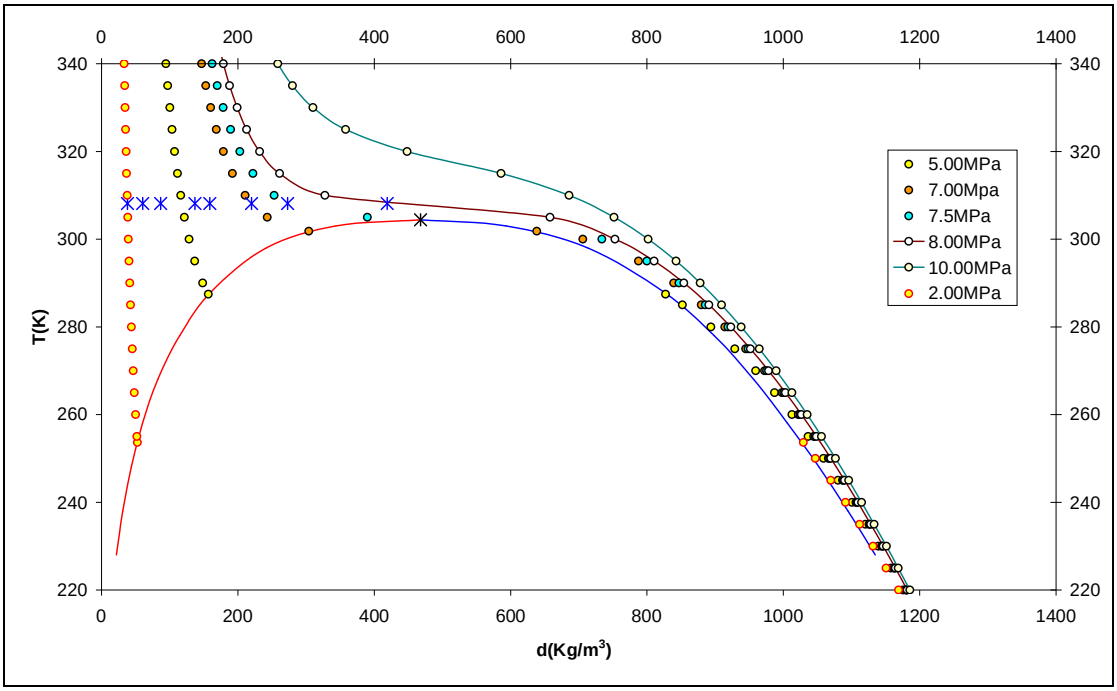

Figure 7-7: Phase diagram for carbon dioxide the blues marks indicate the points we performed molecular simulations at low densities

The conventional Metropolis algorithm used in Monte Carlo molecular simulations requires molecules undergo random unphysical movements and the moves are only accepted based on the system temperature and the energy change of the move. The unphysical nature of MC moves is the only difference of the Monte Carlo method as it allows moves, which would not happen, in molecular dynamics. In order to comprehend, it is better to look at the points we performed simulations and their location on the phase diagram in Figure 7-7. The discrepancy starts to happen at $\rho=0.3\rho_c$ and lower densities.

Let us, assume that one performs two Monte Carlo runs at two different temperatures in the NVT ensemble, sets up the same initial configuration and observes the energy of the systems during the Monte Carlo progress.

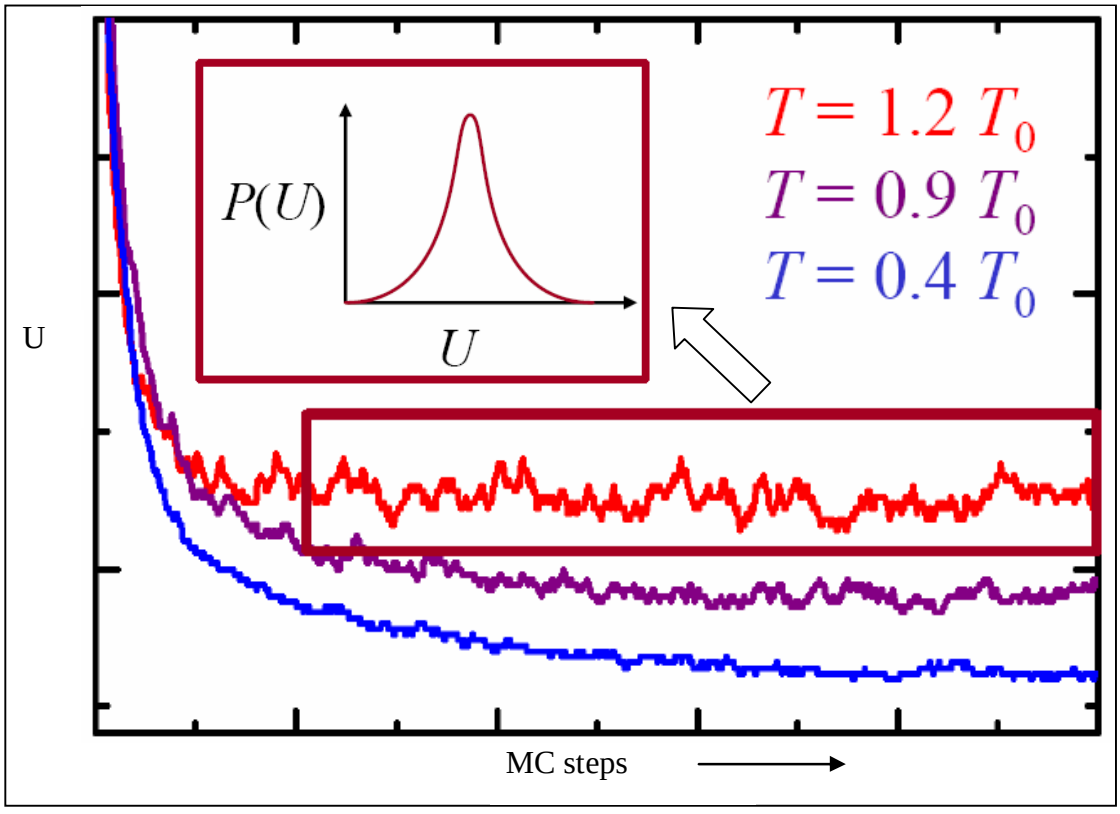

Figure 7-8: Schematic representation of the configurational energy during the Monte Carlo progress at two different temperatures. The figure inside represents the probability functions of each value of the configurational energy.

The deviation should satisfy a Gaussian distribution. The standard deviation of energy in a canonical ensemble is illustrated in Figure 7-8. Given two pairs of data (T_1, U1) and (T_2, U_2) we will extract a relation between U_1 and U_2 at those two different temperatures, using the thermodynamic definition for the constant volume heat capacity C_v:

$$C_V = \left(\frac{dU}{dT} \right)_V \tag{7.3}$$

where U now is the total energy of the fluid.

Considering the assumption that the ideal heat capacity is independent of temperature, the relation between U_1 and U_2 takes the form below

$$U(T_2) = \int_{T_1}^{T_2} C_V(t)dt + U(T_1) \tag{7.4}$$

in the case, that the constant heat capacity is independent of temperature or it changes insignificantly, the corresponding relation being

$$U(T_2) \approx C_V(T_1) \cdot (T_2 - T_1) + U(T_1) \tag{7.5}$$

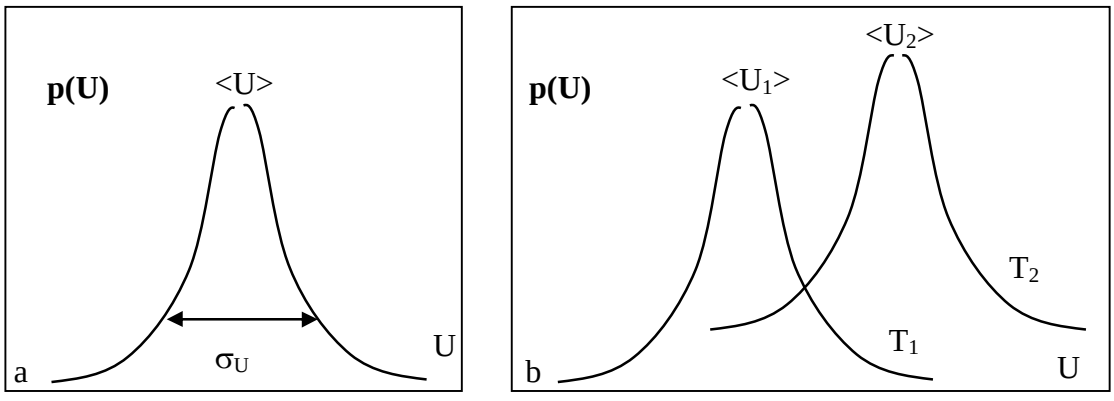

Figure 7-9: A schematic view of the configurational energy distribution function, σ_U the standard deviation of the potential energy U b.) The energy distribution functions are merely overlapping. The mean average of the potential energy increase with temperature

Coming back to our problem, the potential energy distributions overlap if one runs two Monte Carlo simulations in the canonical ensemble at close temperatures as shown in Figure 7-9. It is also well known that at higher temperatures the distribution

of energy is broader than lower temperatures where is narrower and the advantage has been used at replica exchange methods.

Let us assume the case of observing the configurational energy on the critical isochore with temperature, the heat capacity diverges at $T=T_c$. If you are observing the configurational energy on an isochore, different from the critical isochore i.e. $0.8\rho_c$ the heat capacity becomes maximum at the temperature at which there is phase transition and a large difference is found between the configurational energy of the subcritical and the supercritical phase. We can qualitatively draw the temperature dependence of the internal potential energy across the critical isochore. In the range $(0.3\text{-}1\rho_c)$ the divergence of the isochoric capacity is quite large and energy which characterises the subcritical region from supercritical one is quite different, so for Monte Carlo is difficult to sample configurations which belong to lower temperatures. However, at lower densities than $\rho<0.3\rho_c$ that can happen, Monte Carlo can sample phase configurations with lower characteristic energy and can be trapped there, especially at conditions as the two first points in Figure 7-7.

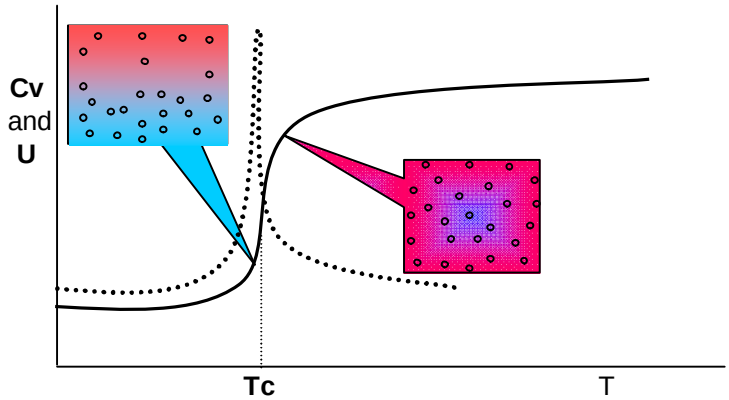

Figure 7-10: Representation of the configurations of the molecules along the critical isotherm. The blue colour indicates a high density region (liquid like) and the red colour a low density region (gas like)

Suspecting this situation, we recorded snapshots during Monte Carlo simulation progress. Indeed, the Monte Carlo samples configurations that belong to subcritical phase. In the Figure 7-11, we present a snapshot, which belongs to

subcritical region. A cross with packed molecules can be seen in the middle of the simulation box. If we suppose three axes x, y, z, which meet in the centre of the box (0, 0, 0) then a high density profile can be seen for x, y, z values around zero value of each axis. The dense area represents the liquid phase.

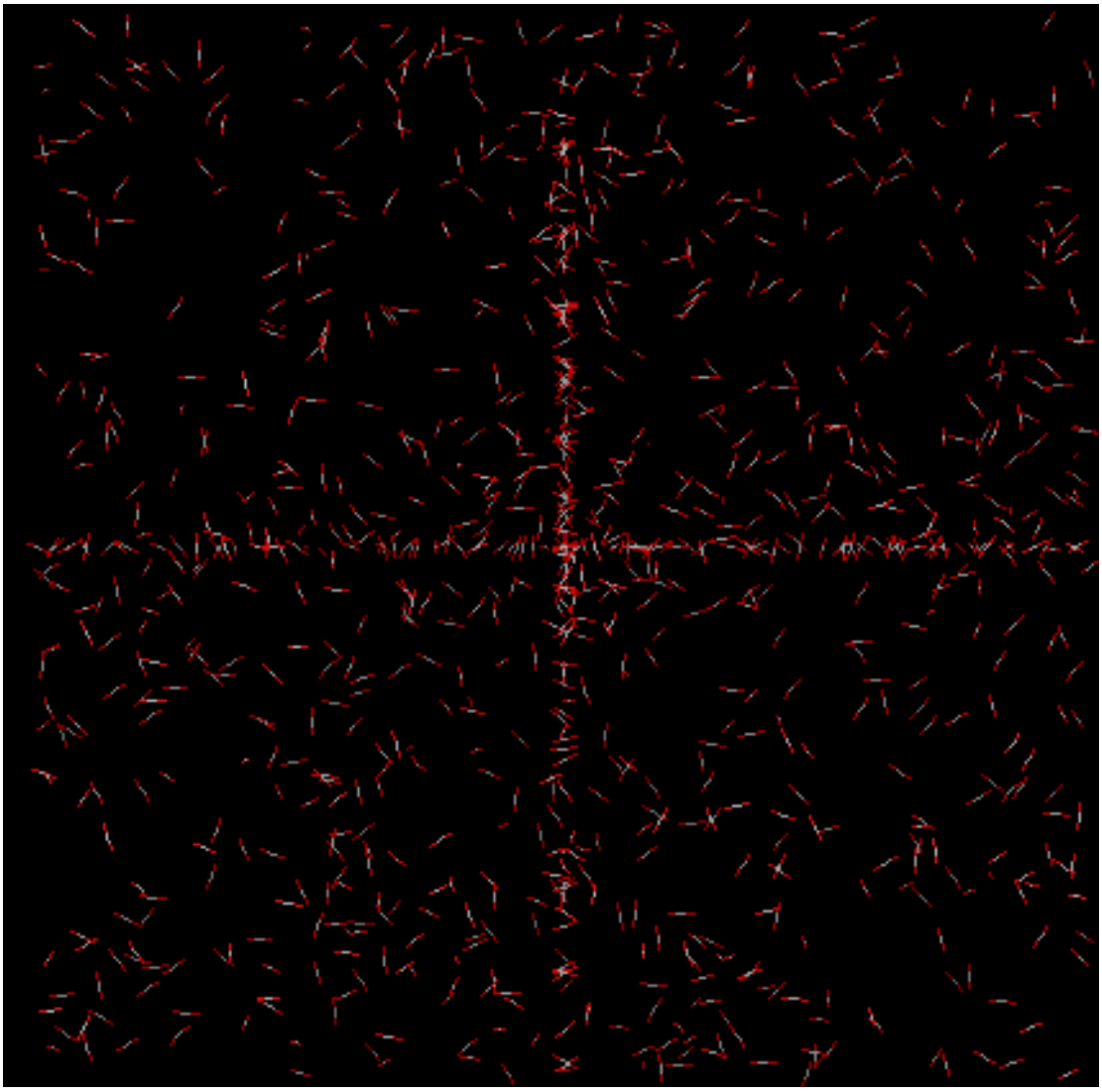

Figure 7-11: A snapshot at pressure P=2MPa and temperature T=1.02Tc. A high density region is formed in the middle of simulation box.

On the other hand, we did not face this situation with fluoroform and ethane simulations. The critical density of fluoroform and ethane is quite high, so all the simulated boxes had kept away from low region densities. Monte Carlo simulations (Song *et al.*, 2002) have been reported on isotherms close to the critical one for fluoroform, but in none of them is at a low density value.

In conclusion, we believe the proper configurations can be sampled during a Monte Carlo simulation if efficient schemes for the construction of new states can be devised. A recipe is need to discharge configurations belonging to subcritical phase.

8 THERMODYNAMIC PROPERTIES OF CARBON DIOXIDE

Investigation into volumetric and thermodynamic properties of the EPM2 model is obligatory, before its usage for studying mixtures of CO_2. In this chapter, we checked the validity of EPM2 model to reproduce thermodynamic properties accurately. The reliability of the EPM2 model is verified by simulating the volumetric properties, isothermal compressibility, isochoric heat capacity and diffusivity as a function of density at 308.15K of pure carbon dioxide. We adopted two kinds of simulation in this study: The NVT molecular–dynamics simulations and the canonical Monte Carlo simulations.

The objective of our work in this chapter is to examine the solvent microstructure on the thermodynamic properties of pure CO_2 in the supercritical region. We have focused our study in an area very close to the critical point ($T=1.02T_c$). We are going to discuss the results as an effect of density inhomogeneities in the real supercritical fluid, the **'correlation induced inhomogeitniies'** and the **'potential-induced inhomogeinities'.** The first inhomogeineities arise from the long-length-scale critical fluctuations and are maximised at the critical point. The second arises from the short-range potential interactions and tends to be maximized at rather low densities.

8.1 INTRODUCTION

Molecular potentials are an integral part of molecular simulations. It is the definition of how a molecule interacts with itself and other molecules. Various levels of complexity are available. Simple models will execute quickly but they can't describe the physical extremes. Models that are more complex will theoretically give a more accurate description of the actual molecular system, but generally take a long time to run. Molecular model EPM2 has chosen for our simulation purposes, since it captures its internal energy and runs in a reasonable amount of time. In the previous chapter, we examined the validity of the model by investigating the reproduction of the potential energy of the model close to the critical isotherm and we verified its appropriateness. In this chapter, we extend its validity by examining its performance on predicting thermodynamic properties near the critical point.

8.2 VOLUMETRIC PROPERTIES

Over the last century, a number of efforts have been devoted to the measurements of volumetric properties of carbon dioxide. In 1996, Span and Wagner (Span and Wagner, 1996) systematically reviewed the available experimental densities over wide range of temperatures and pressure from the triple point to 1100K and 800 MPa and they introduced a very accurate equation of state. The National Institute of Standards and Technology (NIST) approves the equation of state for CO_2 was developed by Span and Wagner as the current standard.

As mentioned, we have carried out a series of NVT-MD simulations of $scCO_2$ in a range of from 60.49 kg/m^3 to 769.3 kg/m^3 at temperature 308.15 K. Figure 8-1 shows the simulated pressures as a function of densities in comparison with values

predicted from the Span-Wagner EOS (Span and Wagner, 1996) at 308.15 K and the experimental data from Zhang et al group (Zhang *et al.*, 2002c).

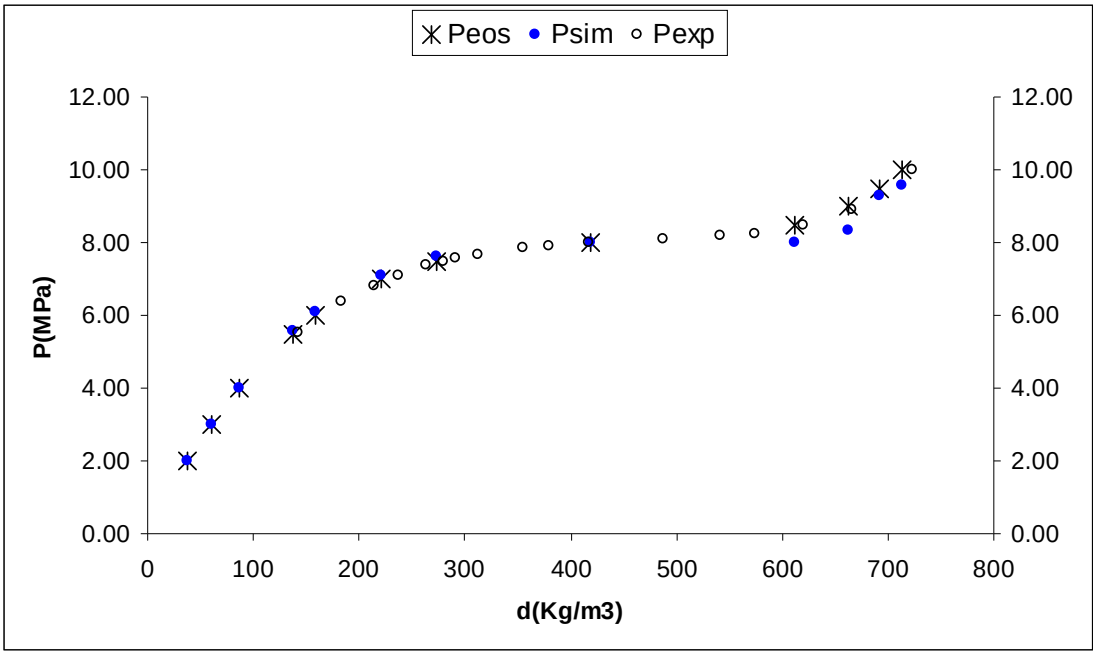

Figure 8-1: The PρT phase diagram of pure CO_2 with comparison with the predicted one from our molecular dynamics studies by using the EPM2 model at temperature 308.15 K and pressure range 2-10 MPa (Peos : values from NIST database using Span and Wagner equation of state, Psim : simulated values, Pexp : experimental studies Zhang et al., 2002c)

The Figure 8-1 shows an excellent agreement between the literature values and our simulation, this fact is very important as it proves the EPM2 has a great performance close to the critical point in predicting volumetric properties. In this study, it was important firstly to validate the choice of the intermolecular potentials by comparison with the volumetric properties, so direct comparisons with experiments can be made. Furthermore, the result is highly encouraging towards an industrial implementation as pressure and temperature are the control parameters.

During the molecular dynamics simulations, we found that the fluctuation of the simulated pressure increasing with the increase of density as we expected as pressure is proportional to the derivative of energy. The application of pressure to gaseous substances causes a significant reduction in the intermolecular distances. The structure is changing from gaseous to liquid-like structure. The packing of molecules

is increasing with density. A small change of the position of a molecule at packing conditions gives a higher change in potential energy and consequently higher fluctuation values for pressure. We present below the fluctuation of pressure at two different points. As the estimation of pressure is an ensemble average, we can conclude that longer simulations are required at higher densities.

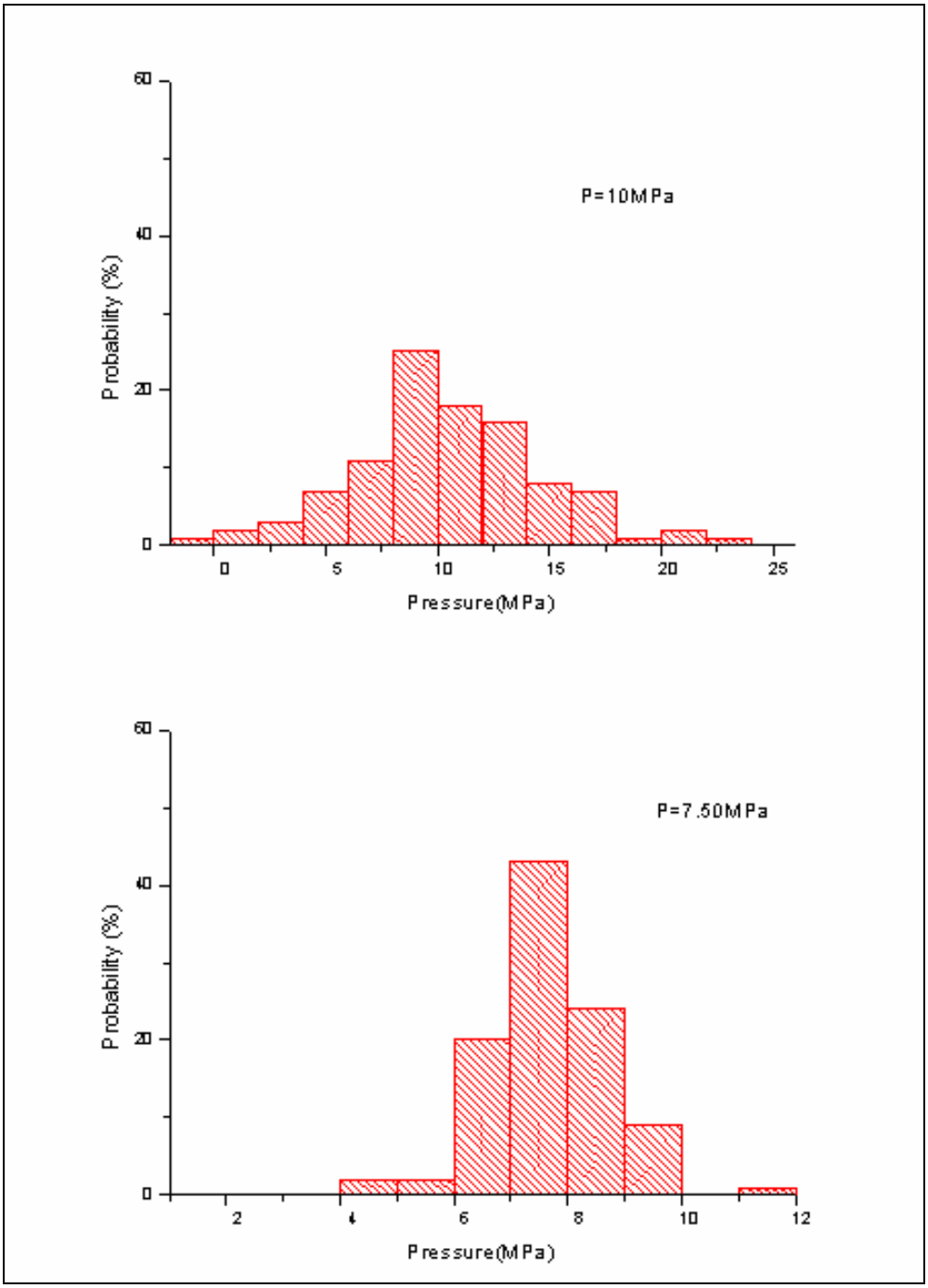

Figure 8-2: Distribution of pressures at two different simulated points.

8.3 STRUCTURAL PROPERTIES

The CO_2 radial distribution functions g(r) were computed from system snapshots generated in constant-NVT simulations. We calculated the g(r) both from molecular dynamics and Monte Carlo, the results we present here come from molecular dynamics simulations which both of the results were almost identical. The carbon-carbon radial distribution functions, reflecting the distributions of molecular centres of mass, over the densities ranging from 60.49 kg/m^3 to 712.91 kg/m^3 (critical density of CO_2 is 468 kg/m^3) is shown in the Figure 8-4. The radial distribution function g(r) has a value of zero for $r \rightarrow 0$, because the coincidence of molecules is not allowed by repulsion. At the lowest density considered, $g_{c\text{-}c}(r)$ is clearly gas like, but with increasing bulk density, a smooth transition is made to a distinctly liquid like form (Clifford, 1999). The peak height decreases with increasing density and a second solvation shell appears. The Figure 8-3, shows the location of the first and the second solvation shell for a typical liquid, the later the g(r) becomes equal to unity, the later the system becomes uncorrelated.

The obvious change obtained upon increasing the density is the appearance of a clear second solvation shell as ones reaches the critical density. One also finds the RDF remains distinctly greater than unity to longer distances at the critical density than it does at the other two densities shown, a result that is consistent with the presence of macroscopic correlation in an SCF in the immediate vicinity of its critical point.

The correlation length becomes maximum at the critical point which translates to large simulation boxes in order to perform simulations close to T_c and P_c but as it is obvious from the figure, the radial distribution function g(r) reaches the values of unity in the box size which means the size of the simulation box is large enough to

describe our system. Experimental (Nakayama *et al.*, 2000) studies close to the critical point reported a correlation length of 20Å. Taking the limitations of molecular simulations into consideration, our box describes properly the supercritical state.

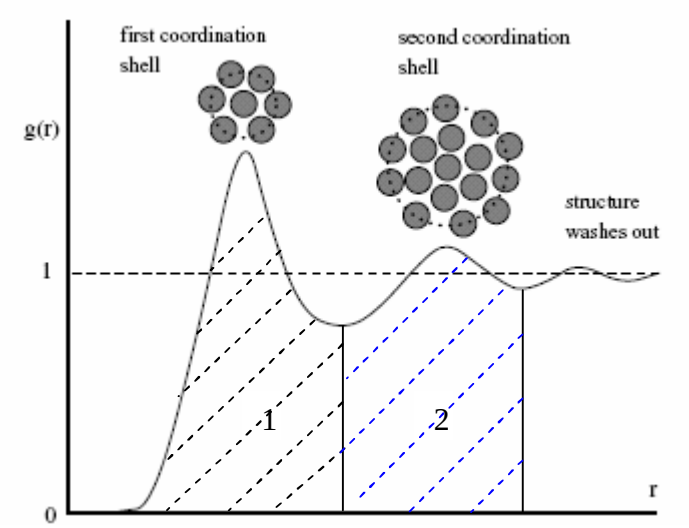

Figure 8-3: Typical form of g(r) for a liquid, we observe short–range order out to at long distances, and the structure from first and second solvation shell. This figure is present for better comprehension of g(r) functions of carbon dioxide.

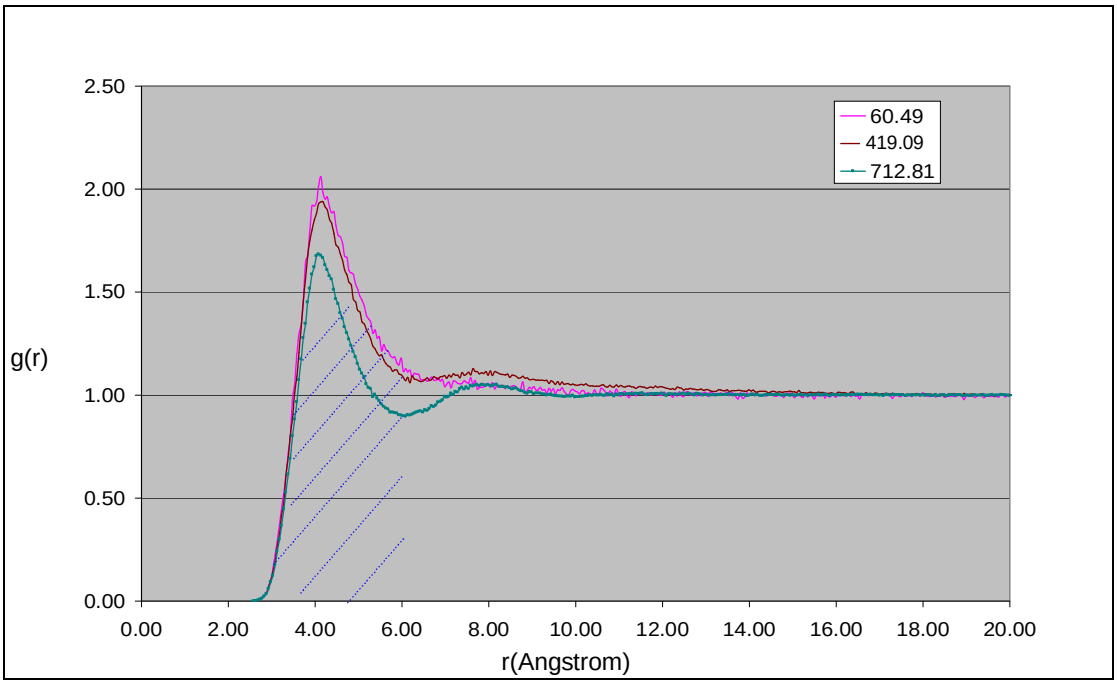

Figure 8-4: CO_2 radial distribution functions for bulk densities of 60.49 kg/m^3 (pink line), 419.09 kg/m^3 (brown line) and 712.81 kg/m^3 (dark green line) at a temperature of 308.12K. The dashed area indicates the area of the first solvation shell.

In Figure 8-5, we also present a configurational snapshot for the same density values, in order to comprehend the phase behaviour with increasing density. Increasing the

system density to the critical density increases the fraction of the total volume that may be deemed high density, but voids are still observed and a fraction of the molecules are either in low-density regions (gas like) or are on the boundary of a high density region (liquid-like). As the system is equilibrated at high densities far from the critical density, we observe only the high density region (bulk density).

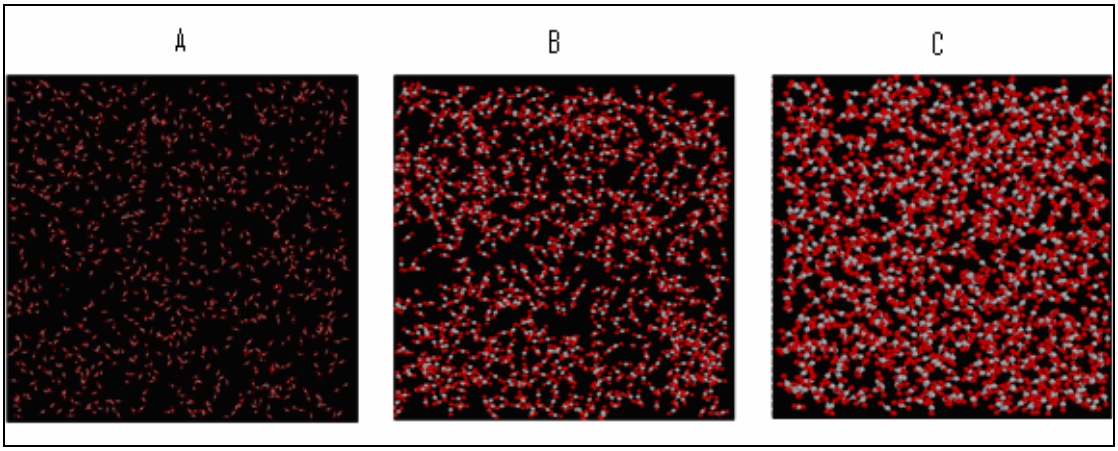

Figure 8-5: Snapshots of supercritical CO_2 at densities (in increasing order from left to right. (a) 60.49 kg/m^3 (b) 419.09 kg/m^3 and (c) 712.81 kg/m^3 each at T = 308.15 K

It is important to begin our discussion, realizing what the radial distribution function expresses. The g(r) function can be thought of as a measure of the structure in a system because, it gives the probability of finding a pair of particles a distance r apart, relative to the probability that would be expected for a random distribution with the same density. In other words, the g(r) can be written like the following equation.

$$g(r) = \frac{\rho(r)d\mathbf{r}}{\rho^{id}d\mathbf{r}} \tag{8.1}$$

where $\rho(r)$ the density of real fluid and $\rho(r)^{id}$ the density of the ideal fluid. One can define local densities in terms of the average numbers of solvent molecules (or atoms) found within a given region surrounding the solute. The number of neighbours, n(r) can be determined by integrating the radial distribution function using the following formula (s notes the distance r in the integral):

$$n(r) = \frac{4\pi N}{V} \int_0^r s^2 g(s) ds \qquad (8.2)$$

This number is called the clustering or coordination number which indicates the number of solvent molecules around a given molecule. Cluster is a simple and practical concept to explain a variety of phenomena in supercritical fluids. We have calculated the coordination number for the first solvation shell. The number is equal to the average number of solvent molecules in this volume. The upper limit of the integral of the radial distribution function, is taken as the position of the first minimum of g(r) (which in the present case for the $g_{C\text{-}C}(r)$ is around 6.18Å. Arithmetic integration has been used.

We present the numbers of solvent molecules in the first solvation shell around a carbon dioxide molecule, plotted as a function of the bulk density at Figure 8-6.

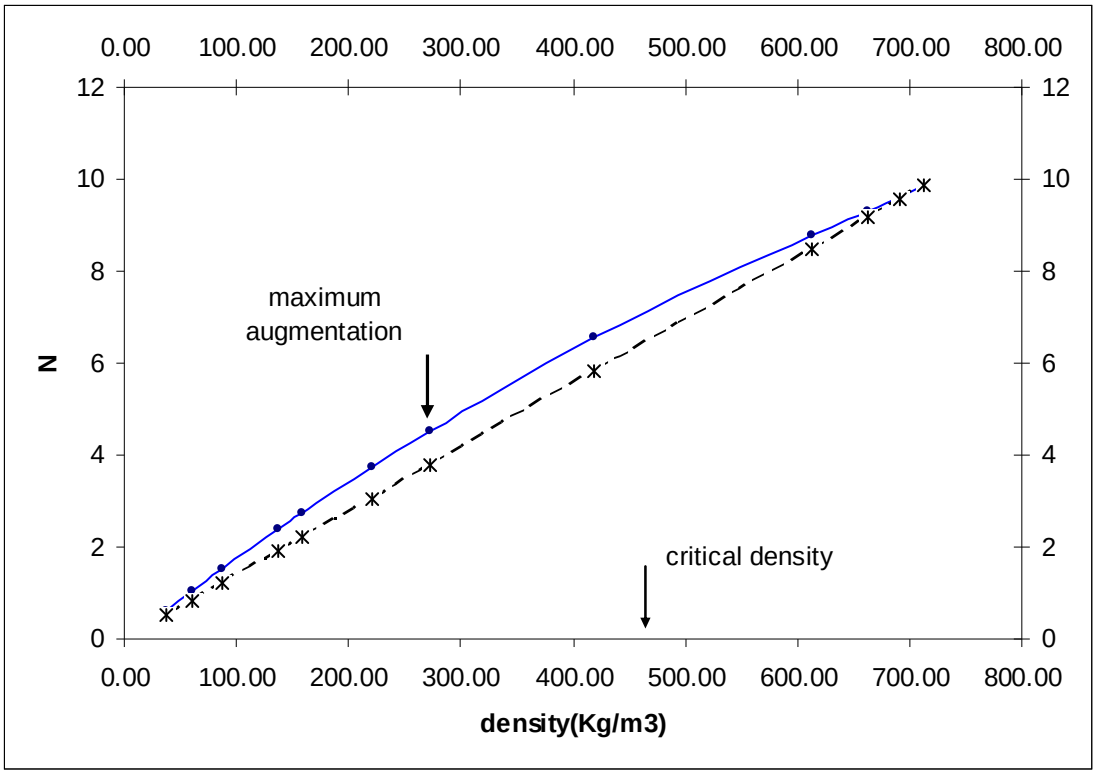

Figure 8-6: Calculated coordination numbers (solid points) as a function of density. The dashed line is the result expected for a homogeneous mass distribution in the system. The maximum augmentation symbol indicates where the maximum augmentation is expected.

As it has been reported firstly by Tucker and co-workers (Tucker, 1999; Tucker and Maddox, 1998) in their two dimensional SCF simulations, local density inhomogeneities become more pronounced at lower densities to the critical density. According to the experimental studies (Song *et al.*, 2000), it is believed that they are maximised at densities around $(2/3)\rho_{c.}$ The local coordination number calculated from the area underneath the first solvation shell as it is shown in the Figure 8-4 though the equation (8.2). The enhancement is quite strong at densities close to the critical one and lower ones. We cannot verify that it takes place at density around $(2/3)\ \rho_c$ exactly. However, our results agree with their observations. The enhancement is becoming less pronounced at the second solvation shell, but still we can observe that there is a difference between the bulk and the local density at Figure 8-7.

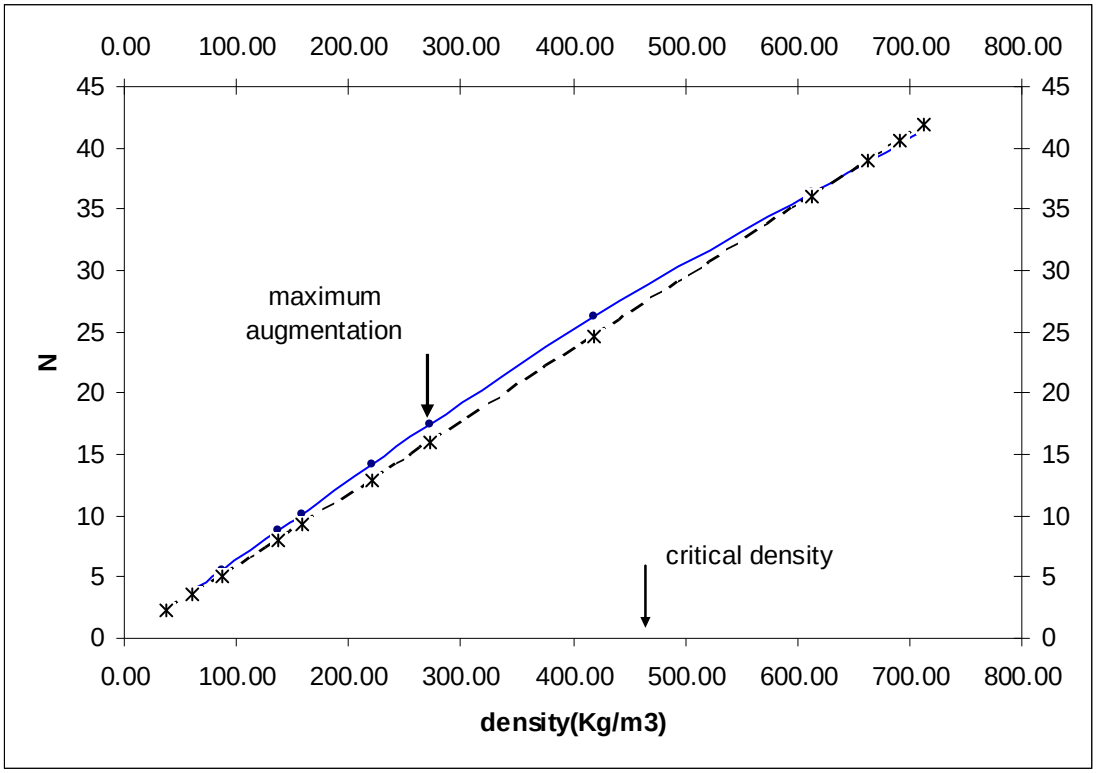

Figure 8-7: Coordination number at the second solvation shell. The layout and the line styles are the same as previous figure.

We believe this 'density augmentation' is a universal behaviour in supercritical fluids, indicating that there is a sponge like structure in supercritical

phase, but as density increases the fluid looks like dense fog. It can be concluded the sponge like structure is pronounced at densities close to critical density, which this local structure enhancement can be seen as regions with high and low density in the supercritical fluid.

The local structure around a molecule is definitely important factor for its behaviour. At the moment, the lifetime of a configuration, which represents a low or a high density structure around a molecule, is not well studied. We can realize the importance of studying the lifetime of the local structure, when we suppose the molecule is a reacting solute.

8.4 ISOTHERMAL COMPRESSIBILITY

Isothermal compressibility is a useful probe of long-range interactions and their effect on the microstructure of a supercritical fluid. The isothermal compressibility expresses the ability of the molecules in a fluid to pack more tightly, and is the macroscopic response of a fluid to an applied pressure. The mathematical relationship between molecular packing and κ_τ can be written in terms of the radial distribution function according to KB theory.

$$\rho_v \kappa_B T \kappa_T = 1 + \rho_v \int_0^\infty 4\pi r^2 (g(r) - 1) dr \tag{8.3}$$

where κ_B is the Boltzmann's constant and ρ_v the density of solvent. The above equation was introduced for a system where N may vary (grand canonical ensemble). However Matubayasi and Levy (Matubayasi and Levy, 1996) introduced an alternative formulation of the KB expression in the Canonical ensemble

$$\rho_v \int_0^\infty 4\pi r^2 (g_{uv}(r)-1)dr = \frac{\int_0^\infty 4\pi r^2 - \rho_v^{-1}\int_0^\infty \rho_{uv}(r)dr}{1-N_v^{-1}\int_0^\infty \rho_{uv}(r)dr} \qquad (8.4)$$

where N_v is the number of solvent molecules in the system, ρ_v is the bulk density of solvent ($\rho_v = N_v / V$), ρ_{uv} is the product of the bulk density of solution and the canonical radial distribution function. However, the authors proved that the KB theory is valid in other ensembles and the formula in equation (8.3) can be used in the Canonical ensemble. Others (Akiya and Savage, 2000a) used KB theory in the Canonical ensemble by applying equation (8.3). Using the equation (8.3) we have calculated the isothermal compressibility. The isothermal compressibility as a function of pressure is shown in Figure 8-8.

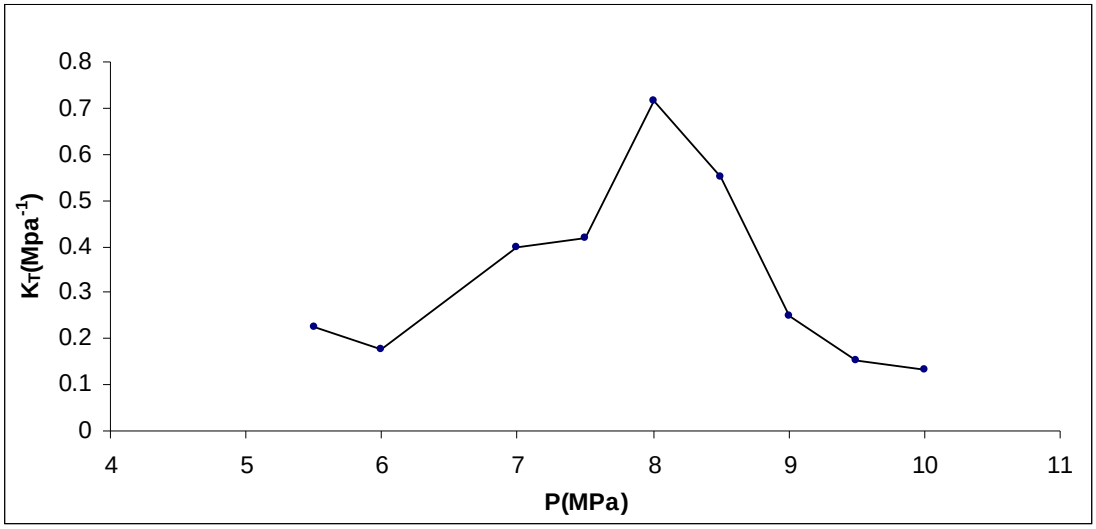

Figure 8-8: Isothermal compressibility of CO_2 κ_T as a function of pressure at temperature T=308.15K. The pressure on axis represents the real pressure of the molecular system.

The simulation results are in good agreement with behaviour of the isothermal compressibility in the supercritical region. However, the absolute value of the peak in Figure 8-8 is different from the one in Figure 8-9 but lets have a better look to this.

The theory of critical phenomena says that κ_T becomes infinite along the critical isotherm as the system moves close to the critical pressure

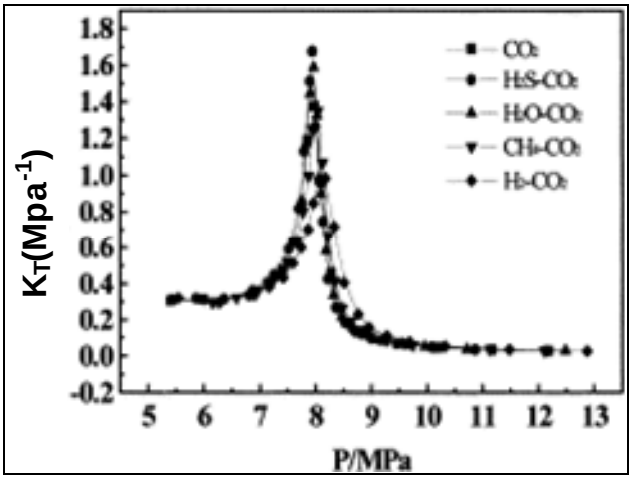

Figure 8-9: Experimental Isothermal compressibility of CO_2 and some mixtures as a function of pressure at temperature T=308.15 K. Data (Zhang *et al.*, 2002a). The maximum value of isothermal compressibility is observed at 8 MPa.

In an open system, the isothermal compressibility as we mentioned can be described by the equation

$$\rho_v \int_0^\infty (g_{vv}(r) - 1) dr = \rho_v G_{vv} = N_{vv}^{ex}$$

The N_{vv}^{ex} is the average excess number of carbon dioxide molecules found around another molecule of carbon dioxide (g(r) in terms of solvent, subscribt $_v$ denotes the solvent), as compared to the number of molecules which would be found in an uncorrelated (random) system. The isothermal compressibility for an ideal gas system is $\kappa_T^0 = 1/P$. Hence, the isothermal compressibility of a real system is $\kappa_T = \dfrac{1 + N_{vv}^{ex}}{P}$

According to the behaviour of isothermal compressibility near the critical point, we can deduce that N_{vv}^{ex} obtains its maximum value near the critical point. If we express the fluctuation of CO_2 molecules around a central CO_2 molecule in a fixed volume

away from the central one, we have $\delta N = N(t) - \langle N \rangle$, in which case the isothermal compressibility can be written as

$$\kappa_T = \frac{\langle N(t) - \langle N \rangle \rangle}{\langle N \rangle}$$

As κ_T reaches its maximum near the critical point, it undergoes large fluctuations about its average value over time. As MD trajectories through solving the Newton equation in order to find the positions of molecules with time, they have a difficulty following the fast movement of the molecules in “real” carbon dioxide, so they underestimate the value of isothermal compressibility. It also has to be considered that these density fluctuations near the critical point are correlated over a long range (radial distribution function decays slowly) so that larger systems are required to describe properly the molecules that are entering a fixed volume and the molecules that are exiting it at a given distance for r in g(r). As fluctuation in local structure is high, possibly more time consuming simulations required to improve the accuracy of the calculated isothermal compressibilities near critical density. It is not so difficult to imagine that this kind of inhomogeneity effects the kinetic energy distribution. Sometimes it can cause a serious breakdown even in the constant-temperature molecular dynamics simulation by Berendsen method.However, even with these improvements it will be a discrepancy between real and of the predicted value because of the nature of molecular dynamics and the nature the microscopic structure of the real world of fluids. This fact does not reduce the incredible value of the molecular dynamics simulations, as they mimic the physical movements of the molecules in the compressible regime at a satisfactory level resulting in quite reliable predictions.

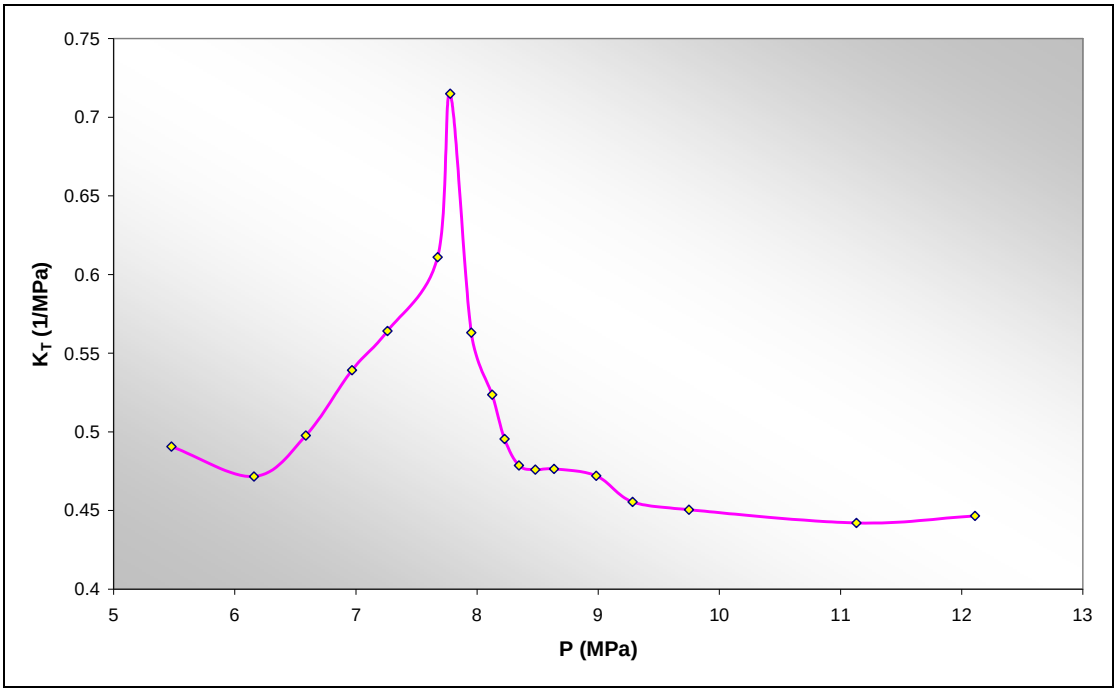

Figure 8-10: MC Simulation results for Isothermal compressibility of pure CO_2 at T = 308.15 K. The pressure on axis represents the real pressure of the molecular system.

The isothermal compressibility was also calculated through Monte Carlo simulation with the same technique. Figure 8-10 shows the isothermal compressibility versus pressure. The prediction from Monte Carlo simulation has the same discrepancy with experimental results. Still, in this case the discrepancy can be attributed to limitations of molecular simulations, but it proves that Monte Carlo and molecular dynamics have the same limitations near the critical point. As Monte Carlo and molecular dynamics give similar results, the limitation can be attributed to potential EPM2.

8.5 DIFFUSIVITY

The diffusion coefficient in the supercritical region is one of the important properties for the design of supercritical fluid extraction and reaction processes. Accurate measurements are, however, very difficult especially in the critical region where density fluctuations become large. Some experimental results have reported an anomalous decrease of diffusion coefficients of solutes at the vicinity of the critical

point (Nishiumi *et al.*, 1996). The restriction to thermal motion of the solute molecule by formation of clusters near the critical region is considered to be one of the reasons for the anomalous diffusivity**.** Because the transport and solvating properties of a fluid depend strongly on its density, an ability to tune the solvent density translates into an ability to manipulate the efficiency of separation processes and reaction outcomes. Molecular dynamics simulations have historically provided the most detailed information about diffusion processes in fluids. However, dynamic properties from simulations turn out to be much more sensitive to the selected potential. We have calculated the self diffusion coefficient for pure carbon dioxide at 308.15 K. The self diffusion coefficient was calculated from the Einstein's relationship:

$$D = \lim_{i \to \infty} \frac{1}{6t} \left\langle \left[r_i(t) - r_i(0) \right]^2 \right\rangle \tag{8.5}$$

Figure 8-11 compares the self diffusion coefficients for pure CO_2 with experimental data. Experimental and simulation are generally limited in the gaseous region with low pressures in the supercritical region. The first experimental data reported on the measurement of self diffusion coefficient was on 1955 (O'Hern and Martin, 1955) and these are the only ones close to the critical point. With the developments of experimental techniques such as nuclear magnetic resonance and theories, measurements under higher pressures with dense gas and liquid phases are available with improved accuracies (Etesse *et al.*, 1992; Gross *et al.*, 1998; O'Hern and Martin, 1955). There are many simulation works of self-diffusion reported in supercritical phase but except the work from Higashi and Iwai (Higashi *et al.*, 2000; Iwai *et al.*, 1997) none is close to the critical point. Up to date, there is a controversial discussion about if an anomalous behaviour of motion exists near the critical (Drozdov and Tucker, 2001; Drozdov and Tucker, 2002) in a pure solvent. What is well known is

that the supercritical fluids exhibit large diffusion coefficients, which resemble those of gases than those of liquids.

The diffusion coefficient in the supercritical region is strongly dependent on temperature and pressure D=D(T, P). The temperature dependence of D in isobaric change can be interpreted through an Arrhenius plot. Transition state theory can be used to interpret the temperature dependence of the diffusion coefficient through the equation $(D)_p = D_0 \times e^{-(\Delta E^{\neq} / RT)}$ (equivalent to Arrhenius equation). These activation energies usually depend on pressure and density (Drozdov and Tucker, 2001). In the same way, the pressure dependence on the diffusion coefficient can be interpreted through an equivalent equation. The slope of the diffusivity with pressure gives the activation volume. The activation volume is defined as

$$\Delta V^{\neq} = R \times T \times \left(\frac{\partial \ln D}{\partial P} \right)_{T=const} \qquad (8.6)$$

Up to now, we really do not know how or even if, local density inhomogeneities affect molecular diffusion coefficients, which is an important transport property necessary for the prediction of chemical reaction rates and the design of SCF reactors.

We present the diffusion coefficient results for the critical isotherm $T=1.02T_c$. The simulation results are in good agreement with experiments studies. Inspection of Figure 8-11 shows that the diffusion coefficient of CO_2 decreases with increasing pressure. Until the pressure reaches the critical pressure, the diffusion coefficient is quite large and resembles the one from gas phase after that, the diffusion coefficient resembles the one from liquid phase. This fact is in a good agreement with the theory of the two supercritical region area divided by a ridge, which the locus of the points where the values of the density fluctuation become maximum in isothermal change (Nakayama *et al.*, 2000; Nishikawa and Morita, 2000). The same can be deducted

from the work of Gross et al (Gross *et al.*, 1998) about their experimental results in the supercritical region, that diffusivities on an isotherm for pressures below the one corresponding to ridge pressures resembling those of gas phase and above the liquid phase ones. Our simulation results agree well with this theory. In the work of Higashi et al (Higashi *et al.*, 2000) the carbon dioxide has been treated as united atom from which we can concluded that an all atom representation is better than a united one for diffusivity prediction close to the critical point.

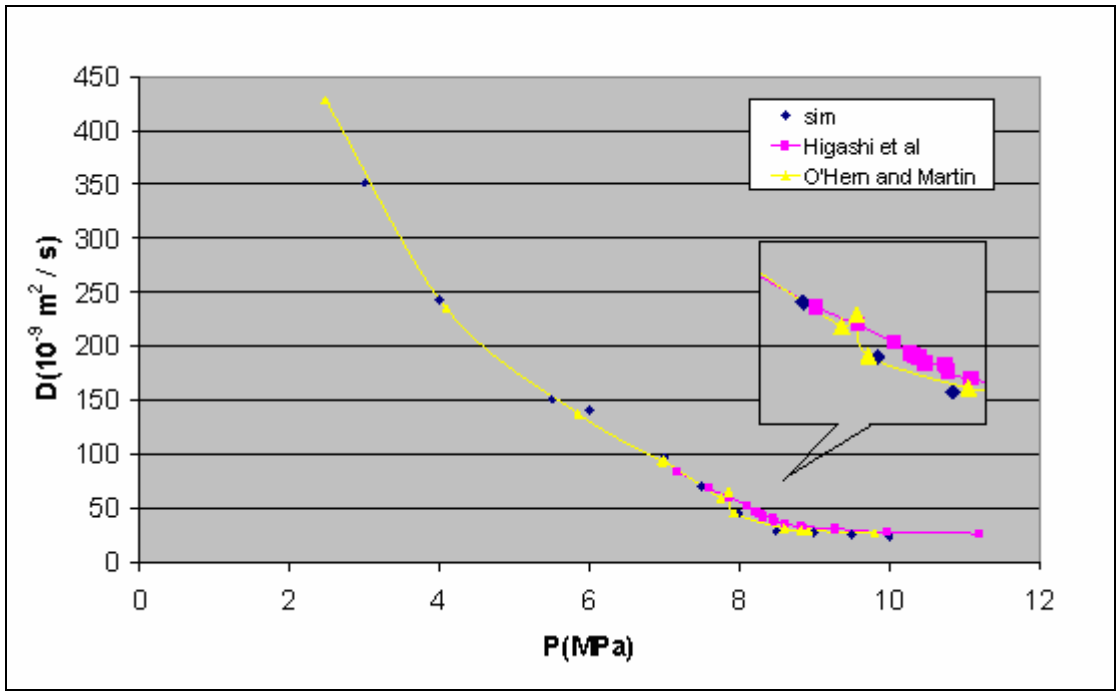

Figure 8-11: Diffusion coefficient versus pressure at 308.2 K for pure carbon dioxide. a) Experimental data (O'Hern and Martin) b) simulation data from our work (sim) c) simulation data (Higashi et al)

On the measurements by O'Hern and Martin we can observe that there is an increment on the self-diffusion near the critical pressure. Unfortunately, some existing experimental results (Trappeniers and Oosting, 1966) on diffusion in SCFs are controversial and do not clarify the situation. On the other hand, experimental observations of the self diffusion coefficient of solutes in dilute SCF solutions (Nishiumi et al., 1996; Nishiumi and Kubota, 2007; Tsekhans, 1971) slows down abruptly near the liquid-gas critical point of these solute-solvent systems. However,

our conventional molecular dynamic studies have not revealed any anomaly close to the critical point.

8.6 ISOCHORIC HEAT CAPACITY

The constant volume heat capacity, C_V can be calculated from the fluctuations in potential energy from MC or MD simulations by

$$C_V = C_V^O + \frac{\left\langle E^2 \right\rangle - \left\langle E \right\rangle^2}{k_B T^2} \tag{8.7}$$

where $\left\langle E^2 \right\rangle - \left\langle E \right\rangle^2$ the potential energy fluctuation, k_B is the Boltzmann constant, and T is the absolute temperature. C_V^O is the ideal gas heat capacity contribution. In case of a polyatomic gas like CO_2 the ideal partition function is a product of electronic, nuclear, rotational, translational and vibrational partition functions. According to the procedure being followed in every statistical mechanic text (Van P.Carey, 1999), the formulation gives the ideal part of heat capacity for a polyatomic gas as

$$C_V = R\left[\frac{3}{2} + \frac{3}{2} + \sum_{j=1}^{3n-6}\left(\frac{\Theta_{\upsilon j}}{T}\right)^2 \frac{e^{\Theta_{\upsilon j}/T}}{(e^{\Theta_{\upsilon j}/T} - 1)^2}\right] \tag{8.8}$$

The first term comes from the translational contribution to the heat capacity, the second term is the rotational contribution and the last term is due to the vibrational degrees of freedom. In the case of carbon dioxide, the rotational contribution is 2/2 since it is a linear molecule. The calculation of ideal heat capacity through statistical mechanics is accurate near the critical temperature, as we can see from Figure 8-12.

In Figure 8-13, we present the simulated heat capacity in comparison to the experimental data and values from Wagner's equation of state. The simulated results are in good agreement, considering the difficulties performing simulations in

supercritical phase and the fact that the heat capacity is calculated as the second derivative of energy.

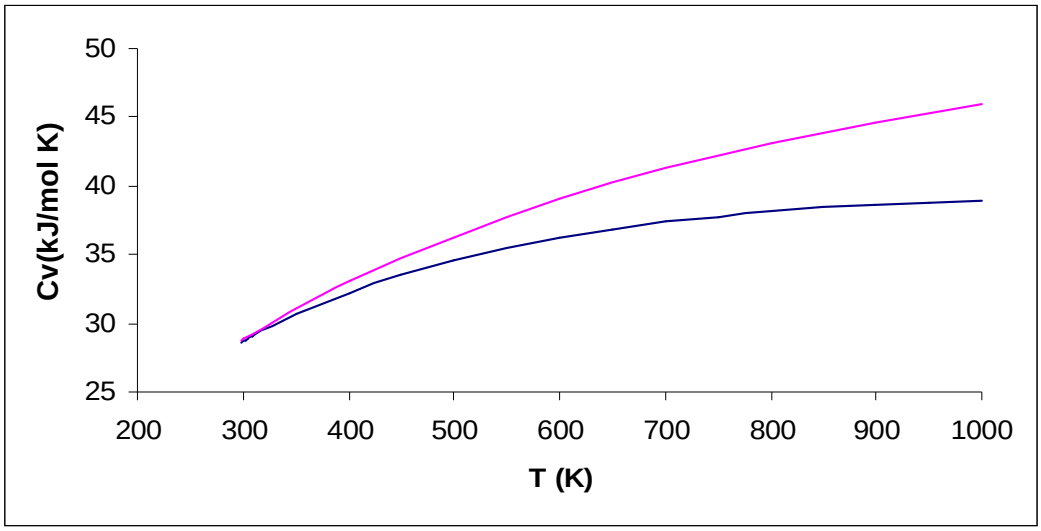

Figure 8-12 . Ideal heat capacity (–).Experimental Values from NIST database (–) Theoretical Values

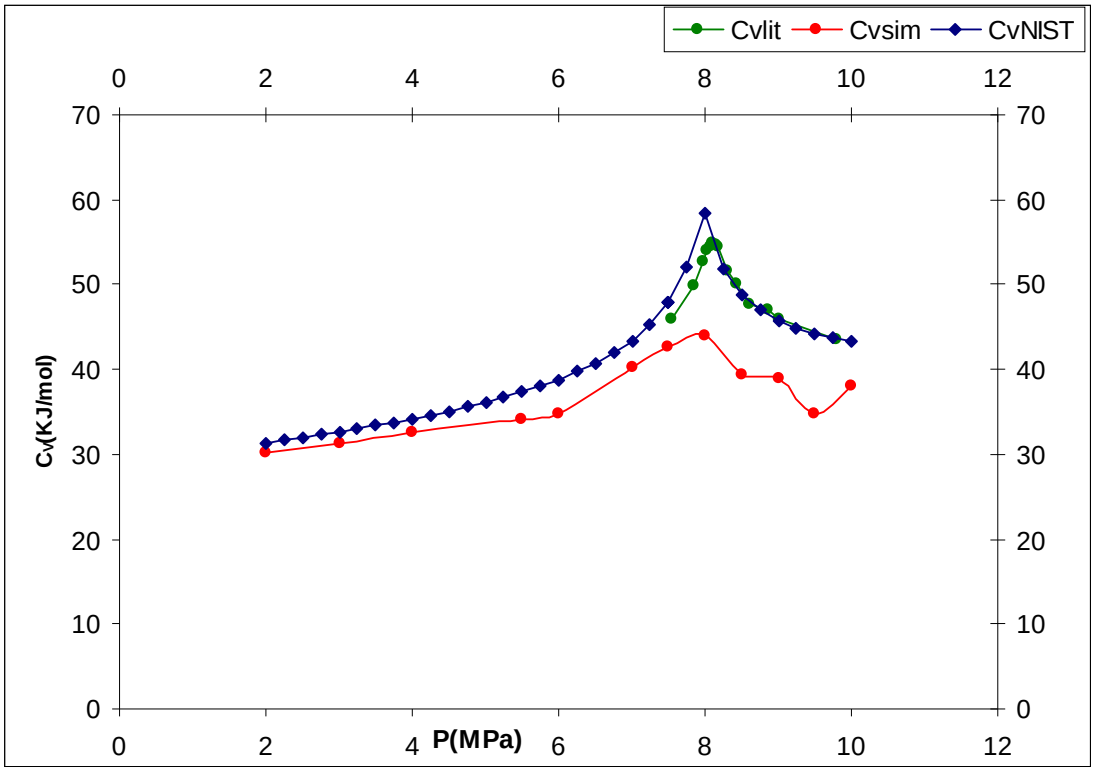

Figure 8-13: Dependence of C_V on pressure for pure CO_2.a) Cvlit data (Zhang *et al.*, 2002c) b) data from Molecular Dynamics simulation c) data from NIST database

It is of great importance that the value of C_V has its maximum close to the critical pressure as we can conclude that the molecular potential we used predict and describes the supercritical region properly; even at temperatures very close to the critical point. The large fluctuations and formation of clusters in the neighbourhood of the critical point therefore result in an abnormally large specific heat capacity. The finite value of isochoric heat capacity near the critical point is a property depending on the number of clusters; in other words, the size and the number of high density and low density regions in the solvent. In order to realize better the concept of a cluster, we should have in mind that is a dynamic process, which has breaking and formation time. The peculiar nature of the supercritical phase, with rapid formation and breakdown of clusters and the rapidly increased number of cluster is the reason for maximizing the value of the isochoric capacity. The discrepancy between the experimental value and the simulated one is because of the limits of molecular simulations as we discussed for isothermal compressibility.

9 SOLUTION PROPERTIES OF MIXTURES AT INFINITE DILUTION

It has been one of the important subjects in supercritical research to understand how the solvent influences chemical reactions. There have been many experiments to investigate the solvent effects on the chemical reactions. Numerous phenomenological data are available on examining the solution effect on reacting solutes, but no universal theory exists to interpret them. The experimental approaches are undoubtedly a powerful tool for the investigation of the solvent effects on chemical reactions, but a strong theory needs to be established to expand the use of supercritical carbon dioxide in industry.

In this chapter, we look deeply into the solvent effect on the solute. The goal of this work is to establish a relation between the degree of aggregation or cavitation and thermodynamic properties, such as diffusivity, heat capacity and partial molar volumes of the solute. Once more, the Kirkwood and Buff fluctuation theory, which is describing non-ideal solutions including supercritical solutions, is used to evaluate the micro-environment of the solutions. The objective is to examine the tendency of the solvent to form clusters or cavitations across different kind of solutes regarding the pressure dependence along a critical isotherm.

9.1 INTRODUCTION

The role of local density in influencing chemistry in supercritical fluids is a key element to our understanding of reaction dynamics. At temperatures appreciably higher than the critical temperature $T>T_c$, the solvent fluid itself is rather uniform and homogeneous and the isothermal compressibility of the fluid is not large. However, when for example a solute with large attractive solute-solvent interactions is placed in the fluid, the solvent molecules form a cluster surrounding the solute molecule. The number of solvent molecules participating in the cluster under such conditions is rather small and they form only the first solvation shells, in contrast to large clusters near the critical point

In traditional solution thermodynamics, the process of solvation can be thought of two steps, finding space and occupying it. In previous chapter, we have seen the random movements of the molecules cause cavities (void spaces in the fluid) to form. The likelihood of a cavity being available to a solute particle is proportional to the density of the fluid; dense systems have few large cavities. According to conventional theories of solution, somebody expects the cavity must be sufficiently sized and shaped to allow a solute particle to move into the cavity during solvation process. The size of cavities is maximized close to the critical point. One expects that the size of cavitations should pass through a maximum with increasing pressure on a critical isotherm.

9.2 INFINITE DILUTION OF METHANE IN SUPERCRITICAL CARBON DIOXIDE

Experimental observations (Zhang *et al.*, 2002a) found that the addition of methane into supercritical carbon dioxide increases the volume of solution. Their

group reported large positive partial molar volumes near the critical pressure, which is evidence that the system volume increases. While the partial molar volume is a macroscopic thermodynamic property, their measurements could be interpreted to show the cavitation of carbon dioxide molecules around methane molecule.

A system, consisting of 999 carbon dioxide molecules and 1 molecule of methane, is used to represent the infinite dilution of methane in the supercritical carbon dioxide. As the addition of one methane molecule into 999 molecules gives a mixture 0,1% per volume, we assume that the critical point of the mixture remains the same. The correlation functions were determined by using the centre of each species, the carbon atom. We sampled the radial distribution function every 1000 configurations during MD simulations

A sampling diagram from the radial distribution functions for T_r = 308.15 K over the densities ranging from 135.79 kg/m^3 to 712.3 kg/m^3 (critical density of CO_2 is 468 kg/m^3) for CO_2-CH_4 is shown in the Figure 9-1. The choppy appearance of the solute-solvent radial distribution function is common and has been observed in other infinite dilute solute mixtures simulations (Akiya and Savage, 2000b). The Figure 9-1 shows that the radial distributions functions exhibit a clear difference in appearance at subcritical and supercritical densities. The peak height decreases with increasing density from subcritical to supercritical ones and a second shell appears which is in agreement with theory (Clifford, 1999). Figure 9-2 shows the solute-solvent and solvent-solvent radial distribution functions for CO_2-CH_4 and CO_2-CO_2 pairs.

Comparing the Figure 9-1 and Figure 8-4, we can see the trend of the RDF for carbon dioxide is strongly dependent on carbon dioxide bulk density compared to carbon dioxide-methane interaction. The height of the peaks and the contrasting

trends demonstrate that the strength of methane-carbon dioxide interactions relative to carbon dioxide-carbon dioxide interactions are lower.

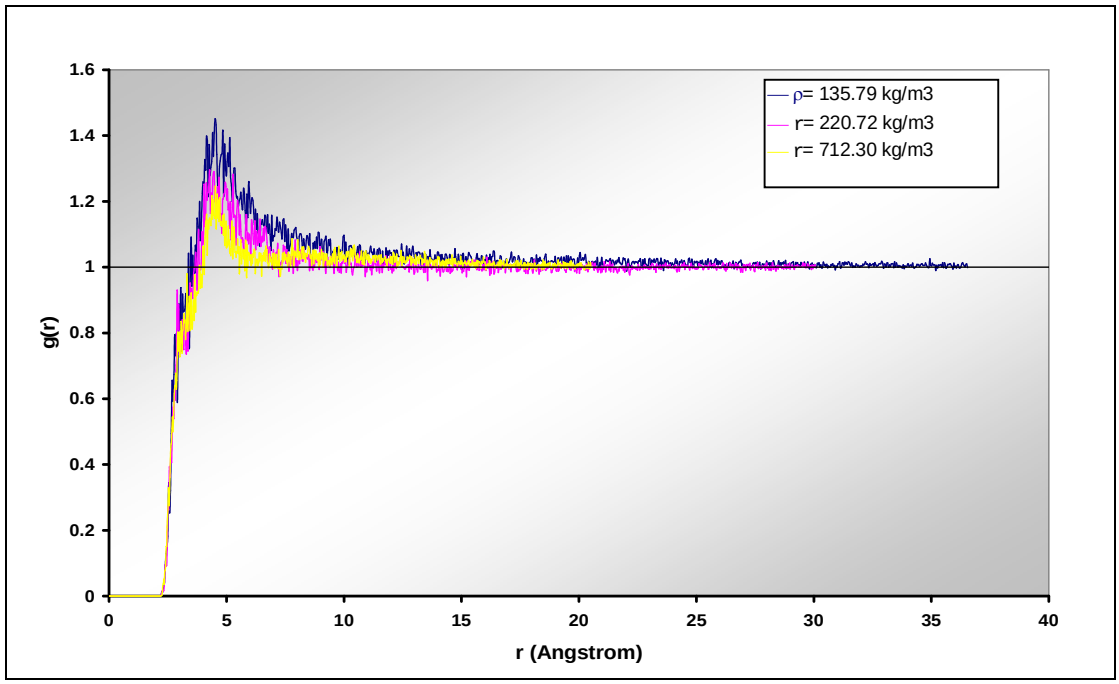

Figure 9-1: Pair correlation function for mixture of CH_4-CO_2 at different densities

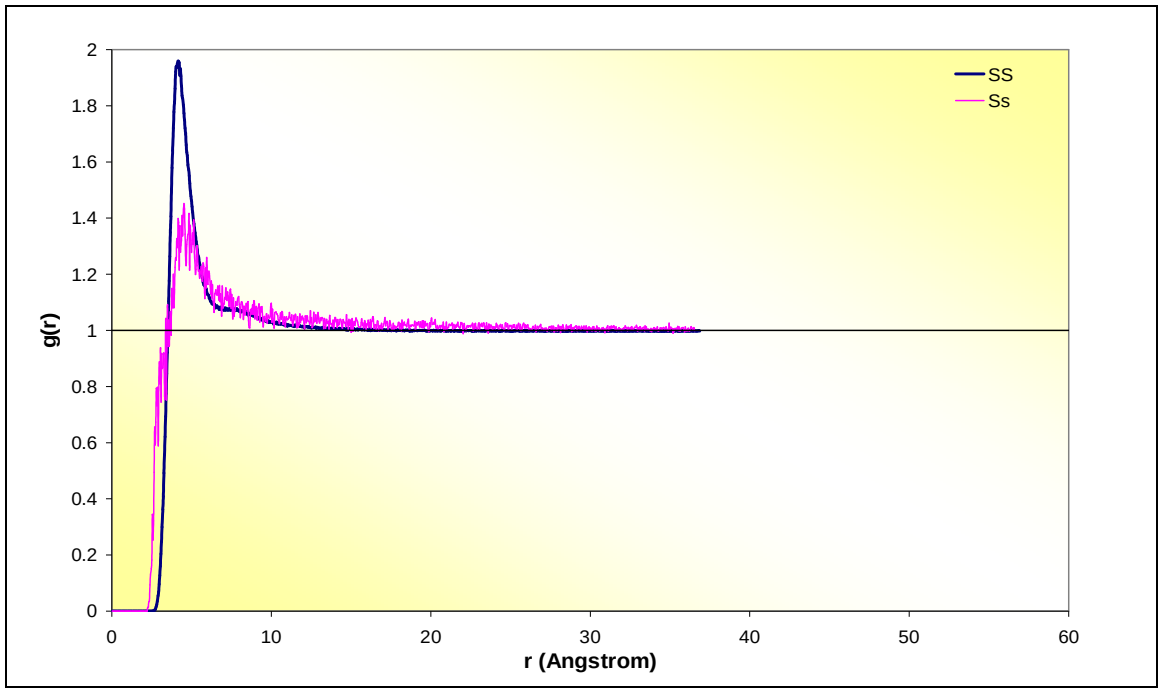

Figure 9-2: Comparison of pair correlation function obtained for pure CO_2 (SS) and mixture of CO_2-CH_4 (Ss) at T = 308.15 K and density equal to 272.79 kg/m^3.

When we compare the RDFs of solute-solvent and solvent-solvent in the same graph (Figure 9-2) it is obvious that the number, N_{ex} which gives the amount of excess molecules around a solute molecule, is negative.

$$N_{ex} = \rho_v (G^{\infty}{}_{uv} - G^{o}{}_{vv}) \tag{9.1}$$

As in our discussion in the previous chapter, we will use the shape of the radial distribution function to interpret the results. The clustering number has been estimated by integrating the radial distribution function within an appropriate range, r_1 to r_2 which defines the solvation shell. It is given by the following equation

$$N_{clus} = 4\pi\rho \int_{r1}^{r2} g_{12}(r) r^2 dr \tag{9.2}$$

In our case, the g_{12} is the radial distribution function between the carbon atom of CH_4 and the one from carbon dioxide. The value of r_1 is equal to zero and the value of r_2 is equal to the distance where the first minimum in g(r) is being observed. In this case the upper bound for the integral in our highest densities results, the position of the minimum is around 6.68 Å. Actually, the value of r_1 is not equal to zero. The value of r_1 it depends on the size of the molecule and it the closest distance which two molecules can approach each other. The values r_1-r_2 in the integration for the calculation of the number of clustering around a methane molecule are different from the values used into the integration around a carbon dioxide molecule. So a directly comparison of the two coordination number can not be made, but a comparison with the coordination number in case that expected when we had a homogeneous fluid can be made.

The isothermal compressibility expresses the gathering of an enormous number of solvent molecules. The range of gathering molecules is quite long, and becomes maximum for $\rho=\rho_c$. The infinite value of the isothermal compressibility near

the critical point can be classified as a long-range phenomenon. On the other hand, depletion or clustering ordinary indicates the gathering of the solvent molecules of a few angstroms and can be classified as a short-range phenomenon.

We present in Figure 9-3 the coordination number of CO_2 molecules around a CH_4 molecule in a homogeneous fluid at same density and the coordination number of CO_2 molecules around a CH_4 molecule in the real fluid. Comparing the Figure 9-3 and Figure 8-6 we can more clearly understand now that the N_{ex} it is a negative number, which means that there is a depletion of CO_2 molecules around the methane, in other words a cavitation exists around the methane molecule. From the two figures, we can deduce that the maximum depletion occurs at densities below the critical one. The higher cavitation around a methane molecule occurs at densities where the maximum local clustering has been observed for the pure carbon dioxide. So, the depletion or the clustering is the kind of process occurs in short range around a solute and belongs to short range phenomena. In other words the addition of a solute molecule in a supercritical fluid in change the microstructure of the supercritical fluid only in a short distance around it, it cannot change dramatically the whole microstructure of the supercritical fluid.

Our observation that the addition of methane molecules into the supercritical carbon dioxide cause depletion around it, agrees well with experiments. The depletion around the methane molecule, leads to expand the volume of solution of the whole mixture. This agrees well with experimental studies as Zhang et al reported positive partial molar volumes of the dilution of methane into supercritical carbon dioxide.

However, the solute partial molar volume is a quantity, which maximised at the point, where the isothermal compressibility obtains its maximum value on a critical isotherm. This means that the partial molar volume at supercritical solutions is

a property is connected more with behaviour of bulk density rather than the local density.

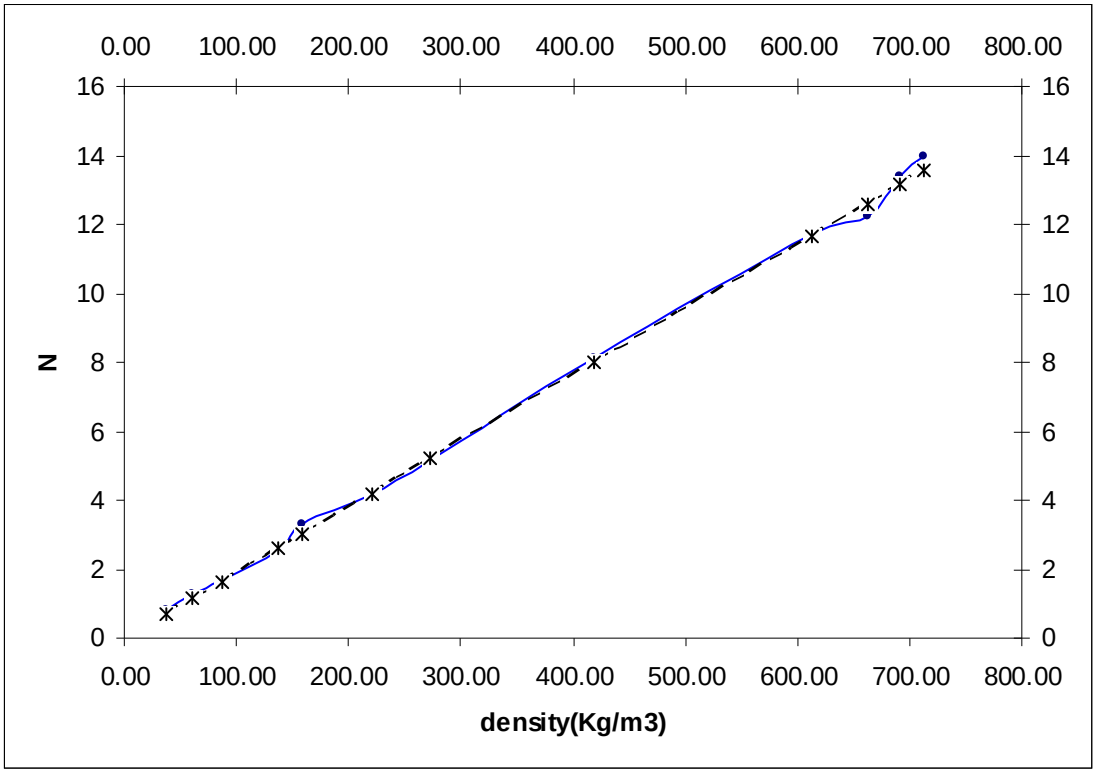

Figure 9-3: Coordination number of CO_2 molecules around a methane molecule` (solid line) and coordination number (dashed line) of a homogeneous fluid at same density.

In addition, combining the equations (9.1) and (4.7) we can extract a formula connecting the excess or depleted number of molecules around a solute, with the solute partial molar volume at infinite dilution. We obtain:

$$V_u^{\infty} = \frac{1 - N^{ex}}{\rho}$$

According to this formula if we calculate the solute partial molar volume in the first solvation shell it will appears to go through a maximum near $(2/3)\rho_{c.}$ However, the solute partial volume diverges close to critical density along an isotherm. Based on the fact we can conclude partial molar volume is a macroscopic property, which reflects more the nature of the solvent rather than the nature of local interactions.

The formation of cavitations around repulsive solutes is an interesting process but to the best of our knowledge, there is no industrial application using this feature. We believe this kind of solvent can used as co-solvents in order to expand the common features (clustering) of supercritical fluids. All the supercritical solutions in technological applications are cases of attractive clustering mixtures e.g., decaffeination of coffee and other examples of supercritical fluid extraction, supercritical chromatography, sorbent regeneration by supercritical fluids. These mixtures are characterised by large negative solute partial molar volumes near the solvent critical point. The mixture of water and supercritical carbon dioxide belongs to that category. We will examine that system in the next section.

9.3 INFINITE DILUTION OF WATER IN SUPERCRITICAL CARBON DIOXIDE

The research group of (Zhang *et al.*, 2002a) reported negative partial molar volumes of water and carbon dioxide at infinite dilution. We followed exactly the same approach as in the case of methane with carbon dioxide, in order to examine the microstructure of the solution. We present the coordination number of CO_2 around a water molecule in Figure 9-4. There is an enhancement of local density around the water molecule. The degree of density enhancement is stronger than those of a CO_2 molecule. According to experimental studies (Song *et al.*, 2000) the larger degree of clustering appears at densities below the critical one. Figure 9-4 shows the maximum clustering occurs at densities around 300 kg/m^3. Our simulation results are in line with experimental observations and we can verify that the maximum degree of clustering occurs at densities around $(2/3)\rho_c$ for an attractive solute.

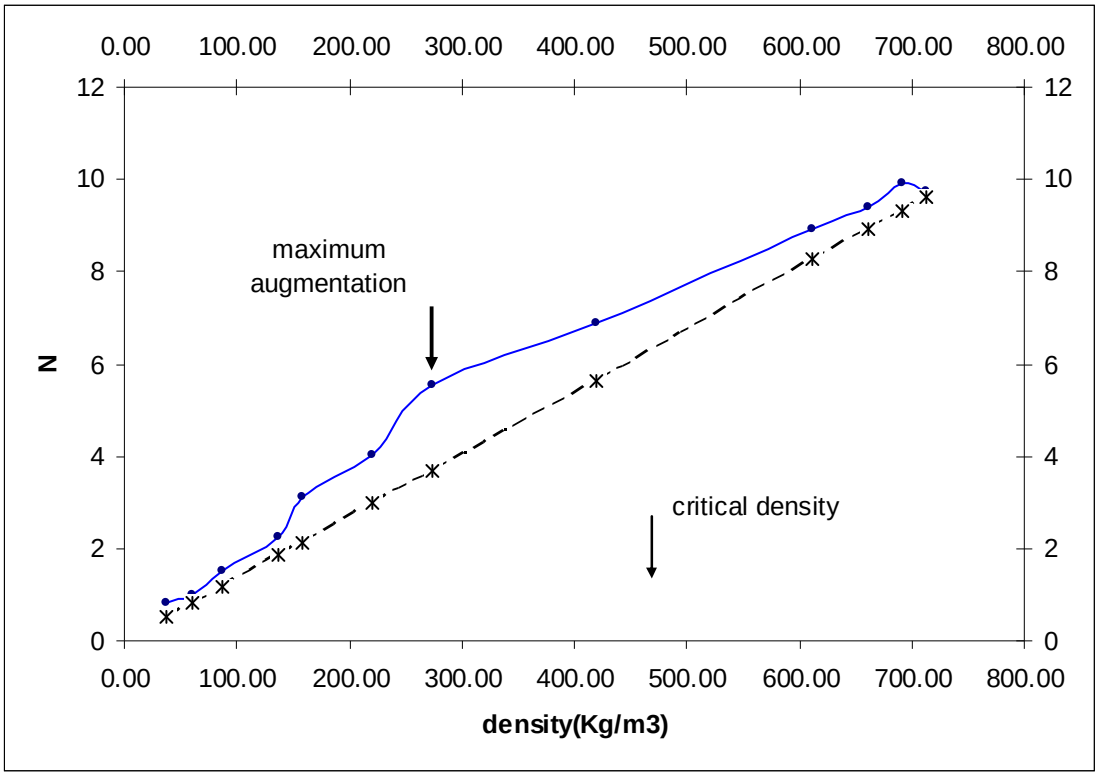

Figure 9-4: Coordination number of CO_2 molecules around a water molecule` (solid line) and coordination number (dashed line) of a homogeneous fluid at same density

9.4 THERMODYNAMIC PROPERTIES OF MIXTURES AT INFINITE DILUTION

9.4.1 Diffusivity

We calculated diffusion coefficients of one methane molecule in supercritical carbon dioxide (repulsive mixture) and one water molecule in supercritical carbon dioxide (attractive mixture). The results are being presented in Figure 9-5. The tracer diffusion coefficient for both methane and water goes abruptly to zero close to the critical point. The reason is to investigate characteristics of the cluster structure around the water molecule and the cavitation structure around the methane molecule. We used the normal Einstein's relation to estimate the diffusion coefficient D. Up to date there two concepts used to explain the reason for the drastic change of the diffusion coefficient near the critical pressure along an isotherm. One is the change in effective mass of the cluster caused by solvent molecules around the solute molecule,

and another is the density fluctuation of the solvent fluid where the solute molecules move. We believe that the first concept is most likely not the origin of the anomalous decrease of diffusivity near the critical point. There are two facts that disagree with this concept. Firstly, if the clustering would have a restrictive role on the solute movement, the diffusivity would be expected to have an anomalous behaviour at densities where the maximum local density enhancement has been observed. Secondly, a repulsive mixture should not exhibit an decrease in diffusivity but rather an increase as the solute molecule is in the middle of a cavitation and has a lot of room to move. In other words it is not the clustering, which forbids the solute from moving. The anomalous diffusivity has been observed for an attractive solute at infinite solution at density close to the critical one as well as a repulsive solute. This phenomenon has been observed for both systems in the region of the phase diagram, which is characterised by spatially extended fluctuations in the fluid density. We believe the extent of these fluctuations is related to the anomalous solute diffusion coefficient for both, the attractive and the repulsive solute.

In order to understand the anomalous diffusivity, it is necessary to realize the nature of the microenvironment around the solute. Furthermore, it is necessary to understand beyond the description provided by the radial distribution function around the solute, as this indicator describes only the average of all the environments found within the fluid. For an attractive solute, the distribution of microstructures containing the solute is changing rapidly over the time near the critical point. The same is happening for a repulsive solute too. The rapid rearrangement of the microstructure around the solute does not give free space for the solute to move. The instantaneous environment around the solute in a short range changes so dramatically with time, that

the free positions for an attractive solute or a repulsive one are always engaged restricting the motion of the solute molecule.

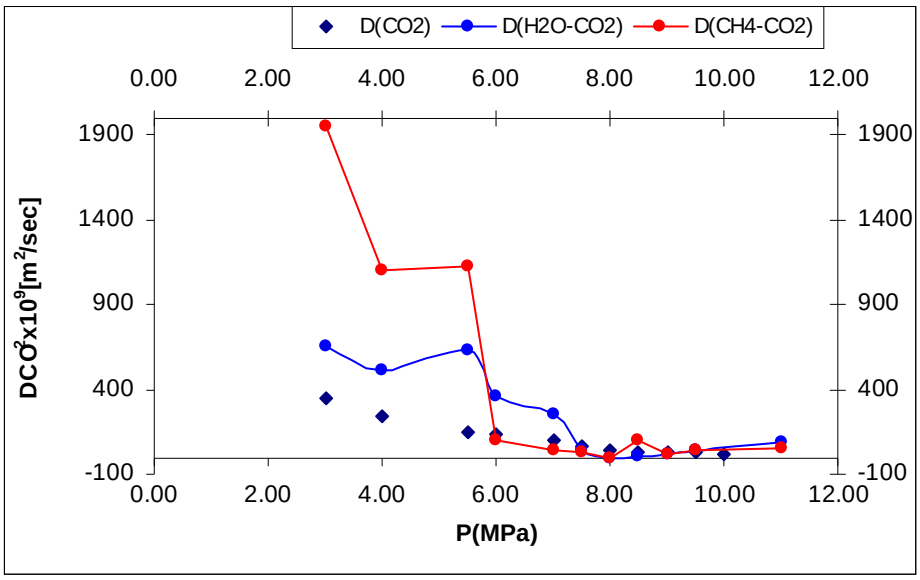

Figure 9-5: Dependence of tracer diffusion coefficient on pressure of i) a CO_2 molecule in pure CO_2 ii) a CH_4 molecule in CO_2 and iii)a H_2O molecule in CO_2 .Solutions 0.1mol% and temperature 308.15K.

Moreover, our explanation is in agreement with the kinetic theory of gases. The molecules in a gas move with quite high speeds. If a little ammonia gas is released at one end of a room, however, an appreciable time elapses before the smell is noticed at the opposite end. The reason for the slowness is that the molecules are constantly entering into collisions, so that the long path, which a single molecule would describe if it were unimpeded, is broken up into a very large number of zigs-zags in all directions. Since, the mobility of solvent molecules is maximed near the critical point; the solute molecule is constantly deflected by collisions with solvent molecules, so the free path is very short. Its position is nearly stationary resulting in zero diffusion coefficients.

9.4.2 Isochoric Heat Capacity

Constant volume heat capacity (C_V) is directly related with internal energy, and thus can provide information about the intermolecular interaction in the system.

C_V of a mixed fluid depends mainly on its composition and intermolecular interactions. At a fixed composition, C_V should depend mainly on the intermolecular interaction. C_V has a weak divergence at the critical point, which implies that is connected with the first and second solvation shell (radial distribution function) instead of the tail, as it is the case with isothermal compressibility. In other words these means that the isochoric heat capacity is related to structure of the molecules in short distance around it compare to molecules at long distance.

Furthermore, C_V of pure components or mixtures is nearly independent of pressure in high pressure region, indicating that the intermolecular interaction is not sensitive to pressure as the fluid is far from the critical region of the mixed fluids. In the critical region, the Cv depends on pressure and is sensitive to composition because of the nature of the supercritical phase.

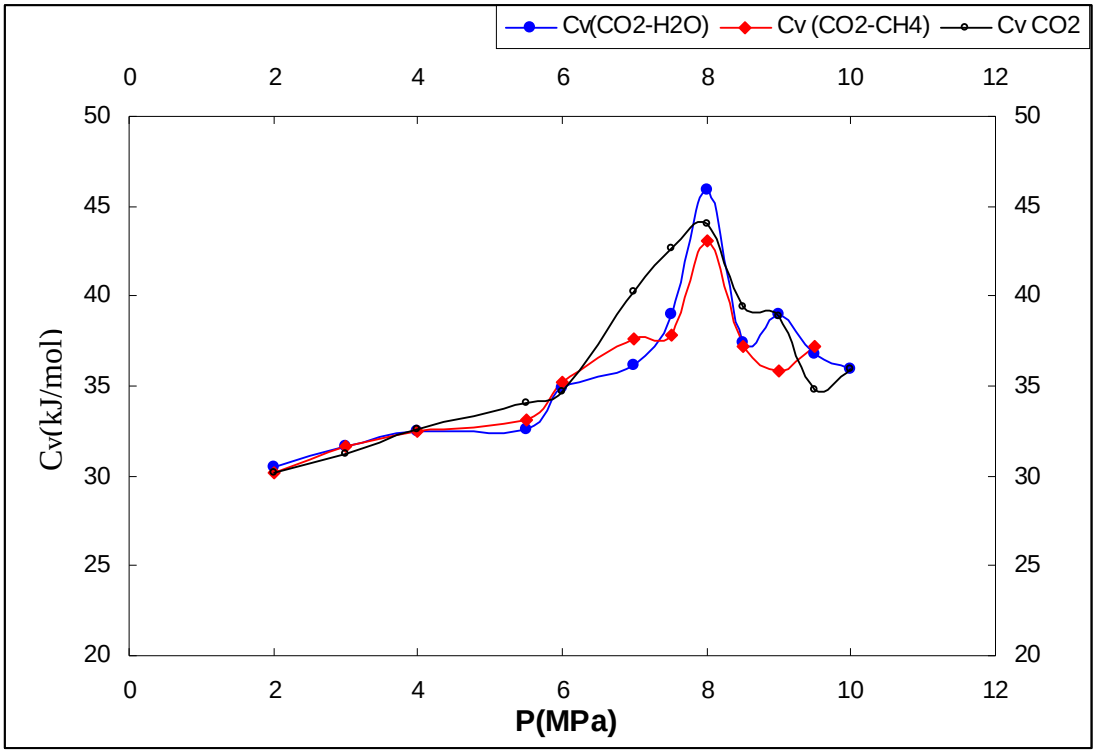

Figure 9-6Dependence of Cv on pressure for pure CO_2, CH_4-CO_2 and H_2O-CO_2 systems (0.1mol% mol) at 308.15K

The first peak of the radial distribution function represents a statistical average of the neighbours around a chosen molecule. As we have explained in the section 8.4, the observed structure around a central molecule, it fluctuates with the time. In the case of methane and carbon dioxide, we have a depletion (lack of molecules) around the methane molecule. In the case of water and carbon dioxide mixture we have an enhancement (excess of molecules) around the water molecule. The way the microenvironment changes around a solute molecule with time become faster when isothermal compressibility obtains its maximum value. We believe that the larger rate, i.e. the speed the molecules come into and leave the tagged area around a solute in the high compressible regime is the reason for the maxima in the curves. An increase in temperature results in decrease in the degree of clustering. Some of the members in the clusters enter into the bulk, which needs some additional energy. Therefore, the largest Cv indicates higher clustering. On the basis of this discussion, it can be deducted that breaking the clusters at the supercritical conditions is an endothermic process. The cluster formed around a water molecule is strongly holding together (strong attractive forces between the solute molecule and solvent molecules) which is more difficult to break than a pure CO_2 cluster. On the other hand, the cluster around the methane molecule is a weak one (weak attractive forces) and can be easier broken than pure CO_2. This fact explains why the solution of water in supercritical carbon dioxide increases the heat capacity while the solution of methane decreases it.

10 CONCLUSION AND FUTURE WORK

In this work, we have successfully employed molecular simulation methods using the potential model EPM2 to derive different thermodynamic properties of pure carbon dioxide, a mixture of methane-carbon dioxide and a mixture of water-carbon dioxide at infinite solution. The transferability of EPM2 model to the supercritical region has been studied through a comprehensive comparison between calculated values of several thermodynamic properties for CO_2 and experimental values.

Molecular simulation, although having plenty of room for improvement, can be reliably used to study difficult systems like supercritical fluids where experimental observations are problematic. Moreover, they provide an insight to the systems on atomic scale which enables us to establish a relationship between intermolecular potential and thermodynamic properties. In our study however, we identified a problem of MC being unable to predict realistic property values in the low density region. The reason for this is the trapping of MC sampling in unphysical configurations.

Beyond pure supercritical fluids, supercritical mixtures at infinite dilution can be studied with the existence of valid molecular force fields. We also observed some deviations in the results of isothermal compressibility and heat capacity from experimental data. These deviations however were due to computational limitations rather than the employed methodology.

Beside the usefulness of molecular simulation in predicting fluid properties in the supercritical region, it gives an insight in events at microscopic level with time and space. It enables us to calculate numerically the radial distribution function which

we used to examine the microstructure of supercritical conditions with regard to local structure using the KB theory

In the application of the KB theory to the systems

1. Pure carbon dioxide

2. Infinite dilution of methane in carbon dioxide

3. Infinite dilution of water in carbon dioxide

We identify three types of local microstructure.

Type A. There is local density enhancement of CO_2 around a CO_2 molecule. This density enhancement is more pronounced at densities below the critical one (ca. $2/3\rho_c$). In other words there is a sponge like structure of CO_2 molecules in supercritical region which is more evident at densities below the critical density along an isotherm. **Type B**. There is also a density enhancement around a water molecule in CO_2 molecules. This has been identified as an excess of CO_2 molecules around a water molecule. Rephrasing, the water molecule prefers to solvate in high density region of carbon dioxide. **Type C**. There is a density depletion of CO_2 molecules around a methane molecule. In this situation, this has been identified as a deficit of CO_2 molecules around a methane molecule. In other words, the water molecule prefers to solvate in areas where there is cavitation.

An apparently counter-intuitive point in the three different pictures of solvation is that they follow the same trend. They show the most anomalous behaviour at the same densities along the critical isotherm. Two unrelated solutes, when being dissolved in supercritical carbon dioxide, follow somehow a ‘universal’ behaviour, despite the fact that they follow a different type of solvation. This universal behaviour is related more to the properties of the supercritical carbon dioxide rather than the properties of the individual solutes, water or methane. In other

words the structure of carbon dioxide is very important in any solvation at supercritical conditions. The density augmentation or depletion is not caused by the solute, but rather it is due to the pre-existing densities inhomogenities in the pure solvent. The solute only shows a preference to dissolve in a high density region or low density region.

Furthermore, this apparently ‘universal’ behaviour is observed also for diffusion coefficients. The diffusion coefficient of methane in the supercritical carbon dioxide drops abruptly to zero, the same as in the case of water. Furthermore, this drop happens around the same density. We noted that the density where this is observed coincides with that where fluctuations in local density obtain their maximum value. We suggest that the rapid movement of CO_2 around a solute molecule is the driving force for zero values of diffusion coefficients. The rapid movement of solvent molecules around a solute restricts the motion of the solute and gives zero values of solute diffusion coefficients.

It can be concluded that the nature of the solvent is crucial in any observed pure or solvation property. This nature is yet not well understood and is still a matter of debate. We believe the preference of the solute to move in a high density region or low density region and the high density fluctuations near the critical point are most likely responsible for any peculiarities in pure or solvation properties. To date little work has been done about the instantaneous environment of a solute molecule in a supercritical fluid. This will help us to understand a second key characteristic of supercritical nature not their fluctuation in space but their fluctuation with time. This is an important factor for reaction dynamics in solvent-influenced chemical reactions. At the present time, the principal source of information on the instantaneous structure

is computer simulations. We believe an important aspect that has to be studied along a supercritical isotherm with pressure is the size a cavitations or clusters with time.

On the basis of our study, one can now imagine a general mechanism of a solution chemical reaction from a microscopic point of view. The solution-chemical reaction is viewed as a passage of a solute molecule over the solute potential-energy barrier, accompanied by solvent influence. The solvent, in general, play three distinct roles.

First, some solvent molecules themselves become involved in the rearrangement of molecules around the solute providing clustering or depletion environment. In turn, they can modify the solute electronic state through electrostatic, exchange, polarization, and dispersion interactions and deform the solute potential-energy surface. Such a modification should influence the potential-energy barrier itself along the reaction coordinate but also the properties of transition state. Second, the interaction energy between the solute and solvent molecules sometimes induces a considerable configurational change of the solute molecule and results in another stabler configuration by reflecting the energetic balance between the solute potential and the solute-solvent interaction energy as we have seen for cases of isothermal heat capacity. Third, the reaction energy required to surmount the potential-energy barrier should be supplied from the surrounding solvent molecules through the solvent energy fluctuation. The solvent-solvent and the solute-solvent interactions should play such roles as the energy source of supply.

We can conclude that new parameters have to be introduced to describe the structure of supercritical phase. The local pressure around a solute with time is one of them, it will help us to explain many reaction phenomena. Alternatively, we have to realize that there is local-bulk anisotropy in pressure which is an important key in any

micro-kinetic analysis, especially at supercritical fluid/solid interfaces, kinetics of adsorption. Furthermore, by defining local pressure we will understand better transition state kinetics and will choose the proper solvation environment in a solvent phase or microporous environment.

Another future research direction is the possibility that reactant-reactant (solute-solute) clustering can occur that in turn will affect reaction kinetics. KB theory with some corrections might still be used for such treatments. We believe this work of fundamental nature will help understand the performance of supercritical fluids as reactions media.

11 APPENDIX

This is program selected at random. It is describing the initialization the equilibration process

```
!----------------
PROGRAM BOX
!----------------

! . Module declarations.
USE DYNAMO

IMPLICIT NONE

! . Program parameters.
INTEGER,            PARAMETER :: NCHANGES = 10
REAL ( KIND = DP ), PARAMETER :: BIGSIZE  = 10.0_DP

! . Thermodynamic conditions (NVT)
REAL ( KIND = DP ), PARAMETER :: DENSITY = 973.1_DP        !kg m^-3.

! . Monte Carlo Simulation Options
REAL ( KIND = DP ), PARAMETER :: P =   14.4_DP/0.101325_DP !atm
REAL ( KIND = DP ), PARAMETER :: T = 310.00_DP             !kelvin
REAL ( KIND = DP ), PARAMETER :: ACC = 0.40_DP             !dimensionless
INTEGER           , PARAMETER :: NVT=0                     !NVT simulation
INTEGER           , PARAMETER :: NPT=500                   !NPT simulation

! . Program scalars.
INTEGER            :: ICHANGE
REAL ( KIND = DP ) :: NEWSIDE, REDUCE, SIDE, TARGET, VOLUME

! . Program arrays.
REAL ( KIND = DP ), ALLOCATABLE, DIMENSION(:,:) :: COORDINATES

! . Output File
open(6,file="results/box=(1000 , 49.68 , 310.00).out")

CALL DYNAMO_HEADER

CALL TIME_PRINT

CALL ZMATRIX_DEFINE ( "../data/zmatrix/CF3.zmatrix" )

CALL ZMATRIX_BUILD

CALL COORDINATES_WRITE

ALLOCATE ( COORDINATES(1:3,1:NATOMS) ) ; COORDINATES = ATMCRD

CALL MM_FILE_PROCESS     ( "solvent.opls_bin",
"../data/opls_aa/solvent.opls" )

CALL MM_SYSTEM_CONSTRUCT ( "solvent.opls_bin", "../data/seq/CF3_box1000.seq"
)

CALL MM_SYSTEM_WRITE     ( "../data/sys_bin/CO2_CF3box1000.sys_bin" )


! . Calculate the volume of a box that gives the appropriate density
(Angstroms^3).
VOLUME = ( SUM ( ATMMAS(1:NATOMS) ) / DENSITY ) * ( AMU_TO_KG * 1.0E+30_DP )

! . Calculate the dimension of a cubic box of the same volume (Angstroms).
TARGET = EXP ( LOG ( VOLUME ) / 3.0_DP )

! . Start off with a very large box.
```

```
SIDE = BIGSIZE * TARGET

! . Calculate the reduction factor.
REDUCE = EXP ( - LOG ( BIGSIZE ) / REAL ( NCHANGES, DP ) )

! . Assign a value to the box size.
CALL SYMMETRY_CUBIC_BOX ( SIDE )

! . Generate coordinates for each molecule.
CALL SET_INITIAL_COORDINATES

! . Initialize the random number seed.
CALL RANDOM_INITIALIZE (314159)

! . Define the options for the Monte Carlo modules.
CALL MONTE_CARLO_ENERGY_OPTIONS ( CUTOFF = 0.45_DP*TARGET, SMOOTH = 0.0_DP )

! . Do a Monte Carlo simulation (at constant volume).
CALL MONTE_CARLO ( 10, 10 * NRESID, VOLUME_FREQUENCY = NVT
,PRESSURE=P,TEMPERATURE=T)

! . Gradually reduce the size of the box to the desired value.
DO ICHANGE = 1,NCHANGES

   ! . Calculate and set the new box length.
   NEWSIDE = REDUCE * SIDE
   CALL SYMMETRY_CUBIC_BOX ( NEWSIDE )

   ! . Scale the coordinates.
   CALL SET_INTERMEDIATE_COORDINATES

   ! . Do a Monte Carlo simulation (at constant volume).
   CALL MONTE_CARLO ( 10, 10 * NRESID, VOLUME_FREQUENCY = NVT
,PRESSURE=P,TEMPERATURE=T)

   ! . Reset SIDE.
   SIDE = NEWSIDE

END DO

! . Save ccordinates
CALL COORDINATES_WRITE ( "../data/box(CF3)/NVT=(1000 , 973.1 ,
310.00)(0).crd" )
CALL PDB_WRITE         ( "../data/box(CF3)/NVT=(1000 , 973.1 ,
310.00)(0).pdb" )

! . Do a final MC calculation for a fuller equilibration.
CALL MONTE_CARLO ( 200, 100000, PRESSURE=P,TEMPERATURE=T,  ACCEPTANCE=ACC,
VOLUME_FREQUENCY = NVT)

! . Save the coordinates
CALL COORDINATES_WRITE ( "../data/box(CF3)/NVT=(1000 , 973.1 ,
310.00)(1).crd" )
CALL PDB_WRITE         ( "../data/box(CF3)/NVT=(1000 , 973.1 ,
310.00)(1).pdb" )

! . Deallocate the temporary arrays.
DEALLOCATE ( COORDINATES )

! . Finish up.
CALL TIME_PRINT

!========================================================================
====
CONTAINS
!========================================================================
====
```

```
   !---------------------------------
   SUBROUTINE SET_INITIAL_COORDINATES
   !---------------------------------

   ! . Local scalars.
   INTEGER :: I, START, STOP

   ! . Loop over the residues.
   DO I = 1,NRESID

      ! . Set the initial values of the coordinates.
      START = RESIND(I)+1
      STOP  = RESIND(I+1)
      ATMCRD(1:3,START:STOP) = COORDINATES

      ! . Randomly translate the molecule within the box.
      CALL TRANSLATE ( ATMCRD(1:3,START:STOP), SIDE * ( RANDOM_VECTOR ( 3 )
- 0.5_DP ) )

   END DO

   END SUBROUTINE SET_INITIAL_COORDINATES

   !--------------------------------------
   SUBROUTINE SET_INTERMEDIATE_COORDINATES
   !--------------------------------------

   ! . Local scalars.
   INTEGER            :: I, START, STOP
   REAL ( KIND = DP ) :: SCALE

   ! . Local arrays.
   REAL ( KIND = DP ), DIMENSION(1:3) :: DR

   ! . Calculate the scale factor for changing the coordinates of the
molecular centers.
   SCALE = NEWSIDE / SIDE

   ! . Translate the coordinates of the atoms in each molecule.
   DO I = 1,NRESID

      ! . Find the atom indices for the molecule.
      START = RESIND(I)+1
      STOP  = RESIND(I+1)

      ! . Find the translation.
      DR = ( SCALE - 1.0_DP ) * CENTER ( ATMCRD(1:3,START:STOP),
ATMMAS(START:STOP) )

      ! . Translate the molecule by the required amount.
      CALL TRANSLATE ( ATMCRD(1:3,START:STOP), DR )

   END DO

   END SUBROUTINE SET_INTERMEDIATE_COORDINATES

END PROGRAM BOX
```

```
DL POLY : Control file
SCO2 at T=308.15 and P=7.5 MPa

integration leapfrog verlet

temperature      308.15
pressure         0.075
ensemble nvt berendsen 0.5

steps              1000000
equilibration       500000
multiple step         4
scale                10
# collect
print                1000
stack                1000
stats                1000
trajectory         500000         500         0
rdf                   100

timestep         0.002
primary cutoff   25.8
cutoff           29.0
delr width       1.2000
rvdw cutoff      29.0
reaction field
eps constant     78.000
cap forces       1000.
#shake tolerance  1.0E-3
quaternion tolerance  1.0E-5
zdensity
print rdf

job time              540000
close time            6600

finish
```

12 REFERENCES

Literature Cited

Akiya, N., and P. E. Savage. 2000a. Effect of Water Density on Hydrogen Peroxide Dissociation in Supercritical Water. 1. Reaction Equilibrium. *J. Phys. Chem. A* **104**:4433-4440.

Akiya, N., and P. E. Savage. 2000b. Effect of Water Density on Hydrogen Peroxide Dissociation in Supercritical Water. 2. Reaction Kinetics. *J. Phys. Chem. A* **104**:4441-4448.

Allen, M. P., and D. J. Tildsley. 1989. Computer simulation of liquids. Oxford University Press, Oxford.

Andrews, T. 1869. *Philos. Trans.***4**:226

Arrhenius, S. A. 1889. *Z. Phy. Chem.***159**:575

Asano, T., and J. Lenoble. 1978. Activation and Reaction Volumes in Solution. *Chem. Rev.* **78**:407-489.

Atkins, P. W. 1994. *Physical Chemistry.* Oxford University Press, Oxford.

Baiker, A. 1999. Supercritical fluids in heterogeneous catalysis. *Chem. Rev.* **99**:453-473.

Berendsen, H. J. C., J. R. Grigera, and T. P. Straatsma. 1987. The missing term in effective pair potentials. *J. Phys. Chem.* **91**:6269-6271.

Blinder, S. M. 1969. *Advanced physical chemistry : a survey of modern theoretical principles.* Collier-Macmillan, London.

Born, M., and R. Oppenheimer. 1927. *Ann. Physik* **84**:457.

Brennecke, J. F., and J. E. Chateauneuf. 1999. Homogeneous Organic Reactions as Mechanistic Probes in Supercritical Fluids. *Chem. Rev.* **99**:433-452.

Chitra, R., and P. E. Smith. 2001a. A comparison of the properties of 2,2,2-trifluoroethanol and 2,2,2-trifluoroethanol/water mixtures using different force fields. *The Journal of Chemical Physics* **115**:5521-5530.

Chitra, R., and P. E. Smith. 2001b. Properties of 2,2,2-trifluoroethanol and water mixtures. *The Journal of Chemical Physics* **114**:426-435.

Clifford, T. 1999. *Fundamentals of Supercritical Fluids.* Oxford Science Publications, Oxford.

Colina, C. M., C. G. Olivera-Fuentes, F. R. Siperstein, M. Lisal, and K. E. Gubbins. 2003. Thermal properties of supercritical carbon dioxide by Monte Carlo simulations. *Molecular Simulation* **29**:405-412.

de Pablo, J. J., J. M. Prausnitz, H. J. Strauch, and P. T. Cummings. 1990. Molecular simulation of water along the liquid--vapor coexistence curve from 25 ^{o}C to the critical point. *The Journal of Chemical Physics* **93**:7355-7359.

Debenedetti, P. G., and R. S. Mohamed. 1989. Attractive, weakly attractive, and repulsive near-critical systems. *The Journal of Chemical Physics* **90**:4528-4536.

Drljaca, A., C. D. Hubbard, R. van Eldik, T. Asano, M. V. Basilevsky, and W. J. le Noble. 1998. Activation and reaction volumes in solution. 3. *Chem. Rev.* **98**:2167-2289.

Drozdov, A. N., and S. C. Tucker. 2001. Self-diffusion near the liquid-vapor critical point. *The Journal of Chemical Physics* **114**:4912-4917.

Drozdov, A. N., and S. C. Tucker. 2002. Response to ``Comment on `Self-diffusion near the liquid-vapor critical point' ". *The Journal of Chemical Physics* **116**:6381-6382.

Eckert, C. A., D. H. Ziger, K. P. Johnston, and S. Kim. 1986. Solute partial molal volumes in supercritical fluids. *J. Phys. Chem.* **90**:2738-2746.

Errington, J. R., K. Kiyohara, K. E. Gubbins, and A. Z. Panagiotopoulos. 1998. Monte Carlo simulation of high-pressure phase equilibria in aqueous systems
41. *Fluid Phase Equilibria* **151**:33-40.

Etesse, P., J. A. Zega, and R. Kobayashi. 1992. High pressure nuclear magnetic resonance measurement of spin--lattice relaxation and self-diffusion in carbon dioxide. *The Journal of Chemical Physics* **97**:2022-2029.

Evans, M. G., and M. Polanyi. 1935. Some applications of the transition state method to the calculation of reaction velocities, especially in solution. *Trans. Faraday Soc*:558-559.

Eyring, H. 1935. The Activated Complex in Chemical Reactions. *The Journal of Chemical Physics* **3**:107-115.

Gao, L., W. Wu, Z. Hou, T. Jiang, B. Han, J. Liu, and Z. Liu. 2003. Transesterification between Ethyl Acetate and n-Butanol in Compressed CO2 in the Critical Region of the Reaction System. *J. Phys. Chem. B* **107**:13093-13099.

Gross, T., J. Buchhauser, and H. D. Ludemann. 1998. Self-diffusion in fluid carbon dioxide at high pressures. *The Journal of Chemical Physics* **109**:4518-4522.

Guo, Y., and A. Akgerman. 1998. Infinite Dilution Partial Molar Volumes of Butanal and 2-Methylpropanal in Supercritical Carbon Dioxide. *J. Chem. Eng. Data* **43**:889-892.

Harris, J. G., and K. H. Yung. 1995. Carbon Dioxides Liquid-Vapor Coexistence Curve and Critical Properties As Predicted by A Simple Molecular-Model. *J. Phys. Chem.* **99**:12021-12024.

Hauthal, W. H. 2001. Advances with supercritical fluids [review]
1. *Chemosphere* **43**:123-135.

Higashi, H., Y. Iwai, and Y. Arai. 2000. Calculation of Self-Diffusion and Tracer Diffusion Coefficients near the Critical Point of Carbon Dioxide Using Molecular Dynamics Simulation. *Ind. Eng. Chem. Res.* **39**:4567-4570.

Hirst, D. M. 1985. *Potential Energy Surface*. Taylor&Francis, London.

Hloucha, M., and U. K. Deiters. 1998. Monte Carlo study of the thermodynamic properties and the static dielectric constant of liquid trifluoromethane. *Fluid Phase Equilibria* **149**:41-56.

Ikushima, Y., N. Saito, and M. Arai. 1992. Supercritical carbon dioxide as reaction medium: examination of its solvent effects in the near-critical region. *J. Phys. Chem.* **96**:2293-2297.

Iwai, Y., H. Higashi, H. Uchida, and Y. Arai. 1997. Molecular dynamics simulation of diffusion coefficients of naphthalene and 2-naphthol in supercritical carbon dioxide. *Fluid Phase Equilibria* **127**:251-261.

Jenner, G. 2002. High-pressure mechanistic delineation based on activation volumes. *Journal of Physical Organic Chemistry* **15**:1-13.

Jorgensen, W. L., D. S. Maxwell, and J. Tirado-Rives. 1996. Development and Testing of the OPLS All-Atom Force Field on Conformational Energetics and Properties of Organic Liquids. *J. Am. Chem. Soc.* **118**:11225-11236.

Jorgensen, W. L., and J. Tirado-Rives. 1996. Monte Carlo vs Molecular Dynamics for Conformational Sampling. *J. Phys. Chem.* **100**:14508-14513.

Jorgensen, W. L. 1981. Quantum and statistical mechanical studies of liquids. 10. Transferable intermolecular potential functions for water, alcohols, and ethers. Application to liquid water. *J. Am. Chem. Soc.* **103**:335-340.

Jorgensen, W. L., J. Chandrasekhar, J. D. Madura, R. W. Impey, and M. L. Klein. 1983. Comparison of simple potential functions for simulating liquid water. *The Journal of Chemical Physics* **79**:926-935.

Jorgensen, W. L., J. D. Madura, and C. J. Swenson. 1984. Optimized intermolecular potential functions for liquid hydrocarbons. *J. Am. Chem. Soc.* **106**:6638-6646.

Kajimoto, O. 1999. Solvation in Supercritical Fluids: Its Effects on Energy Transfer and Chemical Reactions. *Chem. Rev.* **99**:355-390.

Kang, M., and P. E. Smith. 2007. Preferential interaction parameters in biological systems by Kirkwood-Buff theory and computer simulation. *Fluid Phase Equilibria* **256**:14-19.

Kettler, M., I. Nezbeda, A. A. Chialvo, and P. T. Cummings. 2002. Effect of the Range of Interactions on the Properties of Fluids. Phase Equilibria in Pure Carbon Dioxide, Acetone, Methanol, and Water. *J. Phys. Chem. B* **106**:7537-7546.

Kiyohara, K., K. E. Gubbins, and A. Z. Panagiotopoulos. 1998. Phase coexistence properties of polarizable water models
6. *Molecular Physics* **94**:803-808.

Kofke, D. A. 1993. Gibbs-Duhem Integration - A New Method for Direct Evaluation of Phase Coexistence by Molecular Simulation
1. *Molecular Physics* **78**:1331-1336.

Levert Sengers, J. M. H. 1998. *Supercritical Fluids: The properties and applications, Supercritical Fluids Fundamentals and Applications.* NATO publications

Lewis, W. C. M. 1918. *J. Chem. Soc.*

Licence, P., D. Litchfield, M. P. Dellar, and M. Poliakoff. 2004. "Supercriticality"; a dramatic but safe demonstration of the critical point. *Green Chemistry* **6**:497.

Lin, C. L., and R. H. Wood. 1996. Prediction of the Free Energy of Dilute Aqueous Methane, Ethane, and Propane at Temperatures from 600 to 1200 °C and Densities from 0 to 1 g cm-3 Using Molecular Dynamics Simulations. *J. Phys. Chem.* **100**:16399-16409.

Lisal, M., and V. Vacek. 1996. Effective potentials for liquid simulation of the alternative refrigerants HFC-32: CH_2F_2 and HFC-23: CHF_3. *Fluid Phase Equilibria* **118**:61-76.

Lisal, M., J. Kolafa, and I. Nezbeda. 2002. An examination of the five-site potential (TIP5P) for water. *The Journal of Chemical Physics* **117**:8892-8897.

Lue, L., and J. M. Prausnitz. 1998. Thermodynamics of fluid mixtures near to and far from the critical region
11. *Aiche Journal* **44**:1455-1466.

Maillet, J. B., A. Boutin, S. Buttefey, F. Calvo, and A. H. Fuchs. 1998. From molecular clusters to bulk matter. I. Structure and thermodynamics of small CO2, N2, and SF6 clusters. *The Journal of Chemical Physics* **109**:329-337.

Martin, A. C. R., and Martin J.Field. 2000. A Practical Introduction to the Simulation of Molecular Systems. *Computers & Chemistry* **24**:239-240.

Martin, M. G., and J. I. Siepmann. 1998. Transferable Potentials for Phase Equilibria. 1. United-Atom Description of n-Alkanes. *J. Phys. Chem. B* **102**:2569-2577.

Matubayasi, N., and R. M. Levy. 1996. Thermodynamics of the Hydration Shell. 2. Excess Volume and Compressibility of a Hydrophobic Solute. *J. Phys. Chem.* **100**:2681-2688.

McQuarrie, D. A., and J. D. Simon. 1999. Molecular Thermodynamics. University Science Books,Sausalito,California.

Moller, D., and J. Fischer. 1994. Determination of an effective intermolecular potential for carbon dioxide using vapour-liquid phase equilibria from NpT + test particle simulations. *Fluid Phase Equilibria* **100**:35-61.

Moore, J. W., and R. G. Pearson. 1982. *Kinetics and mechanism*. Wiley;New York.

Murthy, C. S., S. F. Oshea, and I. R. Mcdonald. 1983. Electrostatic Interactions in Molecular-Crystals - Lattice-Dynamics of Solid Nitrogen and Carbon-Dioxide. *Molecular Physics* **50**:531-541.

Nakayama, H., K. i. Saitow, M. Sakashita, K. Ishii, and K. Nishikawa. 2000. Raman spectral changes of neat CO2 across the ridge of density fluctuation in supercritical region. *Chemical Physics Letters* **320**:323-327.

Nath, S. K., F. A. Escobedo, and J. J. de Pablo. 1998. On the simulation of vapor--liquid equilibria for alkanes. *The Journal of Chemical Physics* **108**:9905-9911.

Nicolas, J. J., K. E. Gubbins, W. B. Streett, and D. J. Tildesley. 1979. Equation of State for the Lennard-Jones Fluid. *Molecular Physics* **37**:1429-1454.

Nieto-Draghi, C., T. de Bruin, J. Perez-Pellitero, J. B. Avalos, and A. D. Mackie. 2007. Thermodynamic and transport properties of carbon dioxide from molecular simulation. *The Journal of Chemical Physics* **126**:064509-8.

Nishikawa, K., and T. Morita. 2000. Inhomogeneity of molecular distribution in supercritical fluids. *Chemical Physics Letters* **316**:238-242.

Nishiumi, H., M. Fujita, and K. Agou. 1996. Diffusion of acetone in supercritical carbon dioxide. *Fluid Phase Equilibria* **117**:356-363.

Nishiumi, H., and T. Kubota. 2007. Fundamental behavior of benzene-CO_2 mutual diffusion coefficients in the critical region of CO2. *Fluid Phase Equilibria* **261**:146-151.

O'Hern, H. A., and J. J. Martin. 1955. Diffusion in Carbon Dioxide at Elevated Pressures. *Ind. Eng. Chem.* **47**:2081-2087.

Okazaki, S., M. Matsumoto, I. Okada, K. Maeda, and Y. Kataoka. 1995. Density dependence of rotational relaxation of supercritical CF_3H. *The Journal of Chemical Physics* **103**:8594-8601.

Panagiotopoulos, A. Z. 1987. Direct Determination of Phase Coexistence Properties of Fluids by Monte-Carlo Simulation in A New Ensemble
2. *Molecular Physics* **61**:813-826.

Paschek, D. 2004. Temperature dependence of the hydrophobic hydration and interaction of simple solutes: An examination of five popular water models. *The Journal of Chemical Physics* **120**:6674-6690.

Peck, D. G., A. J. Mehta, and K. P. Johnston. 1989. Pressure tuning of chemical reaction equilibria in supercritical fluids. *J. Phys. Chem.* **93**:4297-4304.

Petsche, I. B., and P. G. Debenedetti. 1991. Influence of solute-solvent asymmetry upon the behavior of dilute supercritical mixtures. *J. Phys. Chem.* **95**:386-399.

Potoff, J. J., and J. I. Siepmann. 2001. Vapor-liquid equilibria of mixtures containing alkanes, carbon dioxide, and nitrogen. *Aiche Journal* **47**:1676-1682.

Potter, S. C., D. J. Tildesley, A. N. Burgess, and S. C. Rogers. 1997. A transferable potential model for the liquid-vapour equilibria of fluoromethanes. *Molecular Physics* **92**:825-834.

Quirke, N., and K. E. Gubbins. 1996. *Molecular simulation and industrial applications : methods, examples and prospects*
7. Australia ; United Kingdom : Gordon & Breach Science.

Reid, R. C., J. M. Prausnitz, and T. K. Sherwood. 1977. *The Properties of Gases and Liquids*. McGraw-Hill Book Company: New York, 3th ed.

Sadus, R. J. 2007. *Molecular Simulation of Fluids*. Elsevier, 2002.

Skarmoutsos, I., L. I. Kampanakis, and J. Samios. 2005. Investigation of the vapor-liquid equilibrium and supercritical phase of pure methane via computer simulations. *Journal of Molecular Liquids* **117**:33-41.

Song, W., R. Biswas, and M. Maroncelli. 2000. Intermolecular Interactions and Local Density Augmentation in Supercritical Solvation: A Survey of Simulation and Experimental Results. *J. Phys. Chem. A* **104**:6924-6939.

Song, W., and M. Maroncelli. 2003. Local density augmentation in neat supercritical fluids: the role of electrostatic interactions. *Chemical Physics Letters* **378**:410-419.

Song, W., N. Patel, and M. Maroncelli. 2002. A 2-Site Model for Simulating Supercritical Fluoroform. *J. Phys. Chem. B* **106**:8783-8789.

Span, R., and W. Wagner. 1996. A new equation of state for carbon dioxide covering the fluid region from the triple-point temperature to 1100 K at pressures up to 800 MPa. *Journal of Physical and Chemical Reference Data* **25**:1509-1596.

Stillinger, F. H., and A. Rahman. 1974. Improved simulation of liquid water by molecular dynamics. *The Journal of Chemical Physics* **60**:1545-1557.

Stubbs, J. M., D. D. Drake-Wilhelm, and J. I. Siepmann. 2005. Partial Molar Volume and Solvation Structure of Naphthalene in Supercritical Carbon

Dioxide: A Monte Carlo Simulation Study. *J. Phys. Chem. B* **109**:19885-19892.

Tiltscher, H., and H. Hofmann. 1987. Trends in High-Pressure Chemical-Reaction Engineering. *Chemical Engineering Science* **42**:959-977.

Trappeniers, N. J., and P. H. Oosting. 1966. Selfdiffusion in gaseous and liquid methane. *Physics Letters* **23**:445-447.

Trautz, M. A. 1918. *Z. Anorg. Chem* **102**:81.

Tsekhans, Y. V. 1971. Diffusion of Naphthalene in Carbon Dioxide Near Liquid-Gas Critical Point. *Russian Journal of Physical Chemistry,Ussr* **45**:744-&.

Tucker, S. C. 1999. Solvent Density Inhomogeneities in Supercritical Fluids. *Chem. Rev.* **99**:391-418.

Tucker, S. C., and M. W. Maddox. 1998. The Effect of Solvent Density Inhomogeneities on Solute Dynamics in Supercritical Fluids: A Theoretical Perspective. *J. Phys. Chem. B* **102**:2437-2453.

Tucker, S. C., and D. G. Truhlar. 1990. Effect of Nonequilibrium Solvation on Chemical-Reaction Rates - Variational Transition-State-Theory Studies of the Microsolvated Reaction Cl-(H_2O)N + Ch_3Cl. *J. Am. Chem. Soc.* **112**:3347-3361.

Ulrich Franck, E. 1987. Fluids at high pressures and temperatures. *The Journal of Chemical Thermodynamics* **19**:225-242.

Van P.Carey. 1999. *Statistical Thermodynamics and Microscale Thermophysics.* Cambridge University Press, New York

Vaneldik, R., T. Asano, and W. J. Lenoble. 1989. Activation and Reaction Volumes in Solution .2. *Chem. Rev.* **89**:549-688.

Vaneldik, R., and F. G. Klärner. 2002. High Pressure Chemistry. Wiley-Vch.

Viana, C. A. N., and J. C. R. Reis. 1996. Pressure dependence of rate and equilibrium constants in solution. A guide to analytical equations. *Pure and Applied Chemistry* **68**:1541-1551.

Virnau, P., M. Muller, L. G. MacDowell, and K. Binder. 2004. Phase behavior of n-alkanes in supercritical solution: A Monte Carlo study. *Journal of Chemical Physics* **121**:2169-2179.

Voth, G. A., and R. M. Hochstrasser. 1996. Transition state dynamics and relaxation processes in solutions: A Frontier of physical chemistry. *J. Phys. Chem.* **100**:13034-13049.

Zhang, J., X. Zhang, B. Han, J. He, Z. Liu, and G. Yang. 2002a. Study on intermolecular interactions in supercritical fluids by partial molar volume and isothermal compressibility. *The Journal of Supercritical Fluids* **22**:15-19.

Zhang, X., L. Gao, Z. Liu, J. He, J. Zhang, and B. Han. 2002b. Effect of size and polarity of solutes on partial molar volumes and intermolecular interaction in supercritical fluids. *The Journal of Supercritical Fluids* **23**:233-241.

Zhang, X., X. Zhang, B. Han, L. Shi, H. Li, and G. Yang. 2002c. Determination of constant volume heat capacity of mixed supercritical fluids and study on the intermolecular interaction. *The Journal of Supercritical Fluids* **24**:193-201.

Zhang, Z., and Z. Duan. 2005. An optimized molecular potential for carbon dioxide. *The Journal of Chemical Physics* **122**:214507-214515.